TRACKING
LEARNING
DETECTION

Zdenek Kalal

Submitted for the degree of
Doctor of Philosophy

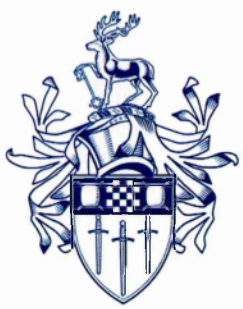

Centre for Vision, Speech and Signal Processing
Faculty of Engineering and Physical Sciences
University of Surrey

April 2011

ProQuest LLC.
789 East Eisenhower Parkway
P.O. Box 1346
Ann Arbor, MI 48106 – 1346

Summary

Visual tracking is the process of locating an object in a video sequence. This thesis investigates visual tracking of an unknown object, which significantly changes its appearance and moves in and out of the camera view. The object is defined by its location and extent in a single frame. In every frame that follows, the task is to determine the object's location and extent or indicate that the object is not present.

We propose a novel tracking paradigm (TLD) that decomposes the visual tracking task into three sub-tasks: Tracking, Learning and Detection. The tracker follows the object from frame to frame. The detector localizes appearances that have been observed during tracking and corrects the tracker if necessary. Exploiting the spatio-temporal structure in the video sequence, the learning component estimates errors performed by the detector and updates it to avoid these errors in the future. The components are analyzed in detail.

In tracking, we develop a method for detection of tracking failures that we call Forward-Backward (FB) error. The FB error allows us to measure the reliability of point trajectories in video. Next, we design a novel object tracker, which represents the object of interest by a grid of points the reliability of which is measured using the FB error. The performance of the tracker is compared with state-of-the-art approaches.

In detection, we focus on supervised learning of object detectors from large data sets. We develop a learning algorithm that optimally combines two popular learning approaches: boosting and bootstrapping. The improvements in terms of classifier speed and accuracy are achieved.

In learning, we focus on incremental, real-time learning of object detectors from a video stream. We develop a novel learning theory, P-N learning, which drives the learning process by a pair of "experts" on estimation of detector errors: (i) P-expert estimates missed detections; (ii) N-expert estimates false alarms. Convergence properties of the learning method are analyzed and conditions that guarantee improvement of the detector are found. The theory is validated on both synthetic and real data and specific examples of the experts are given.

Finally, a real-time implementation of the TLD is described and comparatively evaluated on benchmark sequences. A significant improvement over state-of-the-art methods is achieved.

Key words: tracking, learning, detection, unsupervised bootstrapping

Acknowledgements

I would like to thank my suppervisors Dr. Krystian Mikolajczyk and Prof. Jiri Matas. This thesis would not have been possible without their valuable feedback.

I am grateful to my colleagues: Asish Gupta, Martin Klaudiny and Stuart James for proofreading parts of this thesis and the whole CVSSP for a nice working atmosphere.

Most importantly, I want to thank to my family for endless support throughout my whole studies. My final and very special thanks goes to Sayaka, for her support, comprehension and encouragement.

Contents

Notation and Symbols

I	image
p	image point
b	bounding box
P	image patch extracted around p or within b
x	sample, a representation of P in a feature space $\mathcal{X}$
d	sample weight
$\hat{d}$	approximated sample weight
y	sample label from space of labels $\mathcal{Y}$ = {-1,1}
X	set of samples x
Y	set of labels y
L	labeled set, a set of pairs (x, y)
D	set of weights d
M	object model, a set of patches P
$\hat{D}$	approximated set of weights d
$\overrightarrow{T}_k$	trajectory of an image point tracked for k frames forward in time
$\overleftarrow{T}_k$	trajectory of an image point tracked for k frames backward in time
$f(x\|\Theta)$	classifier that realizes mapping $\mathcal{X} \to \mathcal{Y}$
$h(x)$	weak hypothesis that realizes mapping $\mathcal{X} \to \mathbb{R}$
$H(x)$	strong hypothesis that realizes mapping $\mathcal{X} \to \mathbb{R}$
S	similarity function
S^r	relative similarity function
S^c	conservative similarity function
θ_{NN}	threshold for detecting the object, $S^r > \theta_{\text{NN}}$
θ_{L}	threshold for definition of the core, $S^c > \theta_{\text{L}}$
$Z(h)$	error upper bound of hypothesis h
$n^+(k)$	number of positive examples output by P-expert in iteration k
$n^-(k)$	number of negative examples output by N-expert in iteration k
P^+, P^-, R^+, R^-	quality measures of P-N experts
M	transformation matrix that encodes the stability of P-N learning
λ_1, λ_2	eigenvalues of matrix M

Indexes and Formulas

$\mathbb{R}$	the set of reals
$[\mathbf{11}]^{\mathbf{T}}$	2x2 matrix of ones
t	index of a time series, e.g. I_t means image at time t
i	index of a set, e.g. x_i denotes i-th sample from X
k	index of training iteration
n, m	size of sets, e.g. X_n denotes a set of samples of size n
E[.]	expectation of a random variable
Var[.]	variance of a random variable
$\mathbf{P}$[.]	probability of logical formula
|.|	absolute value
||.||	2-norm

Performance Evaluation

TP	True Positives, correctly accepted examples
FP	False Positives, incorrectly accepted examples
TN	True Negatives, correctly rejected examples
FN	False Negatives, incorrectly rejected examples
P	Predcision
R	Recall
F	F-measure
MF	Median-Flow tracker
FB	Forward-Backward error
NCC	Normalized-Cross Correlation
SSD	Sum of Square Differences
Tr	Trimming
UUS	Unique Uniform Sampling
WS	Weighted Sampling
QWS	Quasi-random Weighted Sampling
QWS+	Quasi-random Weighted Sampling + Trimming

Chapter 1

Introduction

One of the basic tasks of computer vision is to interpret the motion of an object in a video sequence. This task has been studied for several decades and it still remains challenging. To make the problem tractable, a common approach is to make assumptions about the object, its motion or motion of the camera. In contrast, this thesis studies the task with a minimal set of assumptions with the goal to enable real-time, accurate as well as robust tracking of a priori unknown objects.

This chapter provides an overview of the entire thesis. Section 1.1 formalizes our objectives. Section 1.2 introduces possible applications of our research. Section 1.3 discusses the main challenges that have to be tackled. Section 1.4 introduces the contributions made in the thesis. Section 1.5 outlines the rest of the thesis and section 1.6 lists the publications.

1.1 Objectives

Consider a video stream depicting various objects moving in and out of the camera field of view. Given a bounding box defining the object of interest in a single frame, our goal is to automatically determine the object's bounding box or indicate that the

object is not visible in every frame that follows. The video stream is to be processed at full frame-rate and the process should run indefinitely. We refer to this task as *long-term tracking*.

A number of algorithms related to long-term tracking have been proposed in the past. However, these typically make strong assumptions about the task. In particular, tracking-based algorithms assume that the object moves on a smooth trajectory and typically fail if the object moves out of the image. Detection-based algorithms assume that an object is known in advance and require a training stage. In contrast, our goal is to track an arbitrary object that moves in and out of the camera view immediately after initialization. The difficulty of the considered data and the achieved results are shown in figure 1.1.

1.2 Motivation

The research in this thesis is mainly motivated by real-time, interactive applications.

- **Human-computer interaction.** There are already approaches that enable interaction with the computer using natural gestures . These systems are typically based on hard-coded rules. Using a long-term tracker, one can imagine a personalized controller, where the user interacts with the system using gestures or objects that are selected in runtime.

- **Surveillance.** Consider a surveillance camera and an operator. At a certain moment, the operator marks the object of interest. A long-term tracker should be able to monitor the motion of the object while being visible, indicate that the object has moved out of the field of view and re-initialize the monitoring once the objects reappears (possibly in a another camera). This task is essential for security purposes, analysis of customer behavior or even for navigation of robots. Existing systems do not scale well for unexpected objects. An algorithm capable

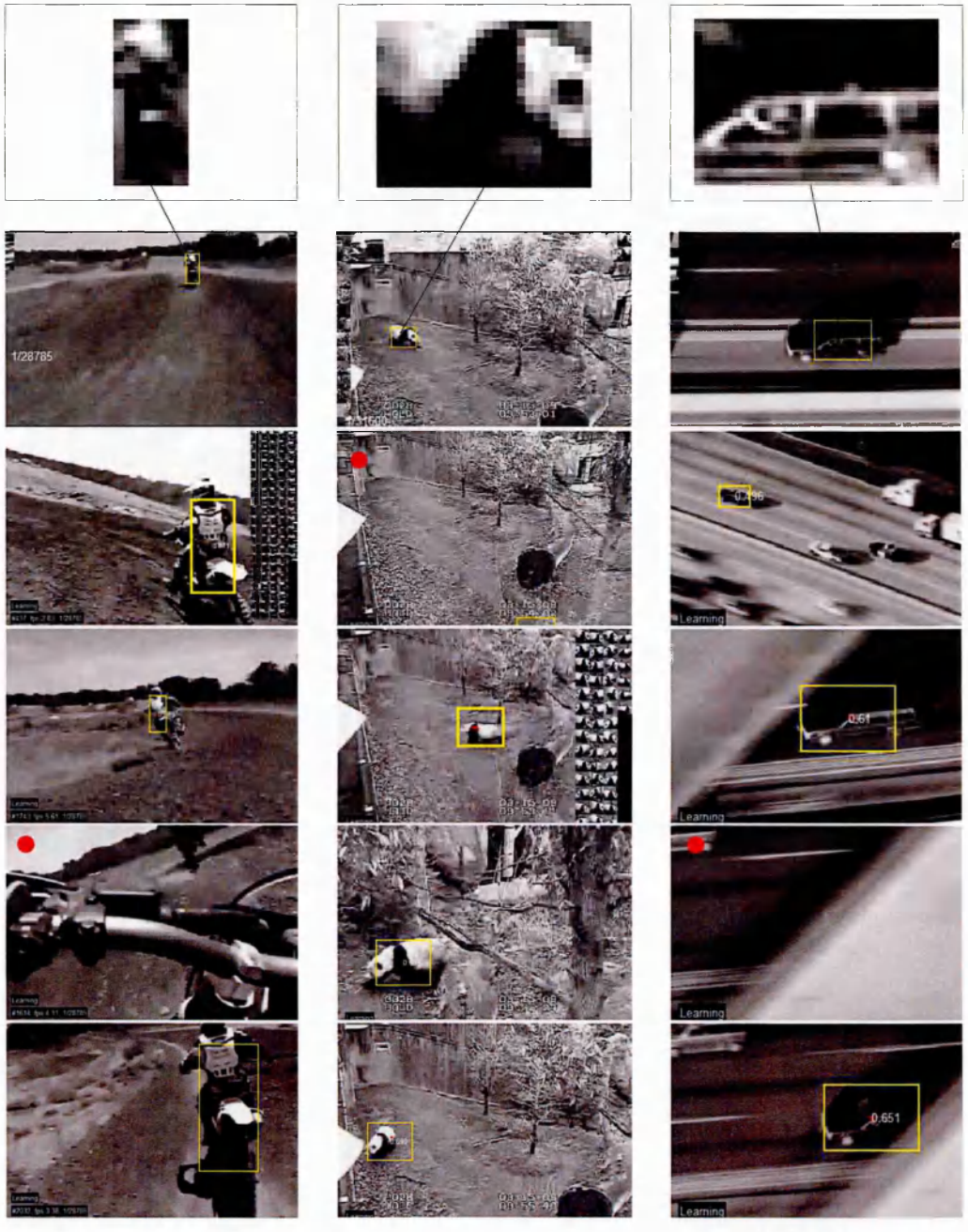

Figure 1.1: The long-term tracking task and the achieved results. The top row depicts the objects of interest selected for tracking. The remaining images show the results of our long-term tracker. The red dots indicate that the object is not visible.

of monitoring the motion of an arbitrary object for long periods of time would find a number of practical applications in surveillance and robot navigation.

- **Augmented reality.** Existing augmented reality applications are often restricted to objects that can be modeled in advance. At the core of these applications is robust tracking which often relies on an offline training stage. The ability to robustly track an arbitrary object without prior training is therefore of great interest with possible applications in games, advertisement, medical, education, tourism or military.

- **Object-centric stabilization.** Consider a hand-held camera and a user that select an arbitrary object. Using object tracking, one can imagine an object-centric video stabilization or adjustment of the camera settings. Existing tracking algorithms would be able to stabilize the video as long as the object is in the field of view, in contrast, a long-term tracker would be able to restart the stabilization whenever the object reappears in the field of view. A typical usage would be when observing a distant object using digital zoom.

- **Object recognition.** Contemporary smart phones feature visual recognition of objects captured by the camera. An emerging approach is to perform client-side tracking of the object of interest to acquire a sufficient number of query images and send them to a server which performs object recognition. Development of robust long-term tracking methods is therefore of high interest.

- **Video analysis.** A number of applications in video analysis (e.g. action recognition, automatic video annotation) require tracking of object or their parts in long video sequences. The long-term tracking methods can be potentially applied in these problems

1.3 Challenges

The range of possible applications of long-term tracking is vast, however, there are a number of issues which need to be addressed.

- **Occlusion and disappearance of the object.** The object may be occluded or disappear from the camera view for an arbitrarily length of time. The object may reappear at any time and at any location. Therefore, the long-term tracker should have mechanism (e.g. detection) to resolve these cases. Figure 1.2 illustrates the scenario.

- **Appearance and viewpoint changes.** The object of interest may change its appearance and viewpoint throughout the sequence. This complicates the tracking process as the only information given to the long-term tracker is a single patch from the initial frame, which may not be relevant throughout the entire sequence. The long-term tracker should have a mechanism (e.g. learning) for dealing with the appearance changes. See figure 1.3 for an illustration.

- **Background clutter and identification.** The object may appear in cluttered environments or may be surrounded by other objects of the same visual class. The long-term tracker should not get distracted by background clutter and should correctly distinguish the object of interest from other objects of the same class in the scene. Figure 1.4 illustrates the scenario where the task is to track a human face.

- **Scale changes.** The object may change scale. While estimation of the scale can be considered as an implementation detail, it brings an additional degree of freedom to the tracking process and as such increases vulnerability of the tracker to failure. The long-term tracker should be able to estimate the scale of an object as illustrated in figure 1.5.

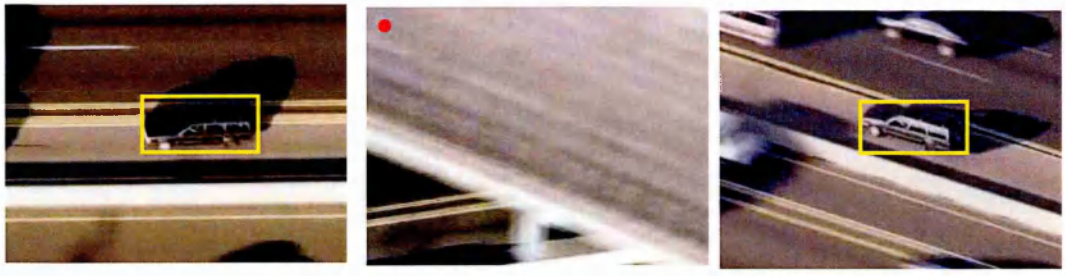

Figure 1.2: Challenges in long-term tracking: occlusion and disappearance.

Figure 1.3: Challenges in long-term tracking: appearance and viewpoint changes.

- **Illumination changes.** The object changes its appearance under different illumination. The long-term tracker should be able to deal with illumination changes as illustrated in figure 1.6.

- **Image noise.** Video sequences may be corrupted by motion blur, interlacing or video compression. This influences the accuracy of features that are extracted from every frame, which may corrupt the output of the tracking algorithm. The long-term tracker should deal with image noise. Figure 1.7 illustrates the object corrupted by motion blur.

- **Real-time performance.** To be useful for interactive applications, the long-term tracker should work at full frame rate. Therefore, the algorithm must be extremely efficient.

Figure 1.4: Challenges in long-term tracking: background clutter and identification.

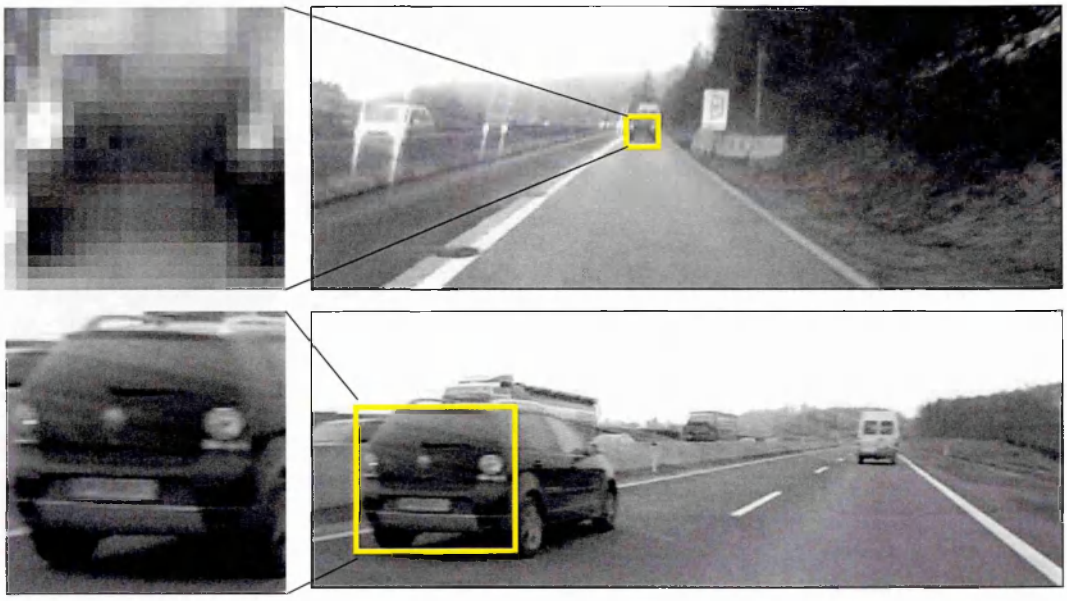

Figure 1.5: Challenges in long-term tracking: scale changes.

Figure 1.6: Challenges in long-term tracking: illumination changes. All images have been equalized.

Figure 1.7: Challenges in long-term tracking: motion blur.

1.4 Contributions

This thesis contributes to the research in long-term tracking with the algorithms summarized below.

- **TLD framework.** We introduce a novel tracking paradigm that decomposes the long-term tracking task into three sub-tasks: Tracking, Learning and Detection, each of which is tackled by a dedicated component. The tracker follows the object from frame to frame. The detector localizes all objects that appear with appearance that have been observed during tracking and corrects the tracker if necessary. Exploiting the spatio-temporal structure in the data, the learning component estimates errors performed by the detector and updates it to avoid these errors in the future. The uniqueness of the approach is in the close integration of all these components which enables mutual compensation of their individual

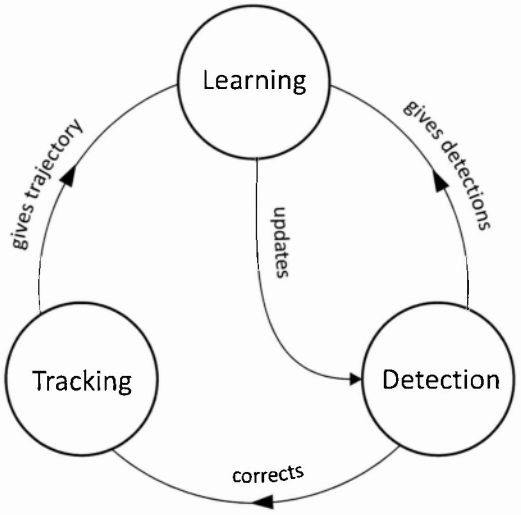

Figure 1.8: The block diagram of the proposed TLD framework.

flaws. The block diagram of the TLD framework is shown in figure 1.9. The components of the framework are studied in detail.

- **Forward-Backward error.** Building on the assumption that correct tracking is forward-backward consistent, we develop a novel measure that estimates the reliability of tracking of an arbitrary object in a video stream.

- **Median-Flow tracker.** We develop an adaptive tracker that is robust to partial occlusions and deals with appearance and illumination changes. The object of interest is represented by a bounding box, within which a sparse motion field is estimated. The reliability of each motion vector is assessed, and the most reliable vectors determine the motion of the object.

- **P-N learning.** We develop an unsupervised learning method for online learning of object detectors from video streams. The learning method is able to learn an object detector from a single example (defined by a bounding box) and a video stream where the object may appear. The learning method is formulated as unsupervised bootstrapping, where the detector errors are estimated by a pair of "experts": (i) P-expert estimates missed detections, and (ii) N-expert estimates

false alarms. Both of these experts are allowed to make errors themselves. The learning process is modeled as a discrete dynamical system and the conditions under which the learning guarantees improvement of the detector are found using stability criteria developed in control theory [Zhou 96, Ogata 09].

- **Boosting+Bootstrap.** Motivated by long-term tracking of human faces, we develop a novel learning method for training efficient object detectors. The learning method is based on a fusion of two popular learning approaches: boosting [Freund 97] and bootstrapping [Sung 98]. We formulate bootstrapping as weighted sampling where the weights are driven by boosting. The optimal sampling strategy is analytically deduced. Extensive experimental evaluation shows superior performance with respect to commonly used methods. The learning method is tested on the task of face detection and state-of-the-art performance is achieved.

- **Implementation.** We show how to implement the TLD framework . An extensive quantitative evaluation shows a significant improvement over state-of-the-art systems. Furthermore, we show how to adapt TLD for face tracking, which combines an offline trained face detector with online face identification.

1.5 Thesis outline

The structure of the thesis is outlined in figure 1.9. In chapter 2, we review the work related to long-term tracking from three points of view: object tracking, object detection and machine learning. In object tracking and object detection, we give special attention to methods that represent the object by a bounding box. In object learning, we focus on methods for training of sliding window-based detectors.

Chapters 3, 4 and 5 consider the tracking, learning and detection problems independently and propose the basic components of TLD that will be tightly integrated later.

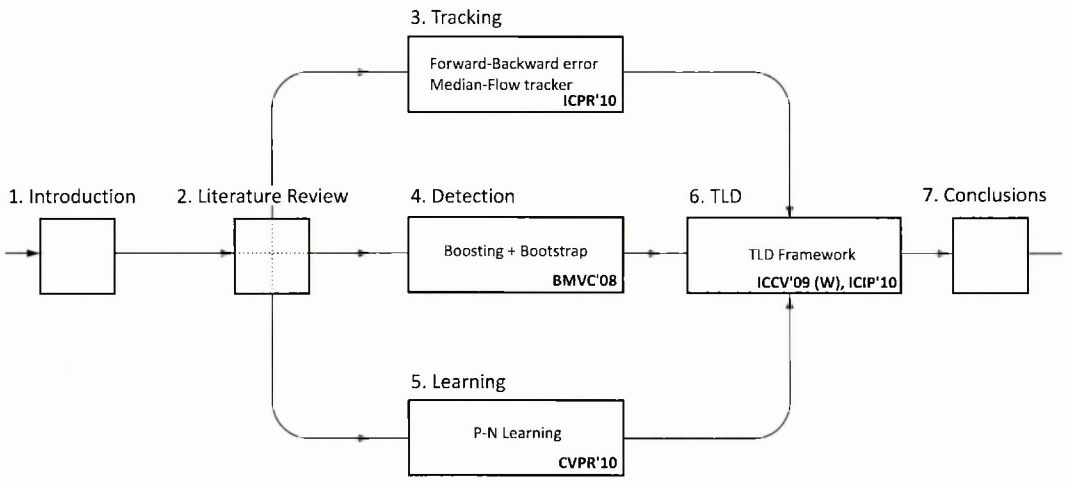

Figure 1.9: Outline and main contributions of the thesis.

Chapter 3 considers tracking algorithms when applied to unconstrained videos. Accepting the fact that every tracker eventually fails is the starting point. First, we study how to detect tracking failures. We define the Forward-Backward error, study its properties and compare to relevant error measures. Second, we study how the detected failures can help tracking itself. We develop the Median-Flow tracker and compare it to state-of-the-art methods on a number of sequences.

Chapter 4 considers offline training of an object detector from large data sets. We review the algorithms often used for this setting, in particular, boosting [Freund 97] and bootstrapping [Sung 98]. The optimal combination of boosting and bootstrapping is developed and evaluated on both synthetic and real data.

Chapter 5 focuses on online learning of an object detector from a single example and a video stream. The P-N learning theory is developed and formalized as a semi-supervised [Chapelle 06] learning method. We show how to design a pair of experts that estimate errors of the detector during learning. We show that tracking can estimate false negatives and non-maxima-suppression can estimate false positives made by the detector. The resulting algorithm is quantitatively evaluated on a number of sequences leading to surprising gains in the detector performance.

Chapter 6 develops the TLD framework and describes its implementation. The performance of TLD is evaluated on two types of experiments: (i) tracking of unknown objects, and (ii) tracking of human faces. A quantitative evaluation is performed on 21 video sequences and compared to 13 relevant tracking algorithms. A significant improvement over state-of-the-art methods is demonstrated. Furthermore, we perform a qualitative evaluation and comment on the pros and cons of the proposed approach.

Chapter 7 summarizes the contributions of the thesis, comments on the recent developments and discusses possible avenues for future research.

1.6 Publications

1. [SUBMITTED] Z. Kalal, K. Mikolajczyk, and J. Matas, "Tracking-Learning-Detection," *Transactions on Pattern Analysis and Machine Intelligence*, 2010.
2. Z. Kalal, K. Mikolajczyk, and J. Matas, "Face-TLD: Tracking-Learning-Detection Applied to Faces," *International Conference on Image Processing*, 2010.
3. Z. Kalal, K. Mikolajczyk, and J. Matas, "Forward-Backward Error: Automatic Detection of Tracking Failures," *International Conference on Pattern Recognition*, 2010.
4. Z. Kalal, J. Matas, and K. Mikolajczyk, "P-N Learning: Bootstrapping Binary Classifiers by Structural Constraints," *Conference on Computer Vision and Pattern Recognition*, 2010.
5. Z. Kalal, J. Matas, and K. Mikolajczyk, "Online Learning of Robust Object Detectors During Unstable Tracking," *On-line Learning for Computer Vision Workshop*, 2009.
6. Z. Kalal, J. Matas, and K. Mikolajczyk, "Weighted Sampling for Large-Scale Boosting," *British Machine Vision Conference*, 2008.

Chapter 2

Related work

Long-term tracking is a complex problem that is closely related to tracking, detection and machine learning and in many cases it is studied from one point of view only. These terms are understood as follows. *Tracking* estimates the object motion between consecutive frames relying on temporal coherence in the video. *Detection* considers the video frames as independent and localizes all objects that correspond to an object model. *Machine learning* is often employed in both of these approaches. Trackers use machine learning to adapt to changes of the object appearance. Detectors use machine learning to build better models that cover various appearances of the object.

To give an overview of the most relevant approaches, the chapter is split into four parts. Section 2.1 gives an overview of tracking approaches ranging from simple template tracking up to trackers that learn online a discriminative classifier. Section 2.2 reviews detection approaches focusing on detection of object instances as well as detection of human faces. Section 2.3 reviews the learning strategies commonly used for the training of object detectors. In particular we review bootstrapping, boosting as well as methods based on semi-supervised learning. Section 2.4 comments on observed trends and outlines challenges that motivated our research.

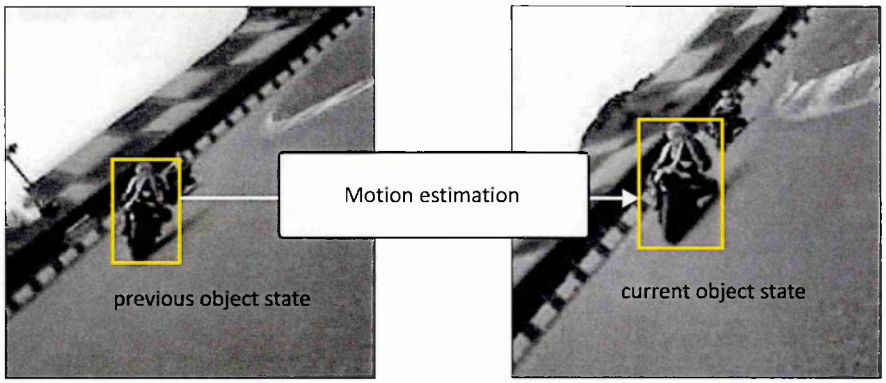

Figure 2.1: Illustration of a typical tracking system.

2.1 Tracking

Tracking is a task of estimating object motion [Yilmaz 06]. Various definitions are considered in the literature. In this thesis we consider tracking as the task of estimating the object motion between consecutive frames. The implicit assumption of such algorithms is that the location of the object in the previous frame is known. This is in contrast to long-term tracking where this location might not be defined. In the following, the term tracking will be sometimes substituted with more accurate frame-to-frame tracking to emphasize the meaning. This review is organized as follows. Sub-section 2.1.1 introduces the terms used in tracking. Sub-section 2.1.2 classifies the tracking approaches based on the object representation. Sub-section 2.1.3 reviews generative trackers, one of which, the Lucas-Kanade [Lucas 81] tracker, is used in our system. Finally, sub-section 2.1.4 reviews in detail discriminative trackers as these represent the closest competitors to our approach.

2.1.1 Prerequisites

At every time instance, trackers characterize the object of interest by several variables (e.g. location, scale, pose), which together represent the so-called *state* of the object.

Figure 2.2: Classification of trackers based the representation of the object: a) points, b) geometric shapes, c) contours, d) articulated models, and e) motion field.

A temporal sequence of states defines the object *trajectory*. Difference of two consecutive states defines the object *motion*. Figure 2.1 illustrates the scenario.

Model. Tracking algorithms represent the object by a *model*. We distinguish two classes of models based on the type of information they represent: (i) generative, and (ii) discriminative. *Generative* models represent the appearance of the object ignoring the environment where the object moves. *Discriminative* models focus on differences between the object and the environment. Both of these models are either *static* – remain fixed during tracking, or *adaptive* – accept new information during tracking.

Motion estimation. Given the object state in the previous frame and the object model, tracking estimates the object motion by fitting the object model to the current frame using some estimation algorithm (e.g. gradient descent). Alternatively, it is possible to maintain a distribution of the object state and propagate it in time, i.e. particle filtering.

Drift & failure. State-of-the-art trackers are often adaptive, i.e. update the object model during tracking, which allows them to handle changes in object appearance, illumination or environment. The drawback of the adaptation is *drift*: the errors of the update accumulate over time and the tracker slowly slips away from the object. Drift is different from tracking *failure*, which is a sudden incorrect estimation of the object state. Tracking failures typically happen when the object dramatically changes appearance, gets fully occluded or moves out of the cameras field of view.

2.1.2 Classification

One of the most distinctive properties of a tracking algorithm is the object state, which determines the variables that are estimated during tracking. Here we use the object state to classify tracking algorithms into five categories shown in figure 2.2.

1. **Points** are often used to represent the smallest objects that do not change their scale dramatically. Algorithms that represent the object by a point will be called *point trackers*. Point trackers estimate only translation of the object. The estimation can be performed using frame-to-frame tracking [Lucas 81, Shi 94], key-point matching [Veenman 01], key-point classification [Lepetit 05], or linear prediction [Zimmermann 09]. Recent work is directed towards optimizing performance of these methods [Takacs 10].

2. **Geometric shapes** such as bounding boxes or ellipses, are often used to represent motion of objects which undergo significant changes in scale. These methods typically estimate object location, scale and in-plane rotation, all other variations are typically modeled as the changes of the object appearance.

3. **3D models** are used to represent rigid objects, for which the 3D geometry is known. These models estimate location, scale and pose of the object. These methods have been applied to various objects including human faces [Vacchetti 04]. A significant effort in tracking is directed towards systems that build the 3D models online such as SLAM [Davison 03] or PTAM [Klein 07].

4. **Contours** are used to represent non-rigid objects. Parametric representation of contours has been used for tracking of human heads [Birchfield 98] or arbitrarily complex shapes [Isard 98]. Non-parametric representations have been applied for the tracking of people in sport footage [Yilmaz 04], or various non-rigid objects including animals and human hands [Bibby 08, Bibby 10].

5. **Articulated models** are used to represent the motion of non-rigid objects consisting of several rigid parts. These models typically consist of several geometric shapes, for which relative motion is restricted by a model of their geometric relations. Articulated models have been used for tracking of humans [Wang 03, Ramanan 07] or human arms [Buehler 08].

6. **Motion field** [Horn 81, Brox 04] is a non-parametric representation of the object motion which gives the displacement of every pixel of the object between two frames. An extensive comparison of these methods can be found in [Barron 94]. Recent developments aim at producing long, continuous trajectories of image points [Sand 08, Goldman 07].

In this thesis we represent the object state by a bounding box. This representation balances the tradeoff between the expressive power of the representation and the difficulty to reliably estimate the object motion. The related methods will be now analyzed in detail.

2.1.3 Generative trackers

Generative trackers model the appearance of the object. In this section we focus on trackers that represent the object by a geometric shape (i.e. rectangle or ellipse) within which the appearance is modeled. Motion estimation will be typically formulated as a search for the best match between an image patch and the model. Even though these methods were not designed for long-term tracking, we review them as our approach is relying on number of ideas from this category.

Template tracking

Template trackers represent the object appearance by a single exemplar – a *template* (e.g. an image patch). They define a *similarity measure* between two templates and

search for such a displacement (or warp) that maximizes the similarity match.

Exhaustive search for the best similarity match is straightforward, but not efficient. To make it faster, the search can be performed using integral images [Schweitzer 02], or in frequency domain [Reddy 02]. Another strategy is to restrict the search to the vicinity of the previous location. Exploration of the neighborhood not only increases the efficiency of the template tracker, but also reduces the number of false matches. On the other hand, the tracker may lose the target if the frame-to-frame motion is larger than expected. In other words, tracker face the tradeoff between speed and robustness. The most popular strategies for searching within the surrounding of the previous location are: (i) gradient-based methods, and (ii) mean-shift.

Gradient-based methods optimize the similarity measure using gradient descent. One of the most popular methods is the Lucas-Kanade [Lucas 81] tracker and its pyramidal implementation [Bouguet 99], which estimates translation of an image patch. Affine warping was later proposed in the Kanade-Lucas-Tomasi tracker [Shi 94]. Both of these approaches have been unified in Inverse Compositional Algorithm [Baker 04]. These methods base the similarity function on SSD. Recently, the similarity function based on mutual information has been proposed [Dowson 08] which demonstrated larger convergence basins.

The mean-shift algorithm [Comaniciu 03, Bradski 98] is another approach to avoid the brute-force search for the best template match. The object is described by a distribution of colors. Given a new image, every pixel is assigned a probability score from the distribution resulting in the so-called back-projection image. Mean-shift then iteratively searches for a mode in the back-projection image. Similarly to the gradient-based methods, mean-shift cannot handle large displacements as the search is local. On the other hand, the histogram-based representation handles large appearance changes as long as the color distribution remains similar.

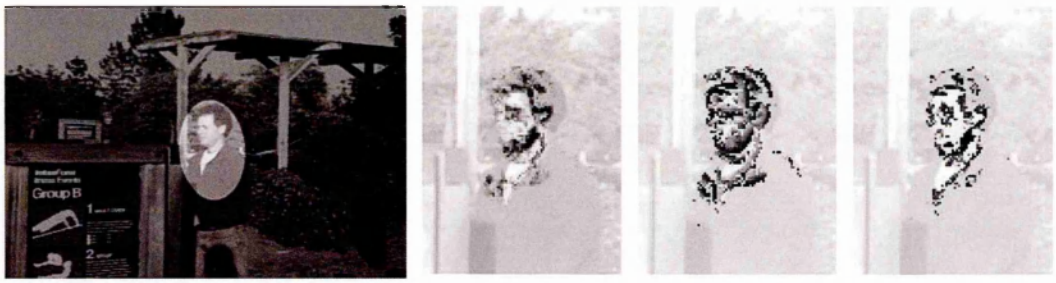

Figure 2.3: The WSL tracker [Jepson 03] estimates components on a template that are reliable for tracking. This increases the tracker's robustness to partial occlusion and appearance changes.

Improvements on template tracking

Template tracking has three main drawbacks. *First*, template tracking faces a tradeoff between static and adaptive tracking. A single static template is often not sufficient to represent all the appearances of the object and adaptation of the template (using the template from the previous frame) suffers from drift. *Second*, template tracking is often sensitive to partial occlusions. *Third*, a single template does not allow encoding of multiple appearances.

To tackle the tradeoff between static and adaptive tracking, the basic idea is to adapt the template only if necessary and re-use the previously observed templates otherwise. For this purpose a function that evaluates the usefulness of the previously observed templates has to be designed. This idea has been used for tracking of image patches [Matthews 04, Dowson 05] as well as 3D pose estimation [Rahimi 08].

To tackle the problem of partial occlusions, the WSL tracker [Jepson 03] decomposes the template into three layers: "Wandering", "Stable" and "Lost". It was shown that by focusing on stable parts of the template, the tracker deals better with partial occlusions and appearance changes. For illustration see figure 2.3. The Fragment-based tracker [Adam 06] decomposes the template into a set of randomly chosen fragments. Motion of each fragment is estimated independently and the global motion is estimated

Figure 2.4: Incremental Visual Tracking [Ross 07] builds online a PCA-based model of the object. The method demonstrated a strong resistance to appearance and illumination variations.

using robust statistics.

To encode multiple appearances of the object, the single image patch can be replaced by multiple projections given by Principal Component Analysis (PCA). EigenTracking [Black 98] considers a scenario when all the object appearances are known in advance and trains an object model offline. This approach has been applied to tracking of non-rigid objects on non-cluttered background. Incremental Visual Tracking [Ross 07] builds the PCA-based model during tracking. It has been demonstrated to handle illumination and appearance variations. See figure 2.4 for illustration.

Research in generative trackers demonstrated that drift can be reduced by reusing already seen examples of the object, and that the resistance to partial occlusions can be achieved by decomposing the template into independent parts. Both of these ideas are used in our system. However, the principle drawback of generative trackers is that they model only the object appearance. As a consequence, generative trackers get confused easily in cluttered background, where the clutter may look similar to the object. To increase the tracker's robustness, methods that consider the background class in the modeling were proposed.

2.1.4 Discriminative trackers

Discriminative trackers encode the differences between the object appearance and the environment where the object moves. A common approach is to build a binary classifier that distinguishes the object from its background. These methods represent the closest competitors to our system as they often demonstrate re-detection capabilities.

Static discriminative trackers

One of the earliest discriminative trackers was proposed by Avidan [Avidan 04], who integrated an offline trained SVM classifier into the tracking process. The motion was estimated by maximizing the classifier confidence using gradient-ascent. The performance was demonstrated on the task of vehicle tracking. The main limitation of static discriminative trackers is in the training data, since all appearances of the object and background have to be captured in advance.

Adaptive discriminative trackers

Adaptive discriminative trackers learn the discriminative classifier during tracking. This allows them to track a wide range of objects immediately after initialization. These trackers typically operate as follows. In the first frame, the tracker builds a simple classifier separating the selected object from its background. The tracking then proceeds in a frame-by-frame fashion. In every frame, the classifier is *evaluated* on the surrounding of the previous object location and the new location is established, e.g. by taking the maximally confident location. The tracker then performs an *update*. The current location of the object is used to sample positive examples, and the surrounding is used to sample negative examples of the object appearance. These labeled examples update the classifier, which is then used in the next frame.

One of the earliest works from this category was by Collins et al. [Collins 05] who

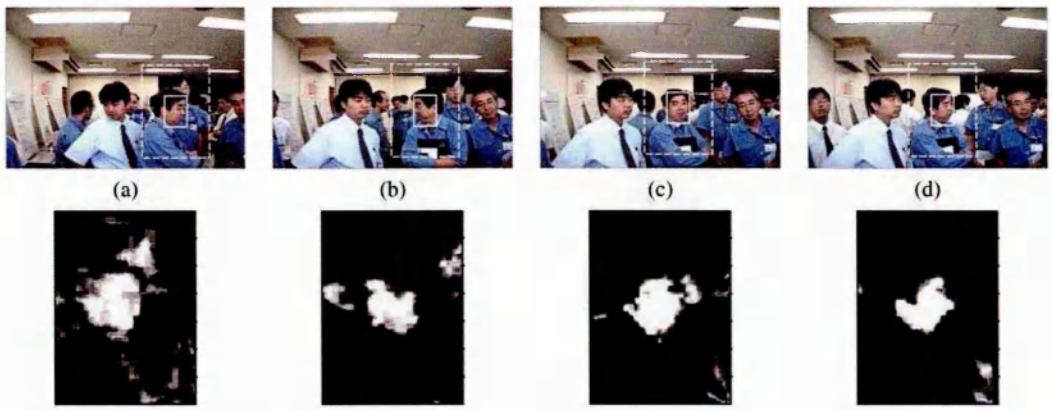

Figure 2.5: Ensemble tracking [Avidan 07] represents the object of interest by a discriminative model classifying every pixel as the object or background. The classifier is adapted in every frame. The tracker demonstrated the ability to handle appearance changes in presence of cluttered environment.

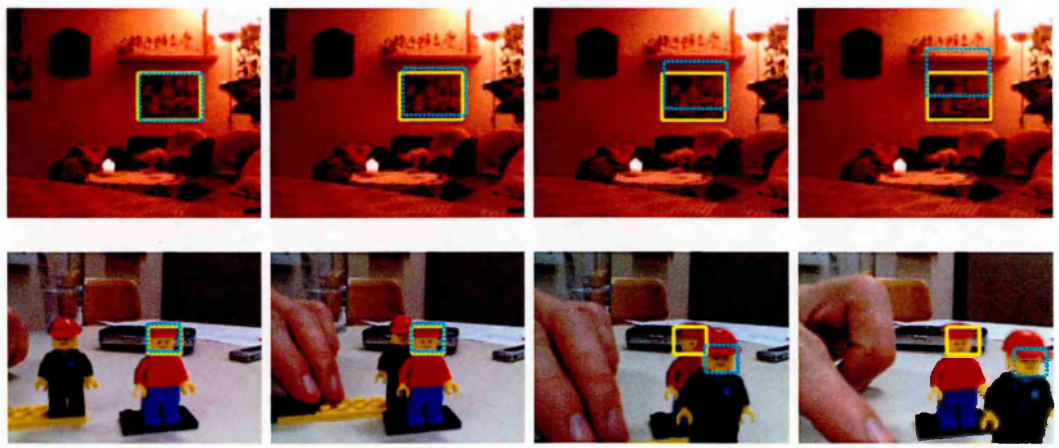

Figure 2.6: The SemiBoost tracker [Grabner 08] reduces drift of discriminative trackers by guiding the update by an offline trained classifier. Performance was demonstrated (among others) on: (TOP) 24h tracking of a still object by static camera, (BOTTOM) re-detection of a stationary object after a brief occlusion.

built a generative model by discriminative training. The object model, based on color projections, was adapted during tracking which made it robust to significant illumination variations. Ensemble Tracking [Avidan 07] updates a boosting-based classifier to discriminate between pixels on the object and pixels on the background. Online Boosting [Grabner 06] applies the same principle to a grid of overlapping bounding boxes instead of individual pixels. Their classifier was based on a set of Haar-like features [Viola 01] and was trained in an online boosting [Oza 05] framework.

The research in adaptive discriminative tracking has enabled tracking of objects that significantly change appearance and move in cluttered background. The speed of adaptation of the classifier plays an important role in these systems. It controls the impact of new appearances on the classifier, but also the speed by which the old information is forgotten. If the speed of adaptation is set correctly for a given problem, these trackers demonstrate robustness to short-term occlusion. On the other hand, if the object is not visible for longer time than expected, the tracker will eventually forget the relevant information and never recover.

Constrained adaptation for discriminative trackers

This section reviews the discriminative tracking approaches that perform *constrained* adaptation of the classifier, which is in contrast to every-frame-update reviewed in the previous sub-section. The constrained adaptation aims at drift reduction as well as long-term tracking resistant to long-lasting full occlusions. Three classes of approaches can be identified: (i) semi-supervised learning, (ii) multiple-instance learning, and (iii) co-training.

Semi-Supervised Learning (SSL) [Chapelle 06] is a learning approach that learns from both labeled and unlabeled training data. SSL has been applied to a number of problems in machine learning [Blum 98] and recently also to adaptive discriminative tracking. Semi-supervised Online Boosting [Grabner 08] is one of the earliest approaches.

The initializing frame is considered as a collection of labeled examples, all the remaining frames from the sequence are considered as unlabeled. The method employs two classifiers: (i) a classifier used for tracking, and (ii) an auxiliary classifier used for update. In the first frame, both classifiers are trained using the labeled data. During the tracking, the auxiliary classifier remained fixed and provides soft-labels to the unlabeled patches, which are then used to update the tracking classifier. The method demonstrated reduction of drift and certain re-detection capabilities. See figure 2.6 for an illustration. Beyond Semi-supervised Online Boosting [Stalder 09] extended the approach with one more auxiliary classifier to increase the adaptability of the system.

Multiple Instance Learning (MIL) [Dietterich 97] is a variant of supervised learning, where examples are delivered in groups. Within each group, the examples share the same label. MILTrack [Babenko 09] combines Online Boosting [Grabner 06] and MIL. In contrast to the every-frame update, the classifier is updated by spatially related groups of patches. The introduction of this spatial-information reduced drift and improved accuracy. Later on, a combination of MILTrack and SSL was proposed [Zeisl 10].

Co-training [Blum 98] is a specific instance of SSL methods, which trains in parallel two independent classifiers. Confident predictions of one classifier train the second classifier and vice versa. The idea behind the co-trained trackers is the following. If the object disappears from the view, neither of the classifiers is confident and the update does not take place. The co-trained Support Vector Machine tracker [Tang 07] represents the object in two feature spaces (color, gradient orientations [Dalal 05]), which were used to train two online-SVM [Cauwenberghs 01] classifiers. The co-trained Generative and Discriminative tracker [Yu 08] exploited the same idea while training a pair of a generative and a discriminative classifiers. A significant improvement in re-detection capability with respect to adaptive discriminative trackers was achieved.

In addition, the task of robust object tracking is often studied in offline setting. It has been shown [Buchanan 06] that points can be tracked very robustly and accurately

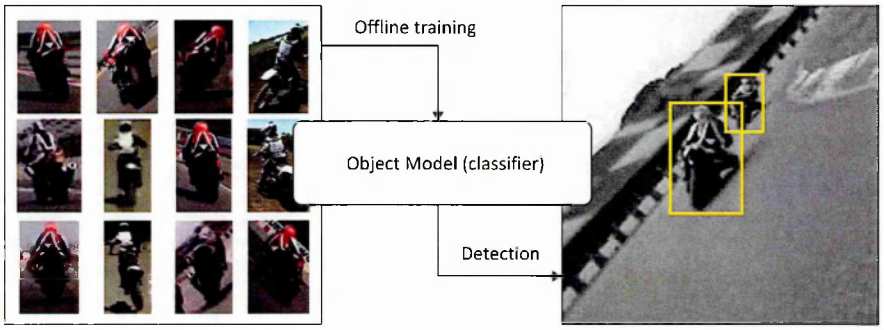

Figure 2.7: Illustration of a typical detection system.

if tracking is tightly integrated with detection using dynamical programming. While the system demonstrated impressive performance it has been designed for interactive post-processing and requires an offline training stage.

2.2 Detection

Object detection is the task of localizing objects in an input image. In long-term tracking, detection capability is essential as the object freely moves in and out of the camera field of view. Object detectors do not make any assumptions about the number of objects nor their location in the image. The objects are described by a model that is built in a training phase. At run-time, the model remains typically fixed. Figure 2.7 illustrates a typical detection system.

This section reviews the detection approaches starting from the simplest up to the most complex. Sub-section 2.2.1 reviews detectors of image features, which represent the basic building blocks of more complex approaches. Sub-section 2.2.2 reviews detectors of object instances (e.g. a specific book cover) and briefly comments on recent methods for online learning of these methods. Finally, as we are also interested in the long-term tracking of human faces, sub-section 2.2.3 reviews the methods for detection of human faces and comments on commonly used features.

2.2.1 Detection of image features

Feature detectors [Tuytelaars 07] are algorithms that are used to localize salient points (or regions) in an input image. We distinguish two approaches for feature detection.

Designed detectors. These detectors design a saliency measure and localize features that maximize it. The widely known approaches are Harris [Harris 88] or Shi-Tomasi detector [Shi 94], which localize image points. These detectors have been extended to scale and affine covariant region detectors with the Hessian-Laplace [Mikolajczyk 05] detector. Other examples from this category are Difference of Gaussians (DoG) [Lowe 04] or Maximally Stable Extremal Regions (MSER) [Matas 04].

Learned detectors. Feature detection has reached a level of maturity and the research was directed toward proposing more efficient solutions that stem from machine learning community. A popular algorithm is FAST [Rosten 06] keypoint detector, which approximates the Harris corner detector [Harris 88]. Efficient approximations of Hessian-Laplace [Mikolajczyk 05] were also proposed [Sochman 09].

2.2.2 Detection of object instances

This section focuses on methods that detect object instances, such as a specific book cover. We distinguish approaches which model the object appearance (i) globally and (ii) locally. We also mention methods for the learning of these detector.

Global appearance models typically represent the object appearance by a collection of examples and define the detection (and the pose estimation) as the search for the most similar example in the database. In one of the earliest works, Murase and Nayar [Murase 95] use a controlled capturing process to collect a large number of examples of various 3D objects. Similar idea underpins more recent methods for detection and rectification of patches [Hinterstoisser 09] or detection of texture-less objects using dominant orientation templates [Hinterstoisser 10]. Global appearance models are

Figure 2.8: Lowe [Lowe 04] proposed a detection system that represented objects locally using keypoints and SIFT descriptors. The detector is based on an approximate nearest neighbor and global geometric constraints. The system demonstrated a significant illumination and pose invariance and robustness to partial occlusions.

appealing due to their simplicity, however they suffer from partial occlusions and background clutter.

Local appearance methods represent the object by a collection of local patches that are related by geometric constraints. Their advantage, with respect to the global appearance representation, is their resistance to partial occlusions. The seminal work in this area was done by Lowe [Lowe 04], where the object is modeled by a collection of SIFT descriptors [Lowe 04] extracted around DoG features. The detection has two stages: (i) the detected DoG features are assigned a nearest neighbor descriptor stored in a database, and (ii) the assignments are validated using geometric constraints (a similarity transformation is considered). Lowe demonstrated near real-time detection of multiple objects, resistant to significant occlusions as shown in figure 2.8. A number of approaches followed this research line [Obdrzalek 05, Lepetit 05, Taylor 09, Pilet 10].

Learning approaches. The methods discussed above typically separate the training and testing stage, which restricts their application to scenarios when the object appearance is known in advance. The training state is therefore essential and often requires

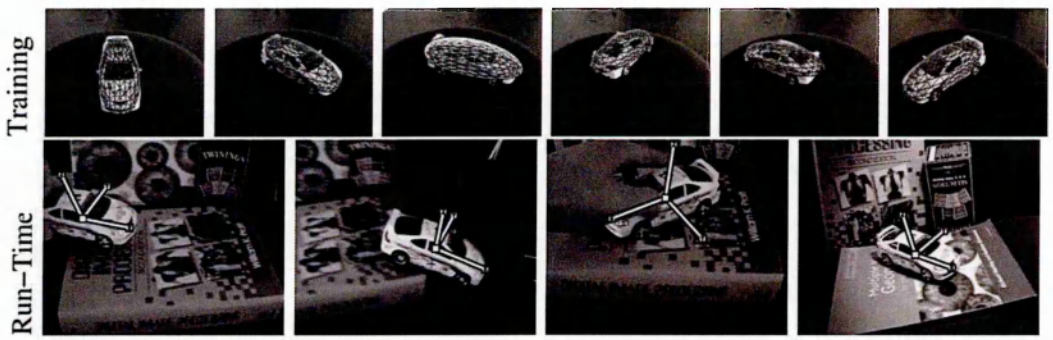

Figure 2.9: Feature harvesting [Ozuysal 06], a method for automatic training of an object detector in a controlled environment (TOP). After the training phase the detector operates in cluttered environments (BOTTOM).

a large number of human-annotated training examples. In order to simplify the training stage, Feature Harvesting [Ozuysal 06] learns the geometry and the appearance of an object automatically from a video. The method assumes a rigid 3D object moving slowly in a video sequence. After the training phase, the algorithm is able to detect the object and estimate its 3D pose in a cluttered background. See figure 2.9 for illustration. Another direction is to make the training instantaneous and thus remove the difference between training and run-time. A common strategy is to simply *add* new templates [Hinterstoisser 10] or to *integrate* new views into the classifier exploiting the computation performed in the offline training [Calonder 08, Hinterstoisser 09, Pilet 10].

For certain classes of objects, the detection of object instances has reached a level of maturity. In particular, planar and textured objects can be reliably detected in real-time and are often used in augmented reality applications. Objects that are non-rigid and non-textured still remain challenging for detection. With respect to online learning, several methods are designed to enable instantaneous online learning, but the decision when to learn new appearances is not directly addressed.

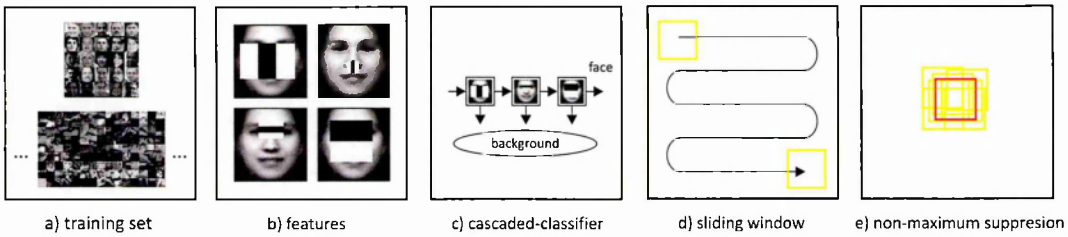

Figure 2.10: Illustration of a typical face detection components.

2.2.3 Detection of faces

Face detection is a task of localizing of human faces in an input image, regardless of their pose, illumination, expression or identity. This section briefly mentions the history of face detection, describes the most popular approaches and comments on the commonly used features.

History. Research in face detection started in early 70' with approaches that modeled the face appearance by a set of *rules* provided by the researcher [Fischler 73, Sinha 94]. This view was mainly motivated by the ease with which rules could be designed (e.g. a face has two eyes) and the lack of computational resources that would enable learning of these rules explicitly. With increasing computational capacity, learning-based methods started to dominate in 90', which learn the rules from training examples [Turk 91, Belhumeur 97, Osuna 97, Sung 98, Rowley 98, Papageorgiou 98]. While a number of these approaches achieved high detection rates [Schneiderman 04], their practical applicability was limited due to their speed. This was changed by Viola and Jones [Viola 01] approach, who introduced the first real-time face detector. Since then, research in face detection iterates over the Viola and Jones approach [Li 04, Fleuret 01, Jones 03, Sochman 05, Huang 07] and is often considered as solved.

Viola and Jones face detector combined a number of techniques previously developed in face detection. Many of these techniques reach beyond face detection and are used in our long-term tracking system as well. Refer to the figure 2.10.

- *Training set.* The face is represented by a model, which is learned from a large collection of labeled training examples. The positive examples depict tightly cropped faces, negative examples depict non-faces.

- *Local features.* The training examples are described by local features. Popular features are Haar wavelets [Papageorgiou 98] which encode intensity patterns. The features are efficiently measured using integral images [Viola 01].

- *Cascaded classifiers.* The face model has a form of a binary classifier which is split into a number of stages. Every stage enabled early rejection of background examples. This cascaded architecture, which leads to a significant increase of the classification speed, was first used in [Yang 94].

- *Sliding window.* The cascaded classifier is evaluated on a grid of locations at multiple scales. At every location, the classifier decides about presence or absence of the face.

- *Non-maximum suppression.* Due to the sliding window approach, the classifier typically produces multiple overlapping responses around the face. A common approach is to take the locally maximal confidence response and suppress all the remaining responses.

- *Boosting+Bootstrap.* The classifier is typically learned using a combination of boosting [Freund 97] and bootstrapping [Sung 98]. As one of the contribution of this thesis is the optimal combination of these methods. A detailed review of these methods is given in section 2.3.

Features used in object detection. Features play an important role in object detection as they encode our knowledge about the object. Here we give a brief overview of features that are commonly used for description of object appearance. See figure 2.11 for an illustration.

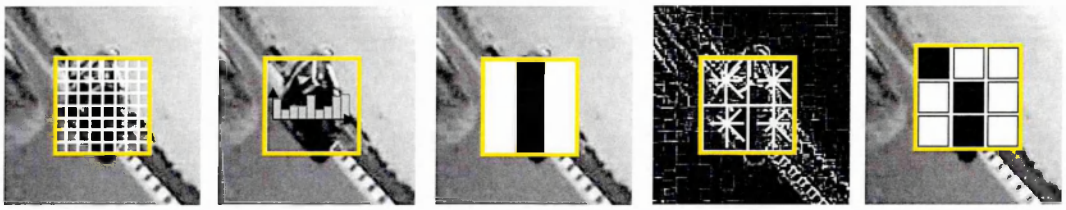

Figure 2.11: Features used to represent appearance in objects detection.

- *Raw pixels.* An image patch can be considered a simple feature. Its advantage is its simplicity and efficiency. The drawback is its high dimensionality as well as low robustness to appearance variations. The similarity is usually measured using Normalized Cross-Correlation (NCC) or by Sum of Square Differences (SSD).

- *Histograms.* A histogram represents the object appearance by a distribution of colors, gray-scale values, edge orientations, etc. Spatial relations between pixels are discarded in histograms.

- *Filter responses.* Filters are used to detect predefined intensity patterns in an image patch. One of the most popular types are Haar-like filters [Papageorgiou 98], which encode difference of average intensities between neighboring rectangular regions. These features can be measured in constant time using integral images [Viola 01]. A number of extensions have been proposed such as the comparison of non-neighboring regions [Li 04], features rotated by 45 degrees [Lienhart 02], or pixel differences measured at different scale-space levels [Huang 07].

- *Gradients.* Gradients represent a significant cue in many object recognition systems. The Scale-invariant Feature Transform [Lowe 04] is probably the most successful. A patch surrounding a keypoint is split into 4x4 cells, within each cell an eight-bin histogram of gradient orientation is measured which produces a feature vector of 128 elements. A number of modifications have been later proposed. Histograms of Oriented Gradients [Dalal 05] uses an arbitrary num-

ber of cells and various normalization schemes. Edge Orientation Histograms [Levi 04] compares just two orientations.

- *Codes.* Codes convert a real-valued intensity patterns to discrete codes. Local Binary Patterns [Ojala 02] are probably the most commonly used. These features were originally designed for texture classification but later were applied to face detection [Hadid 04]. Codes were also used for encoding combinations of wavelet coefficients [Schneiderman 04] or patterns of edge orientations [Mikolajczyk 04].

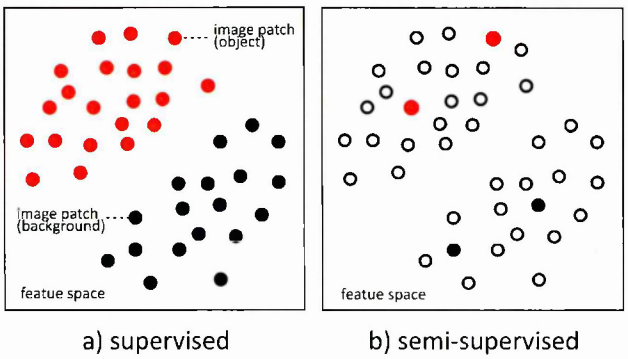

Figure 2.12: Classification of learning methods. Colored dots correspond to labeled training examples; white dots correspond to unlabeled examples.

2.3 Machine learning

This section reviews strategies for learning of sliding window-based object detectors. At the core of these detectors is a binary classifier, which classifies patches in an input image. During training, the image patches are interpreted as points in the feature space (training examples), and the goal is to find a decision boundary that separates the positive examples from the negative examples. Figure 2.12 illustrates two settings discussed in this section: (i) supervised learning, (ii) semi-supervised learning.

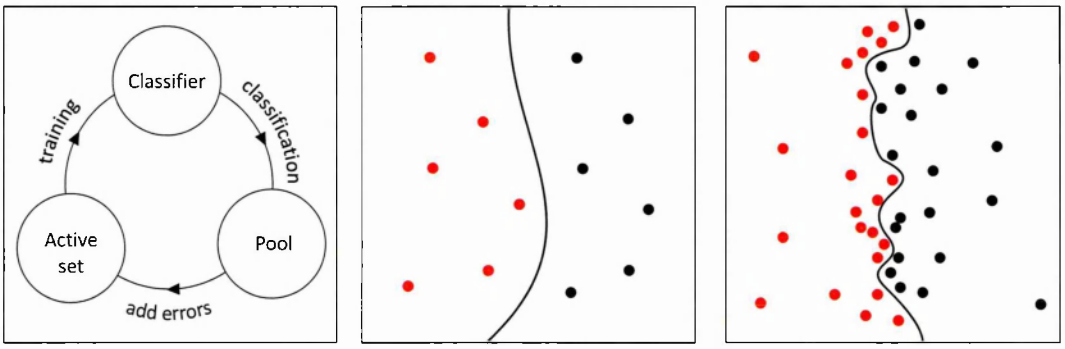

Figure 2.13: Bootstrapping: a) the block diagram, b) an initial training set, c) a training set after several iterations of bootstrapping.

Detectors are traditionally trained using supervised learning. While this setting is not directly relevant for long-term tracking of unknown objects, it becomes valuable when the class of the object is known in advance. For instance, if it is known that the object of interest will be a face, it is possible to train a face detector in advance. Two popular learning methods, namely bootstrapping and boosting will be reviewed in section 2.3.1 and 2.3.2, respectively. Recently, the research in the detector training has focused on semi-supervised learning methods, which, in addition to labeled data, enable processing of unlabeled data. Section 2.3.3 reviews the corresponding methods.

2.3.1 Bootstrapping

Bootstrapping [Sung 98] is a general strategy that iteratively improves a classifier by training it on an increasingly larger and more informative subset of the entire training set. This subset is called an *active set* and the entire training set is reffered to as the *pool*. Bootstrapping first randomly samples the active set from the pool and then iterates over: (i) training a classifier on the active set, (ii) testing of the classifier on the pool, and (iii) enlarging the active set with misclassified examples from the pool. This procedure stops when no more misclassified examples exist or when the performance stabilizes. The result is an augmented active set which is not sampled randomly but

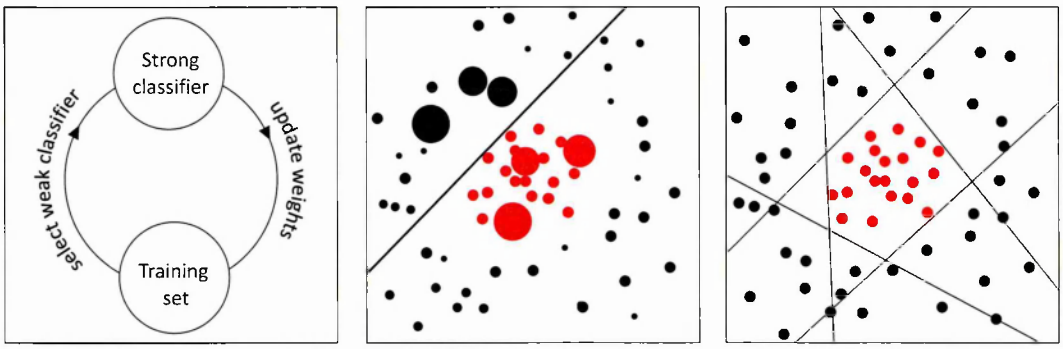

Figure 2.14: Boosting: a) the block diagram, b) a weak classifier and a weighted training set, c) a strong classifier.

with emphasis on the decision boundary. See figure 2.13 for illustration.

Relation to active learning. Bootstrapping is closely related to other methods such as Active Learning [Lewis 94]. Active Learning addresses a problem when a relatively small number of examples are labeled and a large number of examples are unlabeled. Learning starts by training a classifier from labeled examples. The classifier then evaluates the unlabeled set and those examples that are *not* confidently classified are labeled by a human annotator. In contrast, bootstrapping assumes that all training example are already annotated. One of the contributions of this thesis is the extension of bootstrapping for unlabeled data, which we call unsupervised bootstrap. The unsupervised bootstrap is discussed in chapter 5.

Bootstrapping in statistics. The definition of bootstrapping as described above is in line with the one considered in object detection [Sung 98, Papageorgiou 98, Rowley 98, Schneiderman 04, Viola 01], where it is typically used to handle large negative training sets. Notice that in statistics, bootstrapping refers to a set of re-sampling techniques used to measure statistical properties of estimators [Efron 93].

2.3.2 Boosting

Boosting [Freund 97] is a supervised learning strategy which aims to improve the performance of a weak classifier. The intuition behind boosting is: focus on the most difficult training examples. This is achieved by maintaining a distribution of example weights that represent the example's difficulty. This section briefly comments on the history of boosting, its relation to ensemble methods and links to bootstrapping.

Consider a labeled training set and a set of arbitrary weak classifiers. Boosting combines these weak classifiers into a strong classifier which performs better than any of the weak classifiers. Boosting is an iterative process which iterates over: (i) selection of the weak classifier that performs best on current distribution of weights, and (ii) the update of the distribution to emphasize misclassified examples. The set of weak classifiers selected in each round form the strong classifier. Boosting methods differ in the way the example weights are updated, which depends on a particular loss function. A common property of all of boosting methods is that a weak classifier selected in iteration k has 50% error in iteration $k+1$ which prevents it being selected again. The block diagram of boosting, a weak classifier and a strong classifier are illustrated in figure 2.14.

History. Boosting has been studied for two decades now. Schapire [Schapire 90] developed the first boosting procedure that could always improve the performance of a classifier by training two additional classifiers on modified versions of the training data. One year later, Freund [Freund 95] generalized the algorithm to combine an arbitrary number of weak classifiers. Both of these versions assume weak classifiers which have identical error rates. This assumption was dropped by the discrete AdaBoost [Freund 97] algorithm, which enabled to boost classifiers with arbitrary error rates. The strong classifier was defined as weighted majority vote. In a comparative study, Quinlan [Quinlan 96] observed that trees can be boosted into more accurate classifier if each node outputs a confidence value rather than a discrete class. Sub-

sequently, real AdaBoost [Schapire 98b] was proposed, which allowed the classifier to output confidences and achieved a significant improvement in classification over discrete AdaBoost.

Improvements of boosting. Early versions of Boosting [Schapire 90, Freund 95] used a stopping criterion for the number of combined weak classifiers to avoid over-fitting. However, practitioners observed [Schneiderman 04] that testing error keeps decreasing and then stabilizes when the boosting is not terminated. This phenomenon was explained by the "margin theory" [Schapire 98a]. Moreover, the performance of boosting was explained from statistical point of view [Friedman 00] as an additive logistic regression. Boosting algorithms are still evolving. Robustness to noisy data was addressed by BrownBoost [Freund 01] or LogitBoost [Friedman 00]. An online variant of boosting have been also proposed [Oza 05]. A comprehensive review of the methods can be found in [Schapire 02].

Relation to ensemble methods. Boosting has close links to other algorithms which internally maintain a set of weak classifiers and integrate their responses by majority voting, i.e. ensemble classifiers. The underlying assumption of these methods is that the classifiers make independent errors and therefore the majority voting improves their performance [Polikar 06]. The methods differ in the way the independence of the classifiers is achieved. Bagging [Breiman 96] uses sampling with repetition to form different training distributions. If the weak classifiers are trees, bagging becomes a Randomized Forrest [Breiman 01], which has been applied in computer vision to a number of problems [Amit 97, Lepetit 05, Shotton 08]. Apart from sampling with repetition, the classifier independence can be achieved by designing features which are likely to be independent such as in Randomized Ferns [Ozuysal 07]. A similar approach is used in our implementation.

Boosting and sliding-windows. Boosting has been developed for general machine learning problems. However, such algorithm may struggle in some practical scenarios such as face detection using a sliding window. In a typical image, the sliding-window

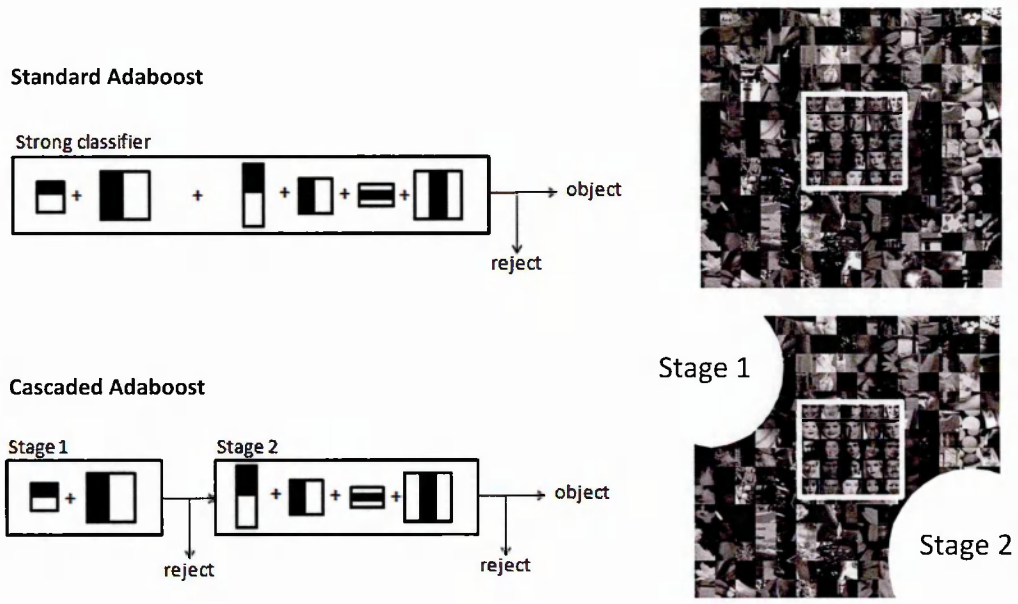

Figure 2.15: Standard AdaBoost versus cascaded AdaBoost: (TOP) standard AdaBoost has to evaluate all weak classifiers (here Haar-like filters), (BOTTOM) cascaded AdaBoost enables to reject negative examples after each stage of the classifier thus reducing the computation demands.

classifier is evaluated on thousands ($\approx 10^5$) of patches and only a small fraction of them (≈ 10) may depict the object of interest. It follows that the positive and negative classes are extremely asymmetric, i.e. majority of windows are negative. The classifier has to be therefore tuned toward precision (probability of false positive should be around $1/10^5$). Another consequence is that the negative class is virtually unlimited and it is not straightforward to maintain a distribution of weights on it.

Boosting and bootstrapping. Boosting has been first applied to object detection by Viola and Jones [Viola 01] with two important modifications: (i) a cascaded classifier, and (ii) bootstrapping. The standard AdaBoost classifier measures all weak classifiers in its ensemble and outputs a decision after that. Such a strategy is too slow and not even necessary for a sliding-window classifier. As noted earlier, the majority of patches

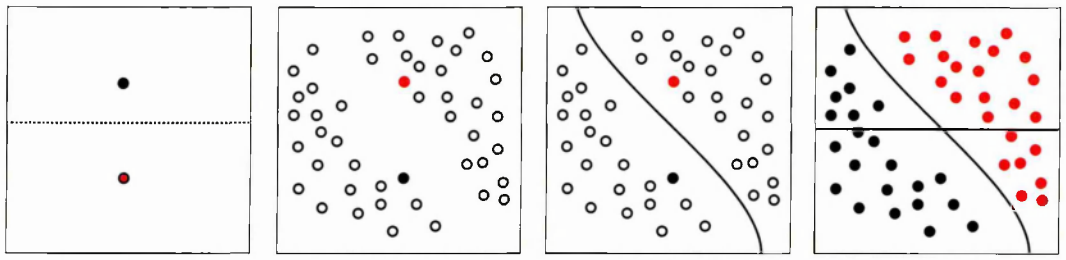

Figure 2.16: Can unlabeled data improve a classifier? Refer to the text for explanation.

in a typical image depict background. Therefore the classifier is split into stages, each of which rejects (classifies as negative) a subset of candidates before progressing to the next stage. This cascaded structure has a great impact on the classifier speed but also influences the quality of training. Standard training maintains only a distribution of weights and considers the training set as fixed. In contrast, training with a cascaded classifier involves resampling of the training set to better represent the examples close to the current decision boundary, which has direct links to bootstrapping [Sung 98].

2.3.3 Semi-supervised learning

This section reviews the semi-supervised learning methods, which, in addition to labeled examples, exploit unlabeled training examples.

A natural question is whether unlabeled data can help in training of a classifier. Consider the mind experiment illustrated in figure 2.16. The goal is to train a classifier in two settings: (i) from two labeled examples, and (ii) from the identical labeled examples and a collection of unlabeled examples. Given the labeled examples only, a number of supervised methods can be used to train a classifier. Figure 2.16 (a) illustrates the decision boundary of a classifier that maximizes the classification margin. If the labeled examples are augmented by unlabeled (b) several semi-supervised learning strategies can be used. One of the simplest is to perform clustering of the unlabeled examples and label each cluster by the corresponding labeled example within it. This

produces a decision boundary that is illustrated in (c). This classifier will make correct predictions as long as the clustering is aligned with the classification that is demanded (d). This example demonstrates that if the underlying distribution of unlabeled examples forms clusters that are aligned with the classification function to be learned, the unlabeled data can help when training a classifier. This property of unlabeled data, also referred to as the "cluster assumption", is often assumed by the semi-supervised learning algorithms [Chapelle 06]. A number of algorithms relying on similar assumptions have been proposed in the past including Expectation-Maximization, self-learning and co-training.

Expectation-Maximization (EM) is a generic method for finding estimates of model parameters given unlabeled data. EM is an iterative process, which in case of binary classification alternates over: (i) estimation of soft-labels of unlabeled data, and (ii) training a classifier exploiting the soft-labels. EM was successfully applied to document classification [Nigam 00] and learning of object categories [Fergus 03]. In the semi-supervised learning terminology, EM algorithm relies on the "low density separation" assumption [Chapelle 06], which means that the classes are well separated in the feature space. EM is sometimes interpreted as a "soft" version of Self-learning [Zhu 09].

Self-learning starts by training an initial classifier from a labeled training set, the classifier is then evaluated on the unlabeled data. The examples with the most confident classifier responses are added to the training set and the classifier is retrained. This is an iterative process. Self-learning has been applied to training of a human eye detector [Rosenberg 05]. However, it was observed that the detector improved more if the unlabeled data was selected by an independent measure rather than the classifier confidence. Rosenberg et al. suggested that the low density separation assumption is not satisfied for object detection and other approaches may work better.

Co-training [Blum 98] is a learning method built on the idea that independent classifiers can mutually train one another. To create such independent classifiers, co-training

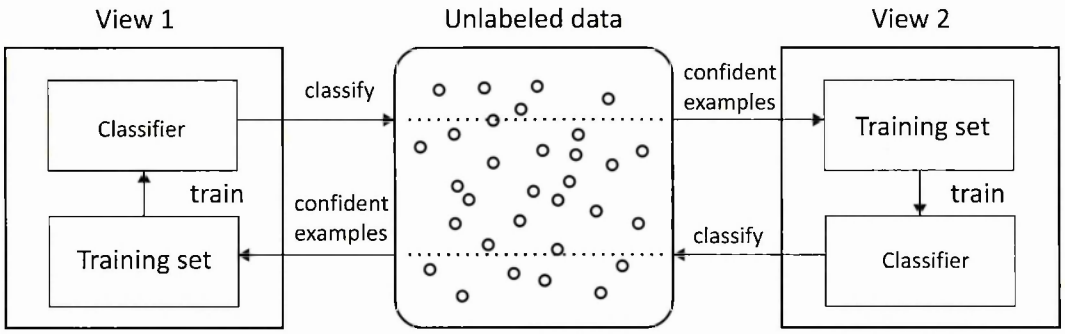

Figure 2.17: Illustration of co-training [Blum 98] of two classifiers.

assumes that two independent feature-spaces are available. See figure 2.17 for illustration of the process. The training is initialized by the training of two separate classifiers using the labeled examples. Both classifiers are then evaluated on unlabeled data. The confidently labeled samples from the first classifier are used to augment the training set of the second classifier and vice versa in an iterative process. Co-training works best for problems with independent modalities, e.g. text classification [Blum 98] (text and hyper-links) or biometric recognition systems [Poh 09] (appearance and voice). In visual object detection, co-training has been applied to car detection in surveillance [Levin 03] or moving object recognition [Javed 05]. We argue that co-training is not a good choice for object detections, since the examples (image patches) are sampled from a single modality. Features extracted from a single modality may be dependent and therefore violate the assumptions of co-training.

2.4 Observations

Tracking. We reviewed methods starting from the most basic approaches such as template tracking, up to complex trackers which define tracking as classification and update the classifier during tracking. Trackers are becoming increasingly complex to handle increasingly challenging environments and appearance changes. The assumption is that the object state in the previous frame is known. In unconstrained video, this assumption is violated and therefore any tracker eventually fails. The tracking failure will be investigated in chapter 3.

Detection. Object instance detection reached a level of maturity for scenarios where a sufficient number of training examples can be either generated or annotated. A cascaded architecture, or fast keypoint detectors enable tracking-by-detection, which overcomes the drift and initialization problems of contemporary trackers. The underlying assumption of object detectors is a separation of training and run-time phase. This limits their applicability to objects that can be modeled in advance. Methods that enable efficient online update of detectors have been proposed, but the problem how to update these detectors was not addressed.

Learning. We reviewed two classes of learning approaches for training of object detectors: supervised and semi-supervised. In the supervised setting the learning is often realized by boosting. However, the standard variants of boosting, do not perform well and have to be combined with bootstrapping to handle large training sets. Chapter 4 closely analyses this relationship between boosting and bootstrapping and proposes a unifying algorithm. In the semi-supervised setting we discussed several approaches popular in text classification, however in object detection the improvements are marginal. One of the reasons is that in object detection it is hard to find independent features that would efficiently drive the learning process. Chapter 5 discusses other information sources (spatio-temporal structure in data) that could be used for training an object detector.

Chapter 3

Tracking: failure detection

This chapter investigates long-term tracking from the perspective of frame-to-frame tracking. The starting point is the observation that any frame-to-frame tracker eventually fails, for instance, when the object moves out of the camera view. Therefore, the primary goal of this chapter is to estimate the reliability of a tracker and use it to detect the tracking failures. The secondary goal is to use the reliability measure to improve the frame-to-frame tracking itself.

The chapter is structured as follows. Section 3.1 focuses on point trackers and proposes a novel error measure that evaluates the reliability of arbitrarily long point trajectories. Section 3.2 develops a novel tracker called Median-Flow. The object is represented by a grid of points, which influence the estimated object motion based on their reliability. The Median-Flow tracker is comparatively evaluated with relevant approaches and superior performance is achieved. The chapter is concluded in section 3.3.

3.1 Detection of tracking failures

This section is concerned with the detection of tracking failures of point trackers, e.g. Lucas-Kanade tracker [Lucas 81]. These trackers build up a point trajectory from a

sequence of frame-to-frame displacements. Such trackers are: (i) prone to drift due to accumulation of localization errors, and (ii) likely to fail if the point suddenly changes appearance, becomes occluded or disappears from the camera view.

Our approach to failure detection is based on so called *forward-backward consistency assumption* that correct tracking should be independent of the direction of time-flow. Algorithmically, this assumption is exploited as follows. First, a tracker produces a trajectory by tracking a point *forward* in time. The trajectory has arbitrary length, and can be obtained by an arbitrary tracker. Second, the point location in the last frame of the forward trajectory initializes a validation trajectory. The validation trajectory is obtained by *backward* tracking. Third, the two trajectories are compared and if they differ significantly, the forward trajectory is considered as incorrect.

Figure 3.1 (TOP) illustrates the method when tracking a point between two images (trajectory of length one). Point no. 1 is visible in both images and the tracker is able to localize it correctly. Tracking this point forward or backward results in consistent trajectories. On the other hand, point no. 2 is not visible in the right image and the tracker localizes a different point. Backward-tracking of this point results in a different location than the original one. The corresponding forward and backward trajectories are significantly different in this case.

Related work. A commonly used approach to detect tracking failures is to compare consecutive point-centered patches using Sum of Square Differences (SSD) [Bouguet 99, Nickels 02]. High SSD means that the patches are dissimilar, which indicates tracking failure. This differential error indicates failures caused by occlusion or rapid movements, but does not detect slowly drifting trajectories. The detection of drift can be approached by defining an absolute error. A popular approach is to consider affine warps of the initial patch [Shi 94] and compare them to the current patch. Recently, a general method for assessing the tracking performance was proposed [Wu 07, Dowson 06], which is based on the "forward-backward" idea. The forward-backward consistency

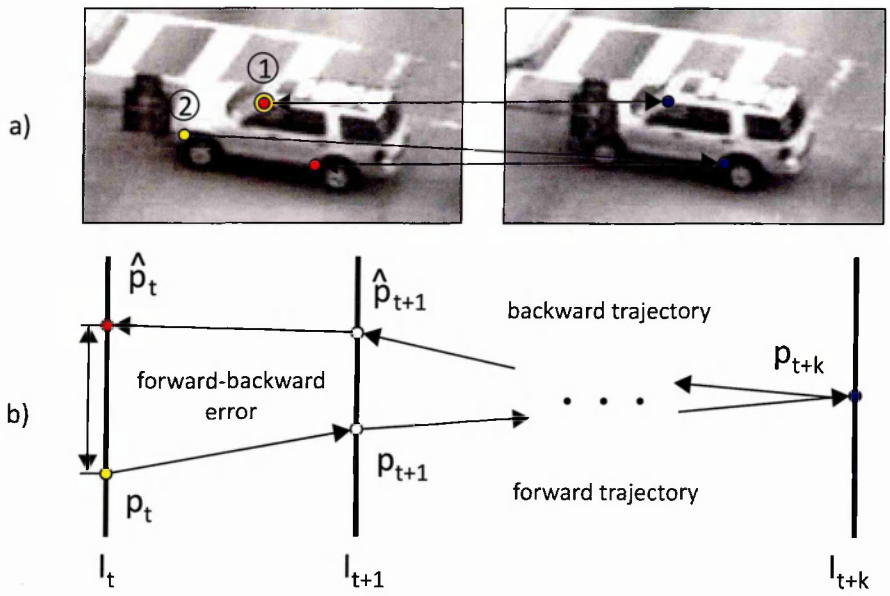

Figure 3.1: Illustration of the Forward-Backward error measure: (TOP) consistent (1) and inconsistent (2) trajectories, (BOTTOM) terms used for the definition of the Forward-Backward error measure.

was used to automatically evaluate the tracking performance without the need to define the ground truth manually. Improvement of the tracking performance based on the forward-backward consistency was not considered. Moreover, the idea of forward-backward consistency is often used wide-baseline matching [Strecha 03] or in optical flow estimation [Alvarez 07]. These methods typically consider a pair of images. In contrast, our approach defines the error for arbitrarily long point trajectories.

3.1.1 Forward-Backward error

This section defines the Forward-Backward (FB) error, see figure 3.1 (BOTTOM) for illustration. Let $(I_t, I_{t+1}..., I_{t+k})$ be an image sequence and p_t be a point location in time t. Using an arbitrary tracker, the point p_t is tracked forward for k steps. The resulting trajectory is $\overrightarrow{T}_k = (p_t, p_{t+1}, ..., p_{t+k})$. Our goal is to estimate the reliability of trajectory $\overrightarrow{T}_k$ given the image sequence. For this purpose, the validation trajectory

is constructed. Point p_{t+k} is tracked *backward* up to the first frame and produces the backward trajectory $\overleftarrow{T}_k = (\hat{p}_t, \hat{p}_{t+1}, ..., \hat{p}_{t+k})$, where $\hat{p}_{t+k} = p_{t+k}$.

The FB error of the forward trajectory given the image sequence is defined as the distance between the forward and the backward trajectory:

$$\mathrm{FB}(\overrightarrow{T}_k | I_t, I_{t+1}..., I_{t+k}) = \mathrm{distance}(\overrightarrow{T}_k, \overleftarrow{T}_k).$$

In our implementation, we use the Euclidean distance between the initial point of the forward trajectory and the end point of the backward trajectory:

$$\mathrm{distance}(\overrightarrow{T}_k, \overleftarrow{T}_k) = ||p_t - \hat{p}_t||.$$

It was observed that distance functions that measure average or maximal distance between trajectories lead to similar performance but are more expensive. On the other hand, distance functions that measure minimal or median distance between the trajectories did not perform well.

The Forward-Backward error provides a real value. Higher values indicate the forward-backward inconsistency and possibility of tracking failures. The hard decision whether the tracker failed is done by a thresholding.

3.1.2 Quantitative evaluation

This experiment quantitatively evaluates the ability of FB and SSD to identify correctly tracked points (inliers) between two frames. One hundred images depicting scenes of nature were warped by random affine transformations and Gaussian noise was added. This process resulted in a set of one hundred image pairs. In the original images, a set of points was initialized on a regular grid. Two types of displacements of these points were then established: (i) ground truth displacements were obtained by projecting the points to the warped images, and (ii) estimated displacements were obtained by tracking the points using Lucas-Kanade tracker [Lucas 81] to the warped images.

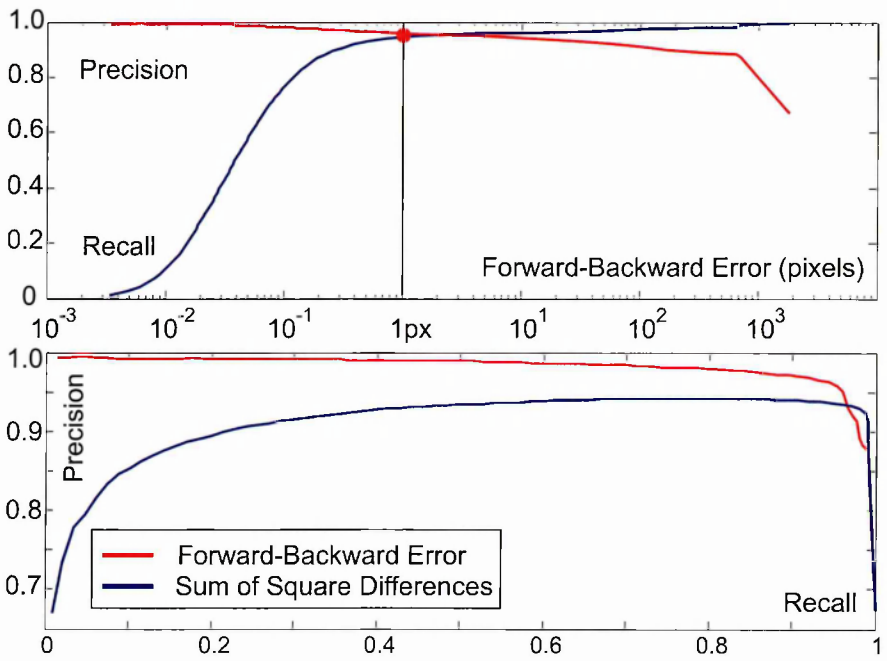

Figure 3.2: Quantitative evaluation of the Forward-Backward error for $k = 1$. (TOP) Precision and recall as a function of threshold θ. (BOTTOM) Precision and recall characteristics in comparison to Sum of Square Differences.

The estimated displacements that ended up closer than 2 pixels from the ground truth were labeled as inliers. We selected the threshold of 2 pixels since Lucas-Kanade does not estimate affine deformation and with too tight threshold, the majority of points would be classified as outliers. By setting the threshold to 2 pixels we are interested in recognition of catastrophic tracking failures. Affine deformation and the Gaussian noise are used as approximations of real variations of the point appearance.

Using the 2 pixel threshold, the inliers represented approximately 65% of all displacements. The estimated displacements were then evaluated by a failure detection measure (FB, SSD), displacements with error below θ were classified as inliers. A correct classification of an inlier is denoted as a true positive (TP), an incorrect classification is denoted as false positive (FP). The quality of the error measures is accessed using precision and recall statistics, which are both function of threshold θ:

$$\text{precision} = \frac{\text{TP}}{\text{TP} + \text{FP}}, \quad \text{recall} = \frac{\text{TP}}{\#\text{inliers}}.$$

Figure 3.2 (TOP) shows the resulting performance of the FB error as a function of the threshold θ. The figure illustrates that the proposed FB error is able to reliably recognize majority of inliers at high precision level. Notice for instance the working point indicated by the red dot. For $\theta = 1$ pixel, the recall is of 95% and precision of 96%. Figure 3.2 (BOTTOM) shows the corresponding precision and recall curves for FB in comparison to SSD. FB outperforms SSD for majority of working points. SSD was unable to detect inliers for small thresholds, its precision starts below 70% (notice that random guessing would start around 65%).

3.1.3 Visualization

This sub-section visualizes the proposed Forward-Backward error for long point trajectories. Given a video sequence, every pixel in the first frame initializes a point trajectory. Every point is tracked forward up to the last frame and then backward up

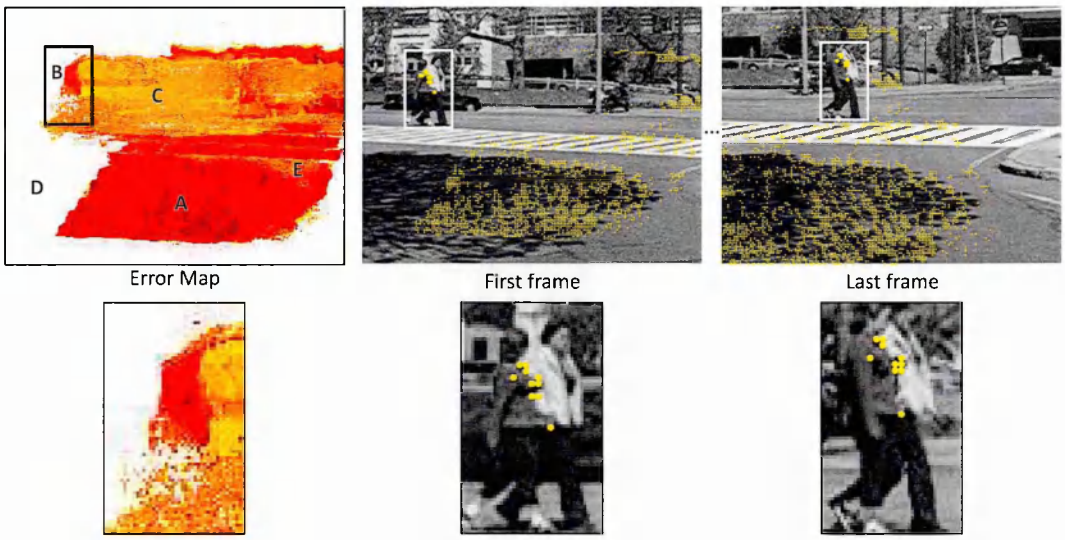

Figure 3.3: Error map: visualization of the Forward-Backward error for $k = 50$. Dark colors in the error map indicate low Forward-Backward error that considers 50 frames. Yellow points in the original frames indicate 5% of the most reliable points. Points on the pedestrians are enlarged for better visibility.

to the first one. Each pixel is then assigned the corresponding Forward-Backward error. The resulting image is called the *error map* and indicates the reliability of the corresponding point-trajectories.

The error map has been constructed for a sequence of 50 frames, with a moving camera following two pedestrians (sequence PEDESTRIAN 1). The figure 3.3 shows the error map as well as the first and the last frame of the sequence. The error map encodes the pixel reliability by colors. Dark colors indicate low FB error: shadow cast by tree branches (a), upper bodies of two pedestrians (b). Any point selected from these "reliable" areas is tracked accurately in the whole sequence. Brighter colors indicate areas which were evaluated as not reliable. These areas may become occluded (c), disappear from the camera view (d) or lack enough texture (e). The first and the last frame also depict the 5% of the most reliable pixels. Notice that these points correspond to identical physical points, which is best visible in the zoomed-in versions.

Application. The error map can be used to detect key-points that can be tracked reliably throughout the entire video. This is in contrast to traditional key-point detectors [Shi 94, Rosten 06], which localize the key-points based on a single frame only and therefore cannot guarantee that the point will be reliably tracked. Moreover, it has been observed [Jepson 03] that tracker performance increases if the tracker focuses on reliably tracked parts of a template. The Forward-Backward error allows identification of such parts. This aspect will be studied in the following section.

3.2 Median-Flow tracker

The aim of this section is to use the proposed Forward-Backward error to build a better bounding box-based tracker. The basic approach is to estimate the bounding box motion using a large number of independent points, measure their reliability and integrate the predictions using a robust statistic. Using this approach, we aim at a tracker that is robust to partial occlusions, is fast and efficient.

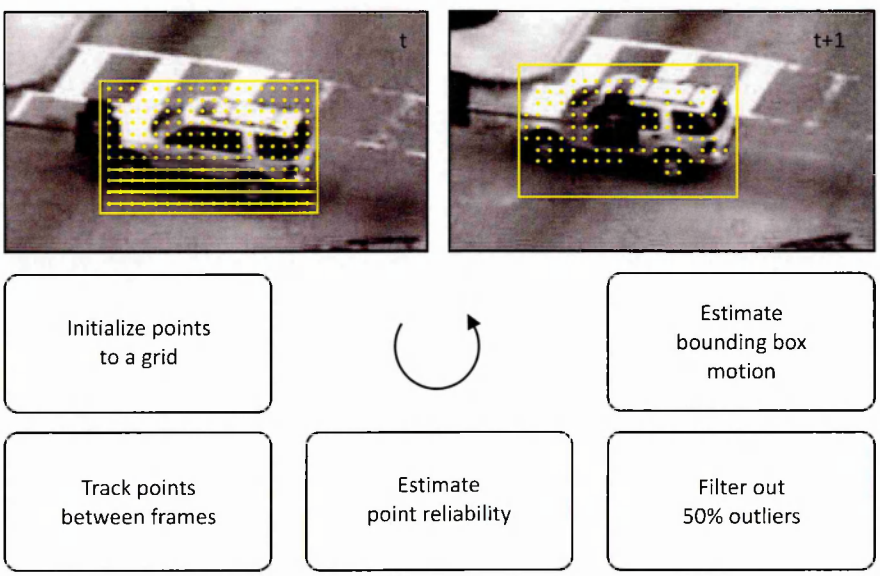

Figure 3.4: The block diagram of the Median-Flow tracker.

The block diagram of the proposed tracker is shown in figure 3.4. The tracker accepts

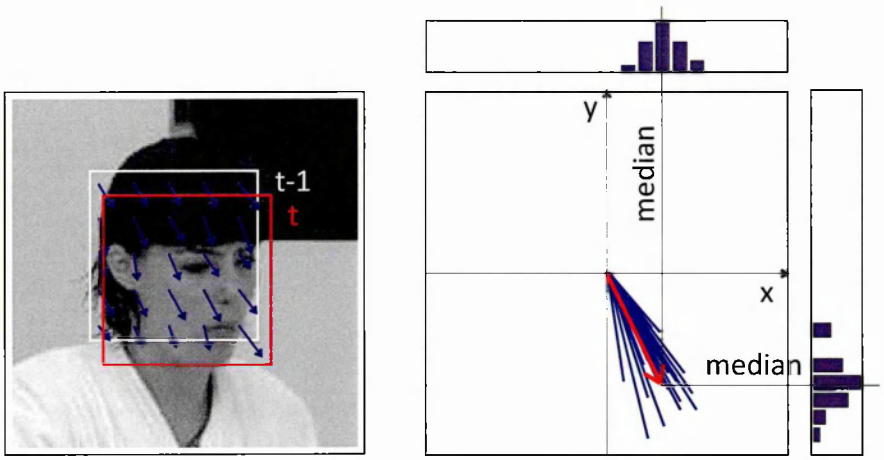

Figure 3.5: Estimation of the object motion using median. Only translation is illustrated, Median-Flow estimates scale as well.

a pair of images I_t, I_{t+1} and a bounding box b_t and outputs the bounding box b_{t+1}. A set of points is initialized on a rectangular grid within the bounding box b_t. These points are tracked by Lucas-Kanade tracker from I_t to I_{t+1}. The quality of the point displacements is then estimated and each point is assigned an error (e.g. FB, SSD or NCC). 50% of the worst predictions is filtered out. The remaining predictions estimate the bounding box motion using median. We refer to this tracker as Median-Flow.

Estimation of the motion by median. The bounding box motion is parameterized by horizontal displacement, vertical displacement and scale change. All three parameters are estimated independently using the median. Figure 3.5 illustrates the estimation of the displacements. The scale change is estimated as follows: for each pair of points, a ratio between current point distance and previous point distance is computed. The bounding box scale change is defined as the median over these ratios.

Median-Flow tracker is related to Flock of Features [Kolsch 04] but differs in several aspects. Flock of Features re-initializes the points only if they are too close to each other or if the point is too far from median. In contrast, Median-Flow re-initializes all points in every frame and therefore the points are always kept on a rectangular grid.

This allows Median-Flow to estimate scale of the object, which is by the Flock of Features not done. Moreover, Flock of Features requires color and has been applied to tracking of hands only.

Median-Flow re-initializes the point locations in every frame. This restricts the error measures that estimate the reliability of the points. In particular, the Forward-Backward error can consider only a pair of frames, which corresponds to $k = 1$. Larger k can not be applied as there are no point trajectories with length $k > 1$.

3.2.1 Quantitative evaluation

A number of variants of the Median-Flow (MF) tracker were tested. The baseline tracker MF_0 estimates the bounding box displacement based on all points on the grid. Trackers $\mathrm{MF}_{\mathrm{FB}}, \mathrm{MF}_{\mathrm{NCC}}, \mathrm{MF}_{\mathrm{SSD}}$ estimate the point reliability using FB, NCC and SSD, respectively. FB performs one backward prediction, NCC and SSD compare consecutive point-centered patches. 50% of the worst points are filtered out. Tracker $\mathrm{MF}_{\mathrm{FB+NCC}}$ combines FB and NCC, each error measure independently filters out 50% of the worst points. These trackers were compared with the following approaches: Incremental Visual Tracking (IVT) [Ross 07], Online Discriminative Features (ODF) [Collins 05], Ensemble Tracking (ET) [Avidan 07] and Multiple Instance Learning (MIL) [Babenko 09]. The evaluation was performed on 6 video sequences from [Yu 08]. The sequences contain appearance changes, fast motion, and partial occlusion and in some cases the object disappears from the camera view and later reappears. The sequences are described in detail in Appendix B.

Evaluation protocol. The objects were manually initialized in the first frame and tracked up to the end of the sequence. The trajectory was considered correct if the bounding box overlap with ground truth was larger than 50%. The overlap was defined as a ratio between intersection and union of two bounding boxes. Performance was assessed as the maximal frame number up to which the tracker was correct.

Sequence	Frames	IVT [Ross 07]	ODF [Collins 05]	ET [Avidan 07]	MIL [Babenko 09]	MF_0	MF_{FB}	MF_{NCC}	MF_{SSD}	MF_{FB+NCC}
David	761	17	n/a	94	135	93	761	144	28	**761**
Jumping	313	75	313	44	313	36	76	87	79	170
Pedestrian 1	140	11	6	22	101	15	37	40	12	**140**
Pedestrian 2	338	33	8	118	37	97	97	97	97	97
Pedestrian 3	184	50	5	53	49	52	52	52	52	52
Car	945	163	n/a	10	45	248	510	394	353	**510**
Best	n/a	0	1	2	1	0	2	0	0	3

Table 3.1: Comparison of the Median-Flow tracker with state-of-the-art approaches in terms of the number of correctly tracked frames.

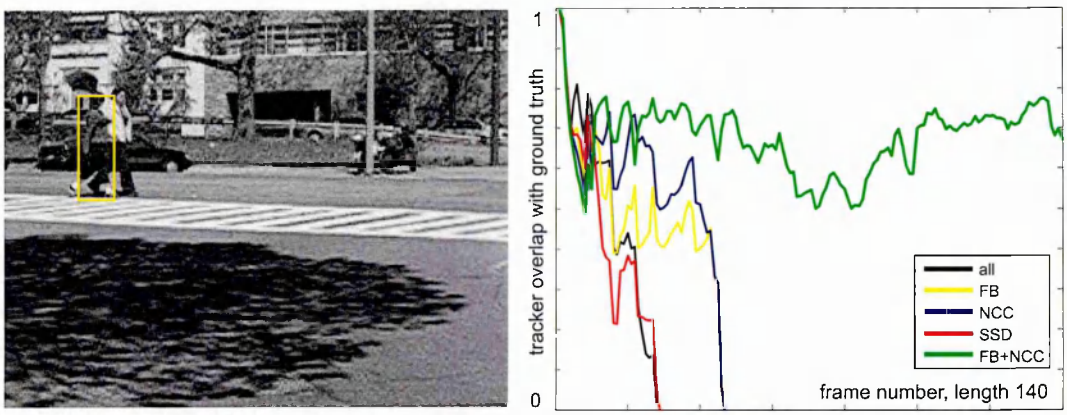

Figure 3.6: Comparison of various variants of the Median-Flow tracker.

Table 3.1 shows the quantitative results for all sequences. The last row shows the number of times the particular algorithm performed best. The best results were obtained by the Median-Flow based on a combination of FB and NCC error. This tracker was able to score best three times.

Figure 3.6 shows the bounding box overlap with the ground truth as a function of time for several variants of the Median-Flow tracker. The baseline T_0 tracker as well as T_{SSD} loose the object quickly after initialization (overlap goes to zero). T_{FB} and T_{NCC} perform better and are able to follow the object for twice as long than the baseline method. T_{FB+NCC} dominates and is able to track the target throughout entire sequence. This result shows partial complementarity of FB and NCC.

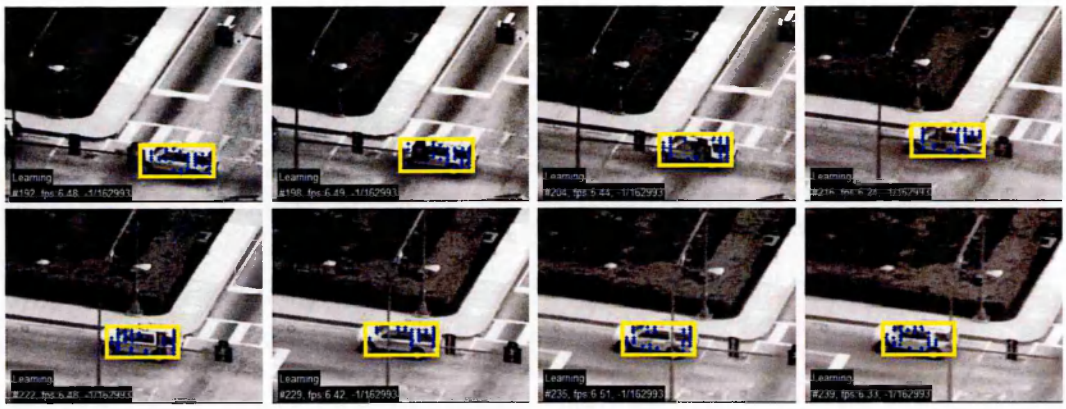

Figure 3.7: Several frames from the sequence CAR overlaid with the output of the Median-Flow tracker (yellow) and 50% of the most reliable points (blue). Notice that the points are covering the visible parts of the tracked object. The points that cover occluded or low-textured parts of the object are automatically filtered out by the Forward-Backward error.

Figure 3.7 shows several frames from the sequence CAR overlaid with the output of the Median-Flow tracker (yellow bounding box) and the 50% of the most reliable points estimated by the combined FB + NCC error measures (blue dots). The car is tracked across a partial occlusion caused by a traffic light. Notice, that the selected points are typicallyBut covering visible, well textured parts of the car, while the occluded parts are filtered out.

3.3 Conclusions

This chapter was concerned with frame-to-frame tracking in unconstrained video sequences and focused on detection of tracking failures. We confirmed two ideas that appeared in tracking literature already: (i) forward-backward consistency assumption can be used to measure tracker's reliability [Wu 07], (ii) frame-by-frame tracking can be improved by focusing on reliable parts [Jepson 03].

First, we proposed a novel measure, Forward-Backward error, which evaluates reliability of arbitrarily long trajectories. The benefits of the measure and complementarity to appearance-based SSD were shown. Second, we developed a novel frame-to-frame tracker, Median-Flow, which internally estimate reliability of its components. We showed that the Median-Flow works best when the reliability is estimated using combined FB and NCC errors. Superior performance in comparison to state-of-the-art trackers was demonstrated on several sequences.

Like any other frame-to-frame tracker, Median-Flow eventually fails. This is apparent in table 3.1 (sequences JUMPING, PEDESTRIAN 2 and PEDESTRIAN 3) where all tested trackers failed due to full occlusion or disappearance of the tracked object. This shows that the frame-to-frame tracking has its limitations and a different model has to be developed in order to handle such sequences. In particular, detection based approaches consider every frame as independent and therefore can handle full occlusions. This approach will be investigated in the following chapter.

Chapter 4

Detection: supervised bootstrap

This chapter investigates long-term tracking from the perspective of object detection. For a large number of tracking scenarios, the *visual class* of the object of interest is known. It is therefore possible to train an object class detector in advance and integrate it into the tracking process. This approach has been successfully applied to a variety of scenarios including tracking of human faces [Li 07], pedestrians [Leibe 07] or ice-hockey players [Okuma 04]. If the information about the object class is available, a long-term tracker should be able to use it. Therefore, our goal is to develop a method for offline learning of object class detectors.

The chapter is organized as follows. In section 4.1 we introduce the problem of large-scale learning of object detectors. Section 4.2 reviews the related work with the focus on two most popular training approaches: boosting [Freund 97] and bootstrapping [Sung 98]. Section 4.3 develops a novel learning method that integrates boosting and bootstrapping optimally. A number of experiments show the properties of the learning method. Section 4.4 applies the learning method to the training of a face detector and state-of-the-art performance is achieved. The chapter is concluded in section 4.5.

4.1 Introduction

Consider a class of detectors that are based on a scanning window and binary classification of image patches [Viola 01]. The crucial problem of these detectors is to train the binary classifier that covers all appearances of the object and discriminates from arbitrary background clutter. Efficient processing of large data sets that cover all the variations is an important problem.

With the information available on the Internet, it is possible to acquire *pools* of training data of virtually unlimited sizes. Large pools sideline the problems related to classifier generalization [Vapnik 98]. Hoverer, due to computational limitations and training complexity, it is rarely the case that the entire pool can be processed at once. As we have reviewed in sub-section 2.3.1, one possible solution is to use bootstrapping and train the classifier iteratively using an *active set* that focuses on the decision boundary only. In object detection, bootstrapping is often combined with boosting [Viola 01, Fleuret 08]. The combination is, however, often ad hoc [Sochman 05], which presents scope for improvements.

Contributions. The main contribution this chapter is the optimal integration of bootstrapping with boosting, where the bootstrapping is formalized as a weighted sampling strategy. We build on the weighted sampling approach [Fleuret 08] and propose a generalized strategy based on *Quasi-random Weighted Sampling + Trimming* (QWS+) that optimally combines its components in order to minimize the variance of hypothesis error in each round of boosting. The QWS+ sampling method is applied to face detection and leads to a significant increase in the classification performance as well as the training efficiency on large pools of data.

4.2 Related work

In object detection, bootstrapping has been used to train a Gaussian mixture model [Sung 98]. In every round of training, the active set was *extended* by examples misclassified in previous round and the entire classifier was retrained. The same approach was applied to refine the decision surface of an SVM classifier [Papageorgiou 98, Dalal 05], to train the neural network [Rowley 98], or to estimate the histograms of Wavelet coefficients [Schneiderman 04].

Viola and Jones [Viola 01] proposed a cascaded classifier composed of a sequence of stages. A bootstrapping strategy based on *re-sampling* of the undecided parts of the pool was used. Many authors followed this approach [Levi 04, Jones 03, Laptev 06]. A number of improvements have been proposed for the classical Viola-Jones cascade. For example, the standard cascade ignores the confidence which is output from each stage thus making the classifier unnecessarily long. This drawback was addressed in [Sochman 05, Wu 04, Xiao 03] where bootstrapping based on (random) *re-sampling* and *re-weighting* of the selected samples according to the confidence was used. Later on, Fleuret and Geman [Fleuret 08] proposed *weighted sampling*. Instead of weighting examples in the active set, examples were sampled with replacement from the pool with respect to their weights. The approach let to improved classifier performance. In machine learning literature, Friedman et al. [Friedman 00] proposed *trimming*, a technique that selects only a fraction of examples with the highest weights resulting in an improvement in training speed.

4.3 Integration of bootstrapping and boosting

This section formalizes the combination of boosting and bootstrapping. The analysis will be performed on AdaBoost formulated as a logistic regression [Friedman 00], but the proposed method is applicable to other boosting methods as well. The bootstrap-

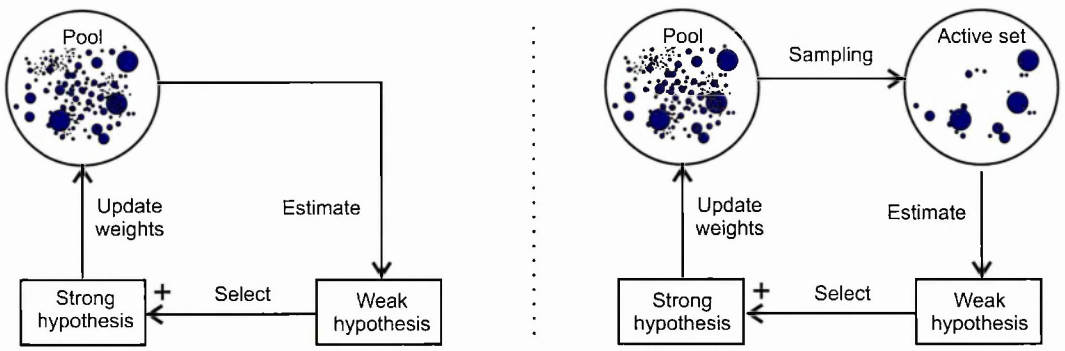

Figure 4.1: Illustration of standard boosting (LEFT) and boosting combined with bootstrapping (RIGHT).

ping will be formulated as a sampling strategy. Next, we present the commonly used approaches within our framework and develop two novel strategies, one of which is optimal. All strategies will be evaluated on several different experiments.

Let $L = \{(x_1, y_1), \ldots, (x_m, y_m)\}$ be a labeled training set where each *example* x_i belongs to an *example space* $\mathcal{X}$, and each *label* y_i belongs to a finite *label space* $\mathcal{Y} = \{-1, 1\}$. This labeled set represent all training data available and will be called the *pool*. Given this input, AdaBoost builds a *strong hypothesis* $H : \mathcal{X} \to \mathbb{R}$ which has the form of $H(x) = \sum_{j=1}^{T} h_j(x)$ where each $h_j(x)$ is a *weak hypothesis*. The sign of $H(x)$ gives the classification, and $|H(x)|$ measure of prediction confidence.

The strong hypothesis is built iteratively. During training, AdaBoost maintains a distribution of weights $D = \{d_i\}$ satisfying $\sum_{i=1}^{m} d_i = 1$ giving higher weights to examples that are "difficult". In each iteration, AdaBoost selects a hypothesis that performs best on current distribution of weights, adds this hypothesis to the strong hypothesis and updates the distribution so that the currently selected hypothesis performs worst in the next round. See figure 4.1 (LEFT) for illustration of the boosting process.

Boosting assumes access to a set of weak classifiers, each of which splits the example space into a number of partitions. For each classifier, AdaBoost estimates a hypothesis

of the form

$$h(x) = \frac{1}{2}\log\frac{\mathbf{P}_D(y=1|x)}{1-\mathbf{P}_D(y=1|x)}, \tag{4.1}$$

where $\mathbf{P}_D(y=1|x)$ is a probability estimated using current distribution of weights d_i. Boosting then selects the optimal hypothesis h^* that minimizes

$$h^* = \arg\min_h Z_D(h) = \arg\min_h \sum_{i=1}^{m} d_i e^{-y_i h(x_i)}, \tag{4.2}$$

where $Z_D(h)$ is the *exponential loss* function. Once such a hypothesis is selected, AdaBoost updates the weights using $d_i \leftarrow d_i e^{-y_i h^*(x_i)}$ and normalizes them to a distribution.

Bootstrapping as a sampling strategy

Standard AdaBoost is not designed for large pools, and therefore, if m is large, the steps 4.1 and 4.2 may be too time consuming or even not feasible. Therefore, some form of approximation is needed. Bootstrapping is a process that approximates the pool of size m by an active set of size n, where $n \ll m$. The hypothesis estimation as well as the selection of the best hypothesis is then performed considering the active set only. The crucial question is how to approximate the pool correctly. We address this question by introducing the so-called *sampling strategy*, which is a process that takes the distribution of weights D of size m and approximates it by a distribution $\hat{D}$ where at most n elements have non-zero value. The approximated distribution must satisfy $\sum_{i=1}^{m} \hat{d}_i = 1$. Notice that in general, $d_i \neq \hat{d}_i$ since both of these weights have to sum-up to one.

Every realization of the sampling strategy results in a different distribution $\hat{D}$ and thus different weights $\hat{d}_i$. It follows that $\hat{d}_i$ is a random variable with expectation $\mathrm{E}[\hat{d}_i]$ and variance $\mathrm{Var}[\hat{d}_i]$. If $\mathrm{E}[\hat{d}_i] = d_i$ we consider the estimated weights unbiased. Suppose we have a hypothesis h with a corresponding exponential loss of $Z_D(h)$ on distribution D. When bootstrap is employed, this value is estimated on the active set $\hat{D}$ according to the following equation:

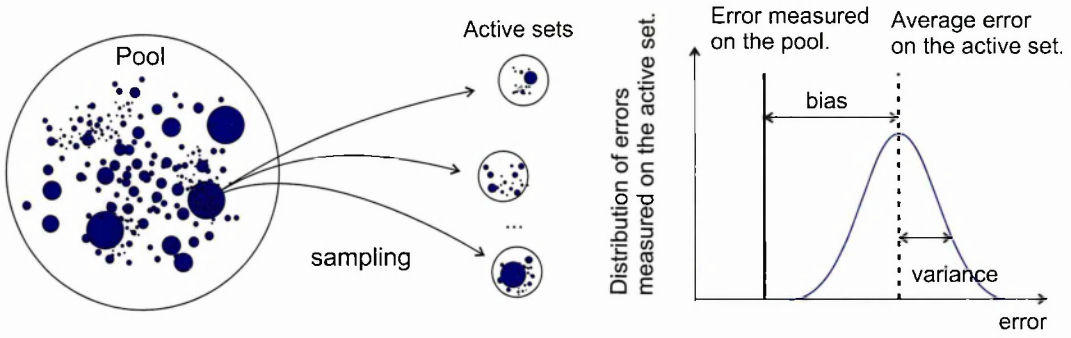

Figure 4.2: Illustration of bias and variance of a bootstrapping strategy.

$$Z_{\hat{D}}(h) = \sum_{i=1}^{m} \hat{d}_i e^{-y_i h(x_i)} \tag{4.3}$$

where the estimated weights are linearly combined by the constant coefficients $e^{-y_i h(x_i)}$. Therefore, if the estimated weights $\hat{d}_i$ are unbiased then the estimated exponential loss is unbiased as well. If $\mathrm{E}[Z_{\hat{D}}(h)] = Z_D(h)$ then the entire strategy is unbiased. $\mathrm{Var}[Z_{\hat{D}}(h)]$ will be referred to as a *variance of error estimate*. The terms bias and variance are illustrated in figure 4.2.

Conditions for the optimal sampling strategy. Our objective is to find the sampling strategy that selects n unique samples out of the pool of size m, is unbiased and with minimal variance of error estimate. Such strategy would guarantee that the approximate hypothesis $\hat{h}$ is as close as possible to the optimal one h^*, which would be trained on the entire pool.

4.3.1 Known sampling strategies

Several bootstrapping strategies have been used in the context of object detection. Here we formalize the most popular approaches within our notation.

Trimming (Tr). This technique selects n samples from the pool with the highest weights. The weights of the selected samples are then normalized so that $\sum_i \hat{d}_i = 1$. This strategy was introduced in [Friedman 00], where n was set so that a predefined fraction $(90 - 99\%)$ of the total weight mass was used for training. If $n < m$ then the weights are biased $\mathrm{E}[\hat{d}_i] \neq d_i$ with zero variance.

Unique Uniform Sampling (UUS). This strategy selects n unique samples from the pool with a probability of selecting sample i equal to $\mathrm{P}(i) = \frac{1}{m}$. The weights of the selected samples are then normalized so that $\sum_i \hat{d}_i = 1$. The estimated weights are in general biased (due to normalization) and have high variance since it is likely to disregard examples that carry significant mass of the distribution. Despite this it is often used in practice [Sochman 05, Wu 04, Xiao 03].

Weighted Sampling (WS). Selects n samples with replacement from the pool. Sample i is selected with probability $\mathrm{P}(i) = d_i$ and assigned weight $\hat{d}_i = \frac{1}{n}$. WS is unbiased, since $\mathrm{E}[\hat{d}_i] = \frac{Nd_i}{n} = d_i$. Possible implementation: the example weights are represented as intervals arranged on a unit line segment. Next we generate n random points on this line segments the positions of which determine the index of the selected sample. Since the example weight are approximated by repeated selection of the sample, this strategy does not guarantee n unique samples in the active set. This strategy was first used in the context of boosting in [Fleuret 08].

4.3.2 Proposed sampling strategies

In this section, we propose new sampling strategies based on WS. These strategies are designed to reduce the variance of error estimate by quasi-random sampling and guarantee selection of n unique samples in the active set.

Quasi-random Weighted Sampling (QWS). QWS reduces variance of the error estimate by pseudo-random sampling [Press 92]. The weights are represented as intervals and arranged to a unit line segment. The line segment is split into n equal intervals. Within each interval, one random number is generated, the position of which determines the index of the selected sample. This process maintains the weights unbiased but significantly reduces their variance. Intuitively, each sample can be selected at most p-times, where p is number of intervals the sample is covering. For standard WS, each sample can be selected at most n-times. Since $p \ll n$, QWS significantly reduces the variance of the estimated weights. However, QWS selects an unknown number of unique samples, which may lead to ineficient usage of available memory.

Quasi-random Weighted Sampling + Trimming (QWS+). The QWS+ is a generalization of Trimming and QWS, parameterized by k, the number of samples with largest weights in the pool that are always selected (trimmed). For $k = n$, QWS+ coincides with trimming. For $k = 0$, QWS+ becomes a QWS. For any $0 \leq k < n$, the QWS+ strategy is unbiased, since weighted sampling is unbiased and calculations of exponential loss on the trimmed set is exact. Parameter k is set to minimize the variance of the error estimate.

Intuitively, QWS+ selects k most dominant samples that would be selected by QWS with probability at least 50% and assigns them their own weights. The remaining weight mass is distributed amongst the remaining $l = n - k$ samples selected by QWS. Trimming of the most dominant samples reduces the variance of their estimated weight and hence the variance of the entire distribution.

In the following theorem, we show the optimal setting of the parameter k. We use the following notation. Index in parenthesis denotes sample with (i)-th largest weight. $S = \{X, D\}$ represents the pool augmented with the distribution of weights that shall be called the *weighted pool*. S_k is the weighted pool without k samples with largest weights, $D_k = 1 - \sum_{i=1}^{k} d_{(i)}$ is the weight mass of S_k, and $Z_{\text{QWS+}}(S, h)$ is the ex-

ponential loss of hypothesis h on weighted pool S when approximated by sampling strategy QWS+.

Theorem: The optimal size of trimming is the largest k that satisfies the condition $\frac{1}{l} \leq \frac{d_{(k)}}{D_k}(2 + \frac{d_{(k)}}{D_k})$, if variance of exponential loss of h changes "slowly" (defined below).

Proof: First, we express the exponential loss of QWS+ strategy as two components (trimming and weighted sampling) parameterized by k:

$$Z_{\text{QWS+}}(S, h) = \sum_{i=1}^{k} d_{(i)} e^{-y_{(i)} h(x_{(i)})} + Z_{\text{QWS}}(S_k, h) \tag{4.4}$$

$$\approx \sum_{i=1}^{k} d_{(i)} e^{-y_{(i)} h(x_{(i)})} + Z_{\text{WS}}(S_k, h). \tag{4.5}$$

We assume that $Z_{\text{QWS}}(S_k, h) \approx Z_{\text{WS}}(S_k, h)$ which results in simplified analysis. The difference between sampling with and without replacement is in this case small since all k dominant samples were already removed by trimming.

Weighted sampling selects $l = n - k$ samples with replacement from S_k. Sample i is selected with probability $P(i) = \frac{d_i}{D_k}$ and assigned weight $\hat{d}_i = \frac{D_k}{l}$. The random variable Z_{WS} is thus a re-scaled sum of l random variables corresponding to each sample:

$$Z_{\text{WS}} = \frac{D_k}{l} \sum_{s=1}^{l} Z_{\text{WS}}^s, \tag{4.6}$$

where random variables Z_{WS}^s attain the value $e^{-y_{i(s)} h(x_{i(s)})}$ with probability $\frac{d_{i(s)}}{D_k}$, $i(s)$ is the index chosen in step s.

Next, we express the variance of the exponential loss. From equation 4.5 we can see that variance of $Z_{\text{QWS+}}$ can be approximated by the variance of Z_{WS} since a trimming

has variance equal to zero. Variance of Z_{WS} is further substituted from equation 4.6 yielding the form:

$$\text{Var}[Z_{\text{QWS+}}] \approx \text{Var}[Z_{\text{WS}}] = \text{Var}[\frac{D_k}{l}\sum_{s=1}^{l} Z^s_{\text{WS}}] = \frac{D_k^2}{l}\sum_{s=1}^{l}\text{Var}[Z^s_{\text{WS}}]. \tag{4.7}$$

After substituting $\sum_{s=1}^{1}\text{Var}[Z^s_{\text{WS}}]$ with c_k, we obtain a simplified equation

$$\text{Var}[Z_{\text{QWS+}}] \approx \frac{D_k^2}{l}c_k. \tag{4.8}$$

Our goal is now to find conditions for k that minimize the variance. We assume that c_k changes slowly as a function of k, i.e. $\frac{c_k}{c_{k-1}} \approx 1$. For interesting cases, where the number of training examples is large and the dominant weights are already removed by trimming, is this condition satisfied. In the following, we express the optimality condition that variance of exponential loss for k must be smaller than for $k-1$:

$$\begin{aligned}
\frac{D_k^2}{l}c_k &\leq \frac{D_{k-1}^2}{l+1}c_{k-1} = \frac{(D_k + d_{(k)})^2}{l+1}c_{k-1}\,, \quad \frac{c_k}{c_{k-1}} \approx 1 \\
\frac{l+1}{l} &\leq \frac{(D_k + d_{(k)})^2}{D_k^2} \qquad (4.9) \\
\frac{1}{l} &\leq \frac{d_{(k)}}{D_k}(2 + \frac{d_{(k)}}{D_k}) \approx \frac{2d_{(k)}}{D_k}, \qquad (4.10)
\end{aligned}$$

which concludes the proof. In practice, the optimal k is found iteratively. Samples are trimmed until the equation 4.10 is satisfied.

4.3.3 Properties of sampling strategies

This sub-section comparatively evaluates the existing and proposed sampling strategies on synthetic data. In particular, the impact of the sampling strategy on the bias and variance is investigated.

Estimation of weights. This experiment visualizes the estimation of weights for the discussed strategies. A pool of size $m = 15$ with randomly assigned weights d_i was

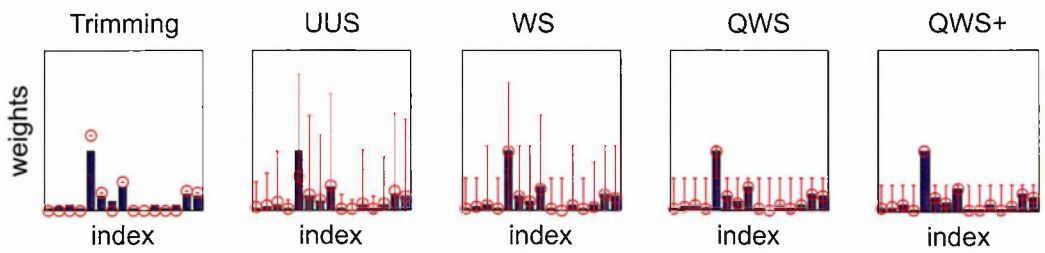

Figure 4.3: Pool with weights d_i (blue bars) is repeatedly sampled to obtain a distribution of the estimated weights. The range of the distribution (1 and 99% quantiles) is depicted by red vertical lines and expected values by circles.

randomly generated. The active set of size $n = 5$ was sampled 1000 times, each realization outputs a set of estimated weights $\hat{d}_i$. For each estimated weight and strategy, the expected value and the variance was computed as shown in figure 4.3. The circles in the figure denote the expectation of the estimated weight. The variance of the estimated weights is depicted by the red error bars. Notice that the expectation of Trimming and UUS is biased, the remaining strategies are not. Note the reduction of variance by Quasi-random Weighted Sampling strategies (QWS, QWS+). Furthermore, QWS+ completely eliminates variance on large examples which leads to the minimal variance of all tested strategies.

Estimation of exponential loss of a given hypothesis. In this experiment, we created a pool containing $m = 95,000$ examples with distribution of weights after the 100th iteration of training a face detector (details later). Using this entire training set, the optimal hypothesis h^* was found and its exponential loss $Z_D(h^*)$ was measured. The pool was than sampled by each strategy to obtain 1000 active sets of size $n = 500$. Next, the optimal hypothesis was tested on each active set to obtain its approximated exponential loss $Z_{\hat{D}}(h^*)$. The expectation and variance of $Z_{\hat{D}}(h^*)$ is shown in figure 4.4 (a). Weighted sampling reduces significantly the variance of $Z_{\hat{D}}(h^*)$ and keeps mean unbiased. Intuitively, the exponential loss is dominated by examples with high weights, weighted sampling forces these examples to be included in every realization

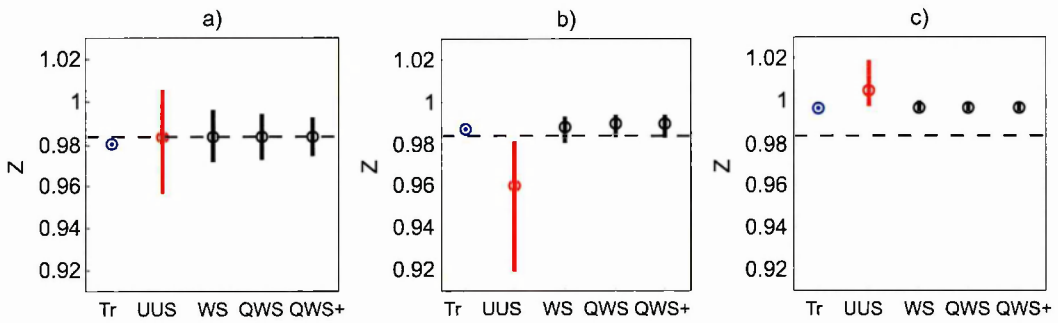

Figure 4.4: The variance and bias of the sampling strategies. The dashed line shows the exponential loss of the optimal hypothesis. (a) Exponential loss measured of a given hypotheis, (b) exponential loss measured on training data, (c) exponential loss measured on testing data. See text for more details.

of the active set, and hence the exponential loss in different trials is similar. Notice that the variance for QWS and QWS+ is further reduced with respect to WS.

Exponential loss estimated on training and testing data. In this experiment we use the same sets as defined in the previous paragraph. The optimal hypothesis h^* was first trained on full pool and the corresponding exponential loss $Z_D(h^*)$ was measured. The hypothesis was trained by the domain partitioning approach [Schapire 99]. Next, for each strategy and realization of an active set, we trained an approximate hypothesis $\hat{h}$. We estimated the *training* exponential loss $Z_{\hat{D}}(\hat{h})$ and *testing* exponential loss $Z_D(\hat{h})$. Figure 4.4 (b, c) shows the mean and variance of the training and testing exponential loss. Note, that UUS sampling overfits the training data more than any of the other strategies, i.e. training loss is lower and testing loss is higher than the optimal loss value. Furthermore, the variance of UUS is the highest of all the strategies. The variance is significantly reduced for WS. QWS and QWS+ further reduce the variance, but the difference with respect to WS is subtle. This apparently insignificant difference in the variance reduction proves to be of importance, when full detector training is evaluated.

Face database	Details
Frontal (L_{FRONT})	3 085 frontal faces collected from www.betaface.com, annotated by a 3rd party face detector + manual check.
Profile (L^{β}_{PROF})	3 384 manually annotated profile faces from 8 movies, β indicates in-plane rotation.
Background (L_{NONE})	3 310 images that were manually checked to contain no faces.

Table 4.1: Data sets used for training of a face detector.

4.4 Application to face detection

This section applies the proposed learning method to training of several face detectors (frontal, profile, specific). We build on WaldBoost [Sochman 05] algorithm, which uses a UUS strategy and extended it with the proposed sampling strategies.

Training details. We have collected three training sets shown in table 4.4 which contain frontal, profile and multi-view faces as well as images depicting background. The training sets consist of tightly cropped face-patches of size 28×28 pixels. The patches are described using three types of features: (i) Haar-like wavelets [Jones 03], (ii) Local Binary Patterns (LBP) [Ojala 02], and (iii) Histogram of Orientated Gradients (HOG) [Dalal 05] projected into one dimension using weighted Linear Discriminant Analysis [Laptev 06]. We generate a feature set of approximately 12 000 Haar, 12 000 LBP and 400 HOG features differing in their localization within the patch, scale and aspect ratio. The resulting detectors are tested on standard CMU-MIT[1] data sets and compared with other approaches using Receiving Operating Characteristic (ROC) and Precision and Recall Curves (PRC).

[1] http://vasc.ri.cmu.edu/idb/html/face/

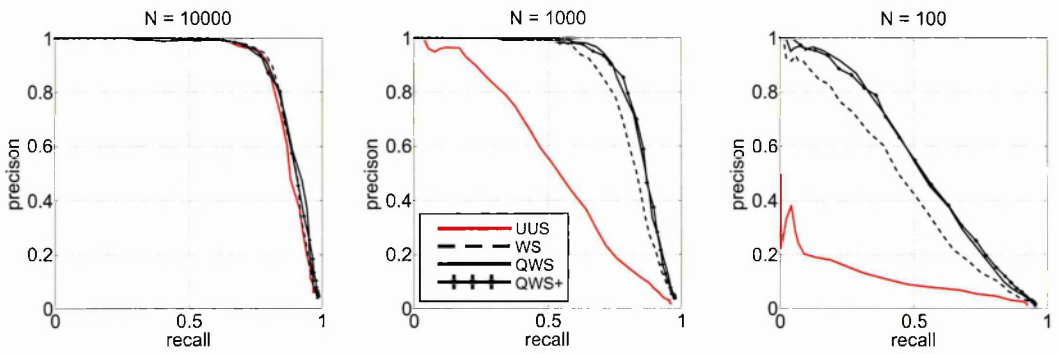

Figure 4.5: The detector performance as a function of the active set size and the sampling strategy. The pool consists of 10 000 positive and 56 million negative examples.

4.4.1 Frontal face detector

This experiment trains a frontal face detector and investigates the influence of relative active set size on the detector performance. We used the pool of 10 000 positive examples and 56 million background patches. The positive examples were generated from L_{FRONT} using shift and in-plane rotation of the original face-patches. The negative patches were sampled from L_{NONE} using a sliding window. This pool was approximated by active sets of three different sizes $n \in \{100, 1\,000, 10\,000\}$. For each size and sampling strategy (UUS, WS, QWS, QWS+), a strong classifier was trained up to the length of 200 features. Trimming was also tested but its performance was much worse than any other strategy.

Figure 4.5 shows the resulting PRC curves on the CMU-MIT data set. The performance of all sampling strategies decreases with smaller active set size. For large active sets ($n = 10\,000$) there is almost no difference in performance between the strategies. For smaller active sets ($n = 1\,000$) the UUS sampling performs significantly worse than the others. WS is in this case slightly worse than QWS and QWS+. For extremely small active sets ($n = 100$) the difference increases. This clearly demonstrates the benefit of QWS and QWS+. The difference between QWS and QWS+ is in this case

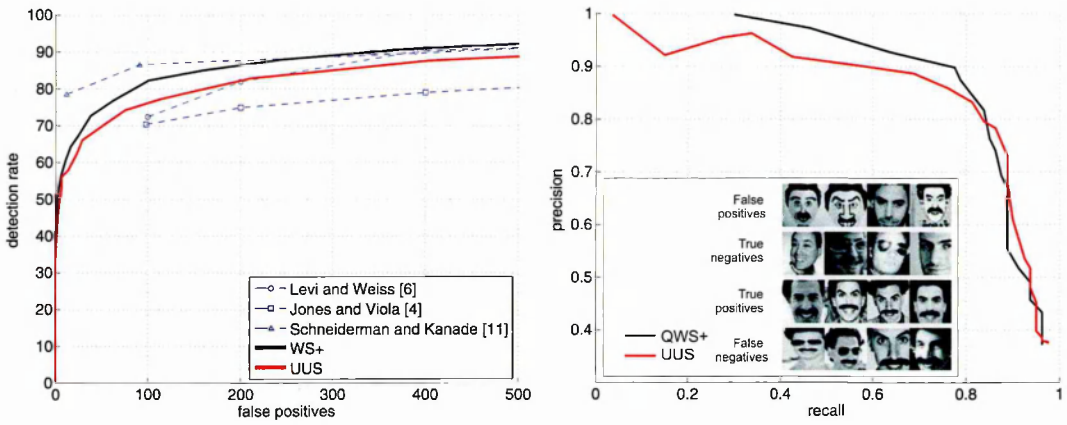

Figure 4.6: Performance evaluation: (LEFT) ROC curves on CMU-MIT profile database (368 profile faces in 208 images). (RIGHT) PRC for specific face detector applied on the results of Google face search.

on a noise level only. The active set size has impact on training efficiency. While training with $n = 10.000$ takes 3 hours, training with $n = 100$ requires 1 hour on the same machine.

This experiment demonstrates that the sampling strategy does not play a crucial role in the case of relatively large active sets, but a significant difference in performance can be achieved when the active set is relatively small with respect to the pool. QWS and QWS+ significantly outperformed UUS and WS in that case.

4.4.2 Profile face detector

This experiment trains a profile face detector and compares it with state-of-the-art approaches. The pool of $41\,000$ positive and 424 million negative patches was generated from L^0_{PROF}, L^{15}_{PROF}, L^{30}_{PROF} and L_{NONE}. Two left-profile detectors of length $2\,000$ were trained with QWS+ and UUS strategy. The right profile detectors were obtained by left-to-right flipping of the model.

The resulting ROC curves are displayed in the left panel of figure 4.6. QWS+ has a

detection rate 5% higher than UUS for 100 false positives. On the same level of false positives, our detector performs better than the results in [Levi 04] and [Jones 03] and slightly worse than [Schneiderman 04]. The average number of evaluated weak classifiers is 5.6 for QWS+ and 7.2 for UUS which shows positive influence of weighted sampling on the classifier speed. Figure 4.7 illustrate the performance of the profile face on several images from CMU/MIT data set.

4.4.3 Specific face detector

Google face search was used to collect 650 images returned for query "Borat"[2]. This set contained 350 true positives (images depicting Borat), and 300 false positives (images containing other faces or background). This set was randomly split into training set and testing set. Using the training set, a specific face detector was trained. The resulting PRC is presented in the right panel of figure 4.6. Notice that also in this task the performance of QWS+ is superior to UUS. The specific face detector successfully finds approximately 80% of faces of Borat with 90% precision.

4.5 Conclusions

We developed an algorithm for training of object detectors from large labeled data sets and integrated boosting and boosting in a unified algorithm.

Two improvements of standard weighted sampling (WS) are introduced. We designed quasi-random weighted sampling (QWS) which reduces the variance of error estimate but does not guarantee unique samples. Next, we introduced a new strategy based on quasi-random weighted sampling + trimming (QWS+) which removes this drawback. We provided the theoretical proof of the variance minimization of QWS+.

[2] A fictional character portrayed by a British comedian Sasha Barron Cohen.

Figure 4.7: Results achieved by our face detector. Bottom row shows the most challenging faces. The binary executable is available at the website of the author.

The performance of the learning method was demonstrated on the task of *generic* face detection. Various characteristics of the learning process were improved: reduction of the active set; better precision/recall curves and speed. The developed face detector operates in real-time on QVGA images [3] and therefore is applicable to tracking scenarios. This detector will be used in chapter 6 for long-term tracking of faces.

We trained a *specific* face detector from manually checked images returned by Google face search. This shows that training a specific face detector is feasible, however, the need of manual preparation of the training set is not practical for long-term tracking scenarios. In long-term tracking, the training of the specific detector has to be done *online* and from *unlabeled* data.

[3] Intel Core 2 Duo, 2.40GHz, 2GB RAM

Chapter 5

Learning: unsupervised bootstrap

This chapter investigates long-term tracking from the perspective of machine learning, the third component of our system. In particular, we study how to improve an offline trained object detector during tracking. Our goal is to design a learning approach that would be suitable for such a scenario as well as general enough to be applicable to other learning problems.

The chapter is structured as follows. Section 5.1 introduces the problem as online learning from labeled and unlabeled data. Section 5.2 develops a novel learning paradigm that we call P-N learning. Section 5.3 applies the P-N learning to training an object detector from a single example and a video stream. The proposed algorithm is evaluated on a number of challenging sequences. The chapter is concluded in section 5.4.

5.1 Introduction

Consider an object detector and a video stream. The object detector is trained offline from a limited number of labeled examples and the video stream is unconstrained. The goal of this chapter is to improve the offline detector by online processing of the video stream. At every time instance, we run the detector on the current frame, estimate its

errors and update the detector so that it does not make such errors in the future. We refer to this process as *unsupervised bootstrap*.

The ability to improve an object detector by online processing of an unlabeled video stream has a large number of applications. Our motivation is long-term tracking where the online learned detector can be used to re-initialize a frame-to-frame tracker after its failure. This aspect is studied in chapter 6.

There are several challenges that have to be tackled in order to enable the unsupervised bootstrap: (i) *large variability* – the learning must deal with arbitrarily complex video streams where the object significantly changes appearance, moves in and out of the camera view, the stream contains background clutter, fast camera motions or motion blur; (ii) *real-time performance* – every learning step has to be done immediately after accepting a new frame; (iii) *robustness* – the learning should never degrade the classifier, if the video stream does not contain relevant information, the detector performance should not degrade.

To tackle all these challenges, we rely on the various information sources contained in the video. Consider, for instance, a single patch denoting the object location in a single frame. This patch defines not only the appearance of the object, but also determines the surrounding patches, which define the appearance of the background. When tracking the patch, one can discover different appearances of the same object as well as more appearances of the background. This is in contrast to standard machine learning approaches, where the training examples are considered to be independent [Blum 98]. This opens interesting questions how to effectively exploit the information in the video during learning.

To exploit the information in the video, we propose a new learning paradigm called *P-N learning*. The detector is evaluated on every frame of the video stream with the aim to find misclassified examples. These misclassified examples are estimated by two types of complementary "experts": (i) *P-expert* – an expert on positive examples, estimates when the object detector missed the object, and (ii) *N-expert* – an expert on negative

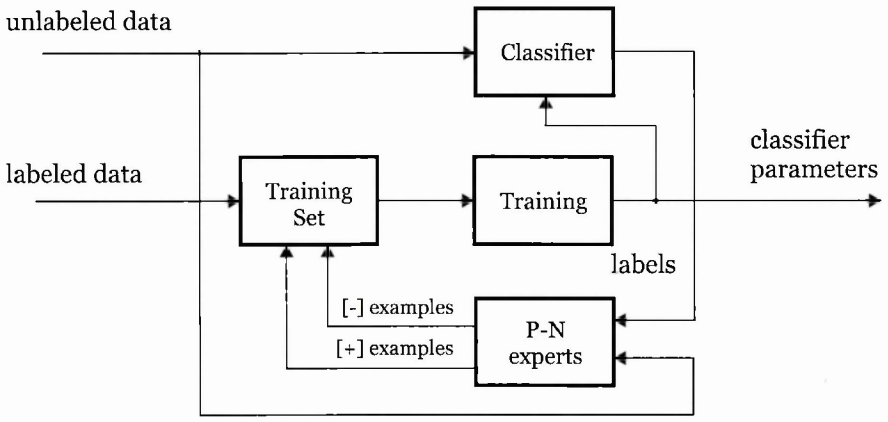

Figure 5.1: The block diagram of the P-N learning.

examples, estimates when a detector made a false detection. The estimated errors augment a training set of the detector, and the detector is retrained in a supervised manner to avoid these errors in the future. As any other process, the P-N experts can make errors themself. However, if the probability of expert error is within certain limits (which will be analytically quantified), the errors are mutually compensated which leads to stable learning.

5.2 P-N learning

This section formalizes the P-N learning without considering any specific application. We assume a set of labeled and unlabeled examples and our goal is to train a binary classifier. The section is split into three parts. Subsection 5.2.1 formalizes the P-N learning and shows its relationship to supervised bootstrapping. Subsection 5.2.2 analyzes the stability of the P-N learning. The conditions that guarantee improvement of the classifier are inferred. Finally, subsection 5.2.3 performs several experiments that validate the proposed theory.

5.2.1 Formalization

Algorithm 1 P-N learning

Require: unlabeled data, labeled data

Require: classifier trained using labeled data

for $t = 1 : \infty$ **do**

Evaluate current classifier on unlabeled data.

Estimate false negatives using N-expert.

Estimate false positives using P-expert.

Add estimated errors to training set.

Retrain or update the classifier.

end for

Let x be an example from a feature-space $\mathcal{X}$ and y be a label from a space of labels $\mathcal{Y} = \{-1, 1\}$. A set of examples X is called an unlabeled set, Y is called a set of labels and $L = \{(x, y)\}$ is called a labeled set. The input to the P-N learning is a labeled set L_l and an unlabeled set X_u, where $l \ll u$. The task of P-N learning is to learn a classifier $f : \mathcal{X} \to \mathcal{Y}$ from labeled set L_l and bootstrap its performance by the unlabeled set X_u. Classifier f is a function from a family $\mathcal{F}$ parameterized by Θ. The family $\mathcal{F}$ is subject to implementation and is considered fixed in training, the training therefore corresponds to estimation of the parameters Θ.

The P-N learning consists of four blocks: (i) *classifier* to be learned, (ii) *training set* – a collection of labeled training examples, (iii) *supervised training* – a method that trains a classifier from the training set, and (iv) *P-N experts* – functions that estimate errors of the classifier and augment the training set with labeled examples. Figure 5.1 shows a block diagram and algorithm 1 defines a pseudo-code.

The training process is initialized by inserting the labeled examples L_l into the training set. The training set is then passed to supervised learning which trains a classifier, i.e. estimates the initial parameters Θ^0. The learning process then proceeds iteratively. In iteration k, the classifier trained in iteration $k-1$ classifies the entire unlabeled set, $y_u^k = f(x_u|\Theta^{k-1})$ for all $x_u \in X_u$. The classification is analyzed by the P-N

experts that estimate, which examples have been classified incorrectly. These examples are added with changed labels to the training set. The iteration finishes by retraining the classifier, i.e. estimation of Θ^k. The process iterates until convergence or other stopping criterion.

The crucial element of P-N learning is the estimation of the classifier errors. The key idea is to treat the estimation of false positives *independent* from estimation of false negatives. For this reason, the unlabeled set is split into two parts based on the current classification and each part is analyzed by an independent expert. The *P-expert* analyzes examples classified as negative, estimates false negatives and adds them to the training set with a positive label. In iteration k, P-expert outputs $n^+(k)$ positive examples. *N-expert* analyzes examples classified as positive, estimates false positives and adds them with negative label to the training set. In iteration k, the N-expert outputs $n^-(k)$ negative examples. The P-expert influences the classifier in positive (growing) sense and increases the classifier generality. The N-expert influences the classifier in a negative (pruning) sense and increases the classifier discriminability. These two forces are working in parallel and independently from each other.

Relation to supervised bootstrap. To put P-N learning into context, let us consider that the labels of set X_u are known. Under this assumption it is straightforward to design P-N experts that identify misclassified examples and add them to the training set with correct labels. Such a strategy corresponds to a supervised bootstrap as discussed in chapter 4. A classifier trained using supervised bootstrap focuses on the decision boundary and often outperforms a classifier trained on a randomly sampled training set [Sung 98]. The same idea of focusing on the decision boundary underpins the P-N learning approach with the difference that the labels of the set X_u are unknown. P-N learning can be therefore viewed as a generalization of standard bootstrapping to unlabeled cases where labels are not given but rather *estimated* using the P-N experts. As any other process, the P-N experts make errors, and estimate the labels incorrectly. Such errors propagate through the training, which will be now theoretically analyzed.

5.2.2 Stability

This section analyses the impact of the P-N learning on the classifier performance and the impact of the errors caused by P-N experts on the stability of the learning. For the purpose of the analysis, let us consider that the ground truth labels of X_u are known and therefore it is possible to measure the errors made by the classifier. Next, consider a classifier that initially classifies the unlabeled set at random and then corrects its classification according to the output of the P-N experts. The performance of such a classifier is characterized by a number of false positives $\mathrm{FP}(k)$ and a number of false negatives $\mathrm{FN}(k)$, where k indicates the iteration of training. The goal of the P-N learning is to reduce these errors to zero.

In iteration k, the P-expert outputs $n_c^+(k)$ positive examples which are correct (positive based on ground truth), and $n_f^+(k)$ positive examples which are false (negative based on ground truth), which forces the classifier to change $n^+(k) = n_c^+(k) + n_f^+(k)$ negatively classified examples to positive. Similarly, the N-experts outputs $n_c^-(k)$ correct negative examples and $n_f^-(k)$ false negative examples, which forces the classifier to change $n^-(k) = n_c^-(k) + n_f^-(k)$ examples classified as positive to negative. The number of false positive and false negative errors of the classifier in the next iteration thus becomes:

$$\mathrm{FP}(k+1) = \mathrm{FP}(k) - n_c^-(k) + n_f^+(k) \tag{5.1a}$$

$$\mathrm{FN}(k+1) = \mathrm{FN}(k) - n_c^+(k) + n_f^-(k). \tag{5.1b}$$

Equation 5.1a shows that false positives $\mathrm{FP}(k)$ decrease if $n_c^-(k) > n_f^+(k)$, i.e. number of examples that were correctly relabeled to negative is higher than the number of examples that were incorrectly relabeled to positive. Similarly, the false negatives $\mathrm{FN}(k)$ decrease if $n_c^+(k) > n_f^-(k)$.

Quality measures. In order to analyze the convergence of the P-N learning, a model needs to be defined that relates the quality of the P-N experts to the absolute number of

positive and negative examples output in each iteration. The quality of the P-N experts is characterized by four *quality measures*:

- *P-precision* – reliability of the positive labels, i.e. the number of correct positive examples divided by the number of all positive examples output by the P-expert, $P^+ = n_c^+/(n_c^+ + n_f^+)$.
- *P-recall* – percentage of identified false negative errors, i.e. the number of correct positive examples divided by the number of false negatives made by the classifier, $R^+ = n_c^+/\,\mathrm{FN}$.
- *N-precision* – reliability of negative labels, i.e. the number of correct negative examples divided by the number positive examples output by the N-expert, $P^- = n_c^-/(n_c^- + n_f^-)$.
- *N-recall* – percentage of recognized false positive errors, i.e. the number of correct negative examples divided by the number of all false positives made by the classifier, $R^- = n_c^-/\,\mathrm{FP}$.

Given these quality measures, the number of correct and false examples output by P-N experts at iteration k have the form:

$$n_c^+(k) = R^+\,\mathrm{FN}(k), \quad n_f^+(k) = \frac{(1-P^+)}{P^+}R^+\,\mathrm{FN}(k) \tag{5.2a}$$

$$n_c^-(k) = R^-\,\mathrm{FP}(k), \quad n_f^-(k) = \frac{(1-P^-)}{P^-}R^-\,\mathrm{FP}(k). \tag{5.2b}$$

By combining the equation 5.1a, 5.1b, 5.2a and 5.2b we obtain:

$$\mathrm{FP}(k+1) = (1-R^-)\,\mathrm{FP}(k) + \frac{(1-P^+)}{P^+}R^+\,\mathrm{FN}(k) \tag{5.3a}$$

$$\mathrm{FN}(k+1) = \frac{(1-P^-)}{P^-}R^-\,\mathrm{FP}(k) + (1-R^+)\,\mathrm{FN}(k). \tag{5.3b}$$

After defining the state vector $\vec{x}(k) = \begin{bmatrix}\mathrm{FP}(k) & \mathrm{FN}(k)\end{bmatrix}^{\mathrm{T}}$ and a 2×2 matrix M as

$$\mathrm{M} = \begin{bmatrix} 1-R^- & \frac{(1-P^+)}{P^+}R^+ \\ \frac{(1-P^-)}{P^-}R^- & (1-R^+) \end{bmatrix} \tag{5.4}$$

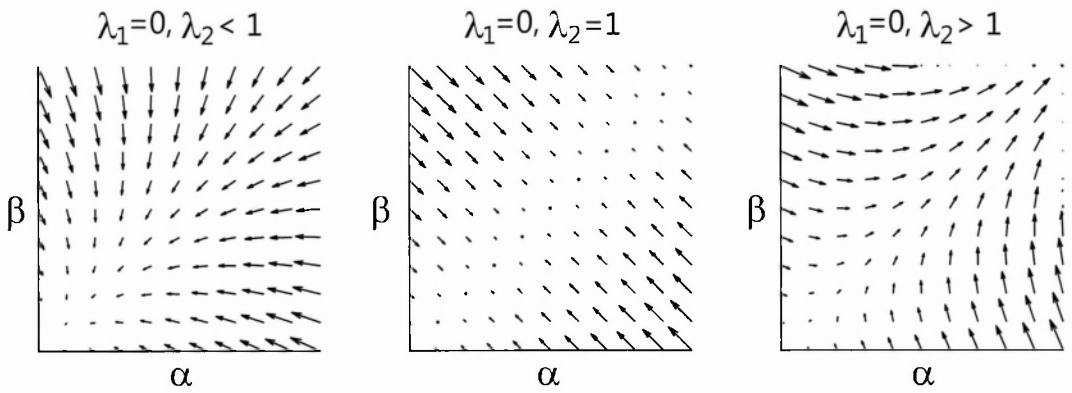

Figure 5.2: The evolution of errors of the classifier depends on the quality of the P-N experts, which is defined in terms of eigenvalues of matrix M. The errors converge to zero (LEFT), are at the edge of stability (MIDDLE) or are growing (RIGHT).

it is possible to rewrite the equations as

$$\vec{x}(k+1) = \mathbf{M}\vec{x}(k).$$

This is a recursive equation that corresponds to a discrete dynamical system. The system models the error propagation during training, i.e. from one iteration of P-N learning to another. Our goal is to show, under which conditions the error in the system drops.

Based on the stability criteria from control theory [Zhou 96, Ogata 09], the state vector $\vec{x}$ converges to zero if both eigenvalues λ_1, λ_2 of the transition matrix M are smaller than one. Note that the matrix M is a function of the expert quality measures. Therefore, if the quality measures are known, it is possible to check whether the error during training converges to zero or not. Experts for which the corresponding matrix M has both eigenvalues smaller than one will be called *error-canceling*. Figure 5.2 illustrates the evolution of error of the classifier when the first eigenvalue is zero and the second eigenvalue attains values (i) $\lambda_2 < 1$, (ii) $\lambda_2 = 1$, and (iii) $\lambda_2 > 1$.

The pragmatic reason for developing the P-N learning theory was the observation, that it is relatively simple to design a large number of experts that correct specific errors

made by the classifier. The combined influence of the experts was, however not understood. P-N learning represents guidelines how to combine a number of weak experts so that the overall learning is stable. Interestingly, P-N learning does not put constraints on the quality of *individual* experts. Even experts with low precision might be used as long as the matrix $\mathbf{M}$ has eigenvalues smaller than one, it is therefore possible to use various (even weak) information sources.

5.2.3 Experiments

This section analyzes the performance of P-N learning as a function of the expert quality measures. Our goal is to experimentally validate the claims about learning stability that have been made in section 5.2.2. The experiment is based on synthetically generated P-N experts.

Experiment setup. The analysis is performed on sequence CAR (see Appendix B). In the first frame of the sequence, a classifier is trained using affine warps of the initial patch and background patches from the surrounding of the object. Details about this step are given in chapter 7. Next, a single run over the sequence is performed. In every frame, the classifier is evaluated. The error of the classifier are recognized using simulated experts that are characterized by chosen quality measures and the classifier is updated. After every update, the classifier is tested on the entire sequence using f-measure. The performance is then drawn as a function of the number of processed frames and the quality of the P-N experts.

The P-N experts are characterized by four quality measures, P^+, R^+, P^-, R^-. To reduce this 4D space of parameters, we analyze the learning at equal error rate. The parameters are set to $P^+ = R^+ = P^- = R^- = 1 - \epsilon$, where ϵ represents *error* of the expert. The transition matrix then becomes $\mathbf{M} = \epsilon[11]^\mathbf{T}$, where $[11]^\mathbf{T}$ is a 2x2 matrix of ones. The eigenvalues of this matrix are $\lambda_1 = 0, \lambda_2 = 2\epsilon$. Therefore, based on the theory, the P-N learning should be improving the performance if $\epsilon < 0.5$.

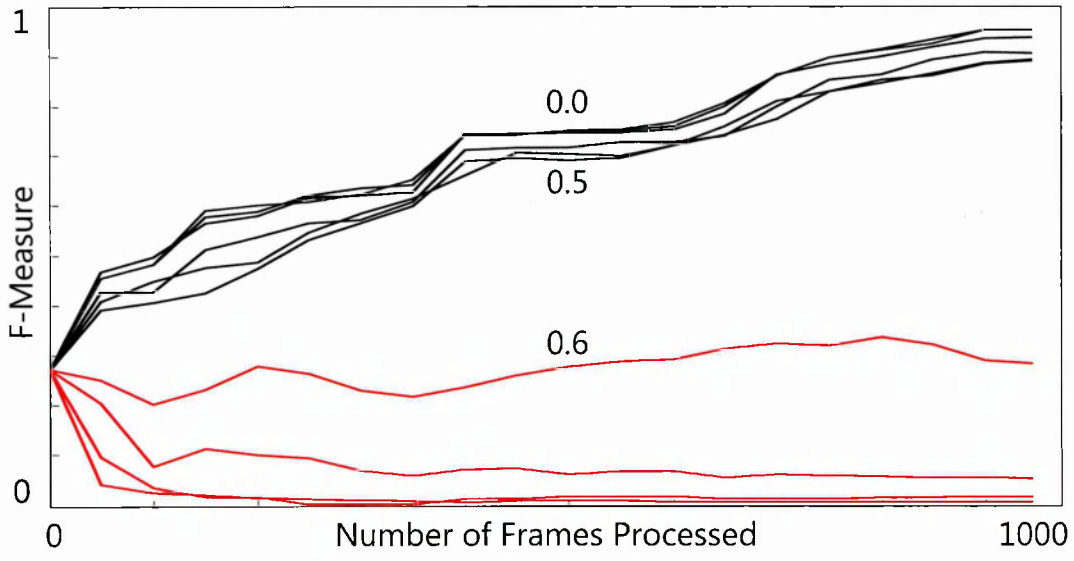

Figure 5.3: Performance of a detector as a function of the number of processed frames. The detectors were trained by synthetic P-N experts with guaranteed level of error. The classifier is improved up to error 50% (BLACK), higher error degrades it (RED).

The experts were realized using the ground truth data as follows. In frame k the classifier generates $\mathrm{FN}(k)$ false negatives. P-experts relabel $n_c^+(k) = (1-\epsilon)\,\mathrm{FN}(k)$ of them to positive which guarantees $R^+ = 1-\epsilon$. In order to satisfy the requirement of precision $P^+ = 1-\epsilon$, the P-expert relabels additional $n_f^+(k) = \epsilon\,\mathrm{FN}(k)$ background samples to positive. Therefore the total number of examples relabeled to positive in iteration k is $n^+ = n_c^+(k) + n_f^+(k) = \mathrm{FN}(k)$. The N-experts were generated similarly.

The performance of the classifier as a function of number of processed frames is depicted in figure 5.3. Notice that if $\epsilon \leq 0.5$ the performance of the detector increases with more processed frames. In theory, $\epsilon = 0.5$ should not alter the classifier performance, although in this sequence it leads to improvements. Increasing the noise-level further leads to sudden degradation of the classifier.

The P-N learning with error-less experts ($\epsilon = 0$) is analyzed in more detail. In this case *all* classifier errors are identified and *no* miss-labeled examples are added to the

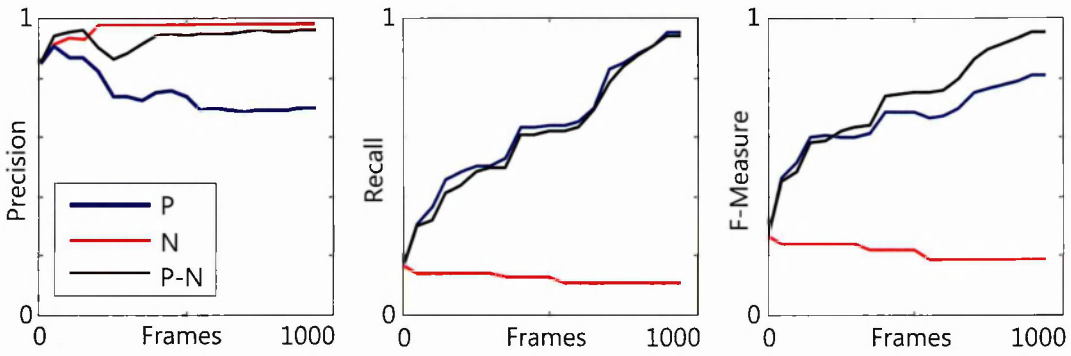

Figure 5.4: Performance of detectors trained by error-less P-expert, N-expert and P-N expert measured by precision (LEFT), recall (MIDDLE) and f-measure (RIGHT).

training set. Three different classifiers were trained using: (i) P-experts, (ii) N-experts, and (iii) P-N experts. The classifier performance was measured using precision, recall and f-measure and the results are shown in figure 5.4. Precision (LEFT) is decreased by P-experts since only positive examples are added to the training set, these cause the classifier to be too generative which results in increase of false positives. Recall (MIDDLE) is decreased by N-experts since these add only negative examples and cause the classifier to be too discriminative. F-measure (RIGHT) shows that P-N experts together work the best. Notice that even error-less experts cause classification errors if used individually, which leads to low precision or low recall of the classifier. Both precision and recall are high if the P-N experts are used together since the errors are mutually compensating.

5.3 Learning an object detector from a video sequence

This section applies the P-N learning to bootstrapping a scanning window-based object detector from a video sequence. The section is split into three parts. Subsection 5.3.1 specifies the learning problem using the P-N learning terminology. Subsection 5.3.2 develops appropriate P-N experts. Finally, subsection 5.3.3 performs quantitative evaluation on a number of challenging sequences. The learning approach will be described

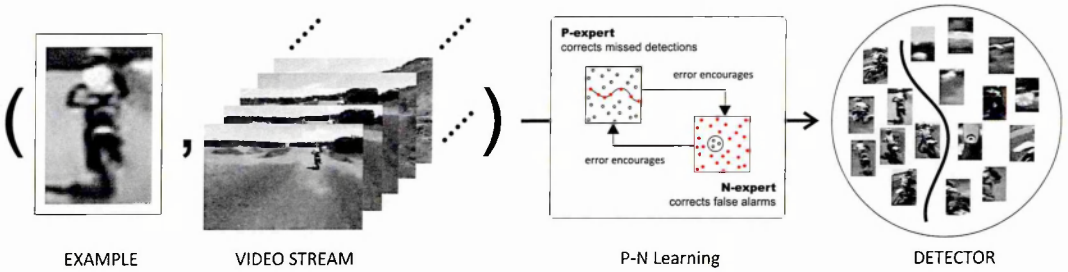

Figure 5.5: Given a single example and a video stream, the goal of P-N learning is to train an accurate object detector.

without considering implementation details, these are given in chapter 6.

5.3.1 Problem specification

The input to the classifier training is a single bounding box and a video sequence. The learning is performed by sequential processing of the video sequence in a frame-by-frame fashion. One iteration of P-N learning corresponds to the processing of one frame of the sequence. The output of the learning is a binary classifier that separates appearances of the object from appearances of the background that appeared in the video sequence. Figure 5.5 illustrates the scenario.

The training examples (both labeled and unlabeled) correspond to image patches. These image patches are sampled at locations and scales determined by a *scanning grid* on which the detector operates. The *labeled* data L_l are extracted from the first frame. Patches that are overlapping with the initial bounding box are positive, patches that are non-overlapping are negative. The *unlabeled* data X_u are contained in the remaining video sequence.

The learning is initialized in the first frame by supervised training of the so called *Initial detector*. The learning then proceeds by sequential processing of the video sequence. In every frame, the P-N learning performs the following steps: (i) evaluation of the detector on the current frame, (ii) estimation of the detector errors using the P-N

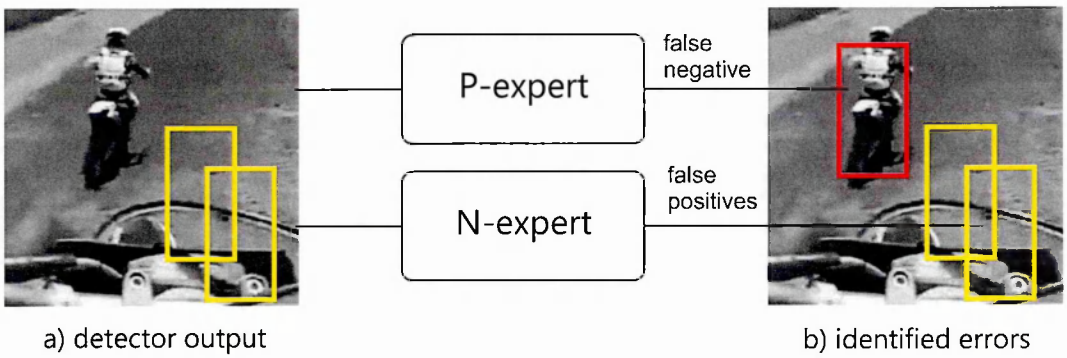

Figure 5.6: Illustration of P-N experts: (a) output of an motorbike detector, (b) errors identified by P-N experts.

experts, (iii) update of the detector by labeled examples output by the experts. The detector obtained at the end of the sequence is called the *Final detector*. We perform the learning in one pass through the video sequence which is analogous to processing live video stream.

5.3.2 P-N experts

This section presents our P-N experts developed for bootstrapping a scanning window-based detector from a video sequence. Consider that our goal is to train a detector of a motorbike. At every iteration of the P-N learning, the detector is evaluated on the current frame. One possible output of the detector is depicted in figure 5.6 (a). Note that the detector performed two false positives and one false negative errors. The goal of the P-N experts is to identify these errors. In particular, P-experts should identify false negatives and N-experts should identify false positives as shown in figure 5.6 (b).

To introduce the P-N experts, consider figure 5.7 (a) that shows three frames of a video sequence overlaid with a scanning grid. Every bounding box in the grid defines an image patch, whose label is represented as a colored dot (b,c). The detector considers every patch to be independent. Therefore, there are 2^N possible label combinations in a single frame, where N is the number of bounding boxes in the grid. Figure 5.7

(b) shows one such labeling. The labeling indicates, that the object appears at several locations in a single frame and there is no temporal continuity in the motion. In natural videos is such labeling not credible and therefore it can be inferred that the detector made a mistake at several locations. On the other hand, if the detector outputs classification as depicted in (c) the labeling is credible since the object appears at one location in a single frame and these locations constitute a smooth trajectory in time.

As we have just shown, it is fairly easy to estimate unlikely behavior of the detector when observing the detector responses in the context of a video volume. We exploited our prior knowledge about the motion of an object which casts constraints on the labeling of the video volume. In other words, every single patch influences labels of other patches. Such a property will be called *structure* and the data that has this property is structured. This is in contrast to the majority of existing learning algorithms in semi-supervised learning, which assume that the unlabeled examples are independent [Blum 98].

The key idea of the P-N experts is to exploit the structure in the data to estimate the detector errors. Our approach to modeling the structure is based on simple rules such as: (i) overlapping patches have the same label, (ii) patches within a single image can have at most one positive label, (iii) patches that are connected by a trajectory have the same label, etc. Based on these rules, the P-N experts are built.

The **P-expert** exploits the temporal structure in the video volume and assumes that the object moves on a smooth trajectory. The P-expert remembers the location of the object in the previous frame and estimates the object location in current frame using a frame-to-frame tracker. If the detector labeled the current location as negative (i.e. made a false negative error), the P-expert generates a positive example from the current location and performs an update of the detector.

The **N-expert** exploits the spatial structure in the video volume and assumes that the object can appear at a single location in a single frame only. The N-expert analyzes all responses of the detector in the current frame and the response produced by the tracker

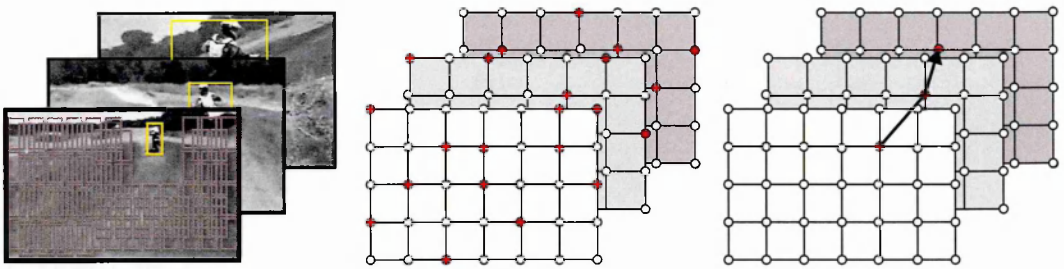

Figure 5.7: Illustration of a scanning grid applied to three consecutive frames (a) and corresponding spatio-temporal volume of labels with unacceptable (b) and acceptable (c) labeling. Red dots correspond to positive labels.

and selects the one that is the most confident. Patches that are not overlapping with the maximally confident patch are labeled as negative and update the detector. The maximally confident patch re-initializes the location of the tracker.

Error compensation. The figure 5.8 depicts a sequence of cam images, the object to be learned is a car within the yellow bounding box. The car is tracked from frame to frame by a tracker. The tracker represents the P-expert that outputs positive training examples. Notice that due to occlusion of the car, the 3rd example is incorrect. The N-expert identifies a maximally confident patch (denoted by a red star) and labels all other patches as negative. Notice that the N-expert is discriminating against another car, and in addition corrected the error made by the P-expert in the 3rd frame. This shows that if the experts use an independent source of information (i.e. temporal and spatial structure in data) they have potential to correct their own errors.

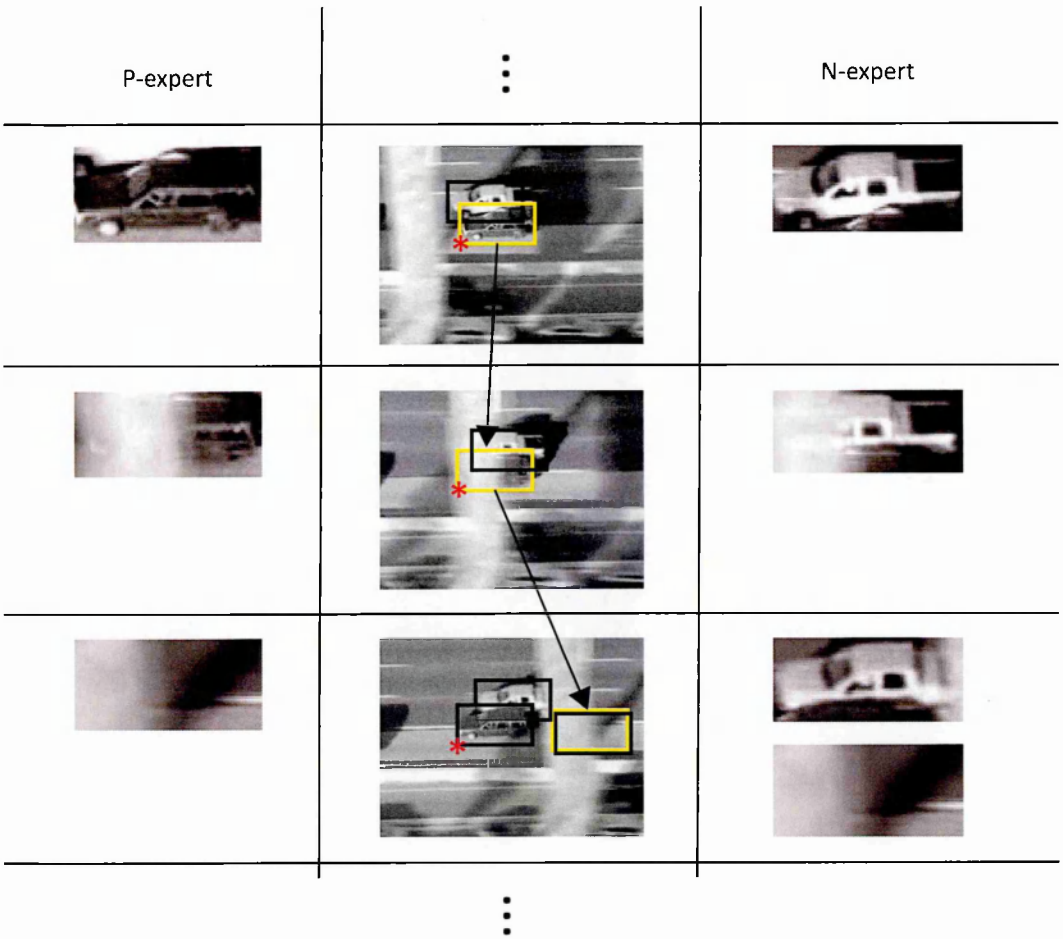

Figure 5.8: Illustration of the P-expert and the N-expert and their error compensation.

5.3.3 Experiments

Components of P-N learning. This experiment investigates the performance of the P-N learning on 10 sequences shown in figure 5.9. The performance is evaluated using precision P, recall R and an f-measure F. P is the number of true positives divided by number of all detections, R is the number of true positives divided by the number of object occurrences that should have been detected. F combines these two measures as $F = 2PR/(P + R)$. Next, the quality of the P-N experts is measured using P^+, R^+, P^- and R^- averaged over all iterations. A detection is considered as true positive if its overlap with ground truth bounding box is larger than 50%. The overlap is defined as the ratio between intersection and union of two bounding boxes.

Table 5.1 (3rd column) shows the resulting scores of the Initial detector. This detector has high precision for most of the sequences with exception of sequence 9 and 10. Sequence 9 is long (9 928 frames) and there is a significant background clutter and objects similar to the target (cars). Recall of the Initial detector is low for the majority of sequences except for sequence 5 where the recall is 73%. This indicates that in this sequence the appearance of the object does not vary significantly. The scores of the Final detector are displayed in the 4th column of the table 5.1. The final detector was evaluated by a single pass through the entire sequence. The recall of the detector was significantly increased with little drop in precision. In sequence 9, even the precision was increased from 36% to 90%, which shows that the false positives of the Initial detector were estimated by N-expert and corrected. The most significant increase of the performance is for sequences 7-10 which are the most challenging of the whole set. The Initial detector fails here but for the Final detector the f-measure is in the range of 25-83%. This demonstrates the benefit of P-N learning. The 5th column of table 5.1 shows the performance of the Online detector that has been jointly trained and evaluated while processing the sequence. For all of the sequences the Online detector achieved higher recall in contrast to Initial detector and slightly worse recall than the Final detector. On the other hand, the precision typically slightly drops with respect to

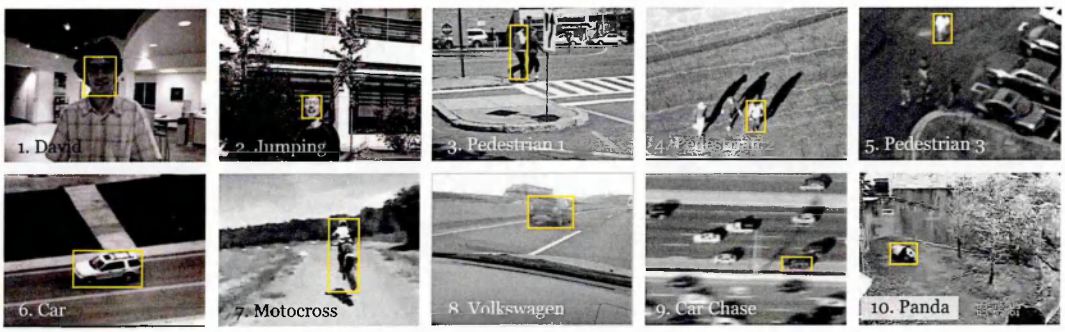

Figure 5.9: Sample images from evaluation sequences with objects marked. See Appendix B for more details.

the Initial detector. The overall performance of the Online detector is between Initial detector and Online detector. The 6th column of table 5.1 shows the performance of Online detector combined with the Tracker. In majority of the sequences, this combination leads to increased recall and slight drop of precision. An exception is sequence 3, where tracking caused a significant drop in precision since the tracker drifted at the beginning of the sequence and remained drifted up to the end. For all remaining sequences tracking improved performance of the online detector.

The last three columns of Table 5.1 report the quality of P-N experts. Both experts have precision higher than 60% except for sequence 10 which has a P-precision of just 31%. Recall of the experts is in the range of 2-78%. The last column shows the corresponding eigenvalues of matrix M. Notice that all eigenvalues are smaller than one. This demonstrates that the proposed experts work across different scenarios and lead to an improvement of the Initial detector. The larger these eigenvalues are, the less the P-N learning improves the performance. For example in sequence 10 one eigenvalue is 0.99 which reflects poor performance of the P-N constraints. The target of this sequence is an animal, which changes its pose throughout the sequence. The Median-Flow tracker is not very reliable in this scenario, but still P-N learning exploits the information provided by the tracker and improves the detector.

Sequence	Frames	Initial Detector Precision / Recall / F-measure	Final Detector Precision / Recall / F-measure	Online Detector Precision / Recall / F-measure	Online Detector + Tracker Precision / Recall / F-measure	P-constraints P^+, R^+	N-constraints P^-, R^-	Eigenvalues λ_1, λ_2
1. David	761	1.00 / 0.01 / **0.02**	1.00 / 0.32 / **0.49**	0.95 / 0.30 / **0.45**	0.94 / 0.94 / **0.94**	1.00 / 0.08	0.99 / 0.17	0.92 / 0.83
2. Jumping	313	1.00 / 0.01 / **0.02**	0.99 / 0.88 / **0.93**	0.89 / 0.60 / **0.72**	0.86 / 0.77 / **0.81**	0.86 / 0.24	0.98 / 0.30	0.70 / 0.77
3. Pedestrian 1	140	1.00 / 0.01 / **0.02**	1.00 / 0.12 / **0.22**	1.00 / 0.10 / **0.18**	0.22 / 0.16 / **0.18**	0.81 / 0.04	1.00 / 0.04	0.96 / 0.96
4. Pedestrian 2	338	1.00 / 0.02 / **0.03**	1.00 / 0.34 / **0.51**	1.00 / 0.27 / **0.42**	1.00 / 0.95 / **0.97**	1.00 / 0.25	1.00 / 0.24	0.76 / 0.75
5. Pedestrian 3	184	1.00 / 0.73 / **0.84**	0.97 / 0.93 / **0.95**	1.00 / 0.85 / **0.92**	1.00 / 0.94 / **0.97**	0.98 / 0.78	0.98 / 0.68	0.32 / 0.22
6. Car	945	1.00 / 0.04 / **0.08**	0.99 / 0.82 / **0.90**	1.00 / 0.55 / **0.71**	0.93 / 0.83 / **0.88**	1.00 / 0.52	1.00 / 0.46	0.48 / 0.54
7. Motocross	2665	1.00 / 0.00 / **0.00**	0.92 / 0.32 / **0.47**	0.93 / 0.28 / **0.43**	0.86 / 0.50 / **0.63**	0.96 / 0.19	0.84 / 0.08	0.92 / 0.81
8. Volkswagen	8576	1.00 / 0.00 / **0.00**	0.92 / 0.75 / **0.83**	0.95 / 0.58 / **0.72**	0.67 / 0.79 / **0.72**	0.70 / 0.23	0.99 / 0.09	0.91 / 0.77
9. Car Chase	9928	0.36 / 0.00 / **0.00**	0.90 / 0.42 / **0.57**	0.60 / 0.33 / **0.42**	0.81 / 0.43 / **0.56**	0.64 / 0.19	0.95 / 0.22	0.76 / 0.83
10. Panda	3000	0.79 / 0.01 / **0.01**	0.51 / 0.16 / **0.25**	0.71 / 0.09 / **0.16**	0.25 / 0.24 / **0.25**	0.31 / 0.02	0.96 / 0.19	0.81 / 0.99

Table 5.1: Performance analysis of P-N learning. The Initial detector is trained on the first frame only. The Final detector is obtained by P-N learning after one pass through the sequence. The P-N Tracker is the adaptive Lucas-Kanade tracker re-initialized by the on-line trained detector. The last three columns display internal statistics of the training process. The statistics were computed for every frame and the table reports the average values.

Figure 5.10: Several snapshot from face sequence that has been used to evaluate repeated runs of P-N learning.

Repeated run over one sequence. This experiment investigates the stability of P-N learning when run multiple times over a single sequence. We use a benchmark face sequence that has been first introduced in [Maggio 07]. The sequence contains 1006 frames and shows four face targets in an indoor environment that undergo a variety of changes including: fast motion, out of plane rotation, partial and full occlusions. The subject that undergoes the most significant changes was selected for tracking. Figure 5.10 shows several frames from the sequence.

P-N learning has been run repeatedly on this sequence. After every run, the trained

$\theta_L = 0.95$		1	2	3	4	5	6	7
Online detector + Tracker	Prec	1.00	1.00	1.00	1.00	1.00	1.00	1.00
	Rec	0.01	0.01	0.02	0.02	0.03	0.03	0.03
Final Detector	Prec	1.00	1.00	1.00	1.00	1.00	1.00	1.00
	Rec	0.00	0.01	0.01	0.01	0.02	0.02	0.02
$\theta_L = 0.90$								
Online detector + Tracker	Prec	1.00	1.00	0.99	0.99	0.99	0.95	0.95
	Rec	0.04	0.35	0.59	0.68	0.70	0.69	0.71
Final Detector	Prec	1.00	0.99	1.00	0.99	0.99	0.98	0.98
	Rec	0.01	0.25	0.49	0.58	0.58	0.61	0.63
$\theta_L = 0.80$								
Online detector +Tracker	Prec	1.00	0.97	0.94	0.91	0.91	0.90	0.87
	Rec	0.22	0.59	0.70	0.72	0.72	0.71	0.72
Final Detector	Prec	1.00	1.00	0.97	0.93	0.95	0.94	0.89
	Rec	0.08	0.46	0.59	0.61	0.65	0.65	0.64
$\theta_L = 0.70$								
Online detector +Tracker	Prec	0.98	0.99	0.94	0.94	0.90	0.87	0.87
	Rec	0.09	0.57	0.73	0.79	0.78	0.77	0.65
Final Detector	Pre	1.00	1.00	0.99	0.97	0.94	0.90	0.93
	Rec	0.01	0.35	0.57	0.66	0.68	0.67	0.59

Table 5.2: Performance of P-N learning as a number of runs through the video.

classifier was kept in memory and used as the initial classifier in the next run. The performance was then accessed using precision and recall as a function of number of runs over the sequence. We investigated both the performance of the Final detector as well as the Online detector + Tracker. This experiment was repeated four-times for different parameter θ_L which corresponds to rate of learning. The parameter θ_L is discussed in chapter 6 section 6.3.6.

The results are presented in table 5.2. Notice the third sub-table with $\theta_L = 0.80$. In the first iteration, Online detector + Tracker discovers 22% of the trajectory, while the Final detector only 8% at the same precision of 100%. With every iteration, the recall of both of them increases. For $\theta_L = 0.95$ the learning process does not start at all. The learning is too conservative in that case. For $\theta_L = 0.70$ the overall performance first increases but around 5th iteration it slightly drops and oscillates.

5.4 Conclusions

In P-N learning, a novel approach for the processing of labeled and unlabeled examples, has been proposed. The underlying assumption of the learning process is that the unlabeled data are structured. The structure of the data is exploited by positive and negative experts that restrict the labeling of the unlabeled data. These experts provide a feedback about the performance of the classifier which is iteratively improved in a bootstrapping fashion. We have formulated conditions under which the P-N learning guarantees improvement of the classifier. The conditions have been validated on synthetic and real data. The P-N learning has been applied to the problem of learning of an object detector from a single example and an unlabeled video sequence. We have proposed experts that exploit the spatio-temporal properties of a video. These results open questions such as: (i) under what conditions these experts fail, and (ii) how to design other experts. These questions are covered chapters 6 and 7.

Chapter 6

Tracking-Learning-Detection (TLD)

This chapter defines, implements and evaluates a new tracking paradigm that we reffer to as Tracking-Learning-Detection (TLD). The chapter is structured as follows. Section 6.1 introduces the main idea behind TLD. Section 6.2 formalizes the TLD framework. Section 6.3 describes our implementation. Section 6.4 performs a set of comparative experiments with state-of-the-art approaches. Section 6.5 applies the TLD framework to long-term tracking of human faces. Finally, section 6.6 performs a set of qualitative experiments and discusses the pros and cons.

6.1 Introduction

Consider a video stream and a single bounding box defining the object of interest in one frame. The goal of long-term tracking is to track the object "forever": every time, the object appears in the camera view, a long-term tracker should draw a bounding box around it. As we have discussed in chapter 2, the long-term tracking problem is closely related to frame-to-frame tracking and tracking-by-detection.

Frame-to-frame tracking assumes that the object moves on a smooth trajectory. Trackers are able to adapt to changes of the object appearance, however, they typically fail if

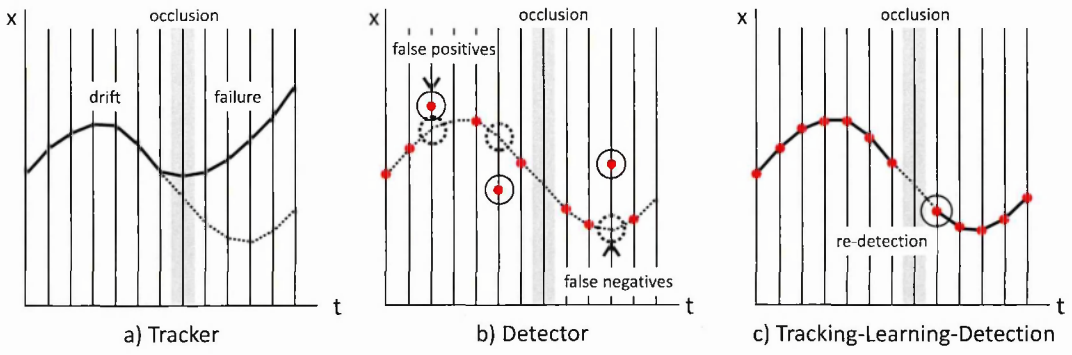

Figure 6.1: Illustration of a tracker (a), detector (b), and a tractor (c). Dotted line shows ground truth trajectory, gray bar represents full occlusion, thick line is the trajectory of a tracker, red dots are responses of a detector.

the object gets fully occluded or disappears. In contrast, tracking-by-detection assumes that the object model is known in advance. The detectors never fail due to occlusion or disappearance, however, the object model is fixed which means that unexpected appearances cannot be detected (false positives) and cluttered background may generate false detections (false positives). Obviously, both of these assumptions are too restrictive for the long-term tracking problem.

In a number of tracking problems, the objects occasionally reappear with previously observed appearance. This has been already used to reduce drift of frame-to-frame tracking [Dowson 05, Rahimi 08], closing loops in SLAM [Newman 06] or tracking of people [Ramanan 05]. The idea of this chapter is to build online an object detector that represents all appearances observed so far. This detector shall run in parallel with an object tracker and correct or re-initalize it when necessary. Tracking is then understood not only as a way to determine the location of the object, but also as a way to provide training examples for the online trained object detector. Any algorithm, that combines an object **trac**ker with an online learned detec**tor** will be refered to as **tractor**. See figure 6.1 for comparison of a tracker, a detector and a tractor.

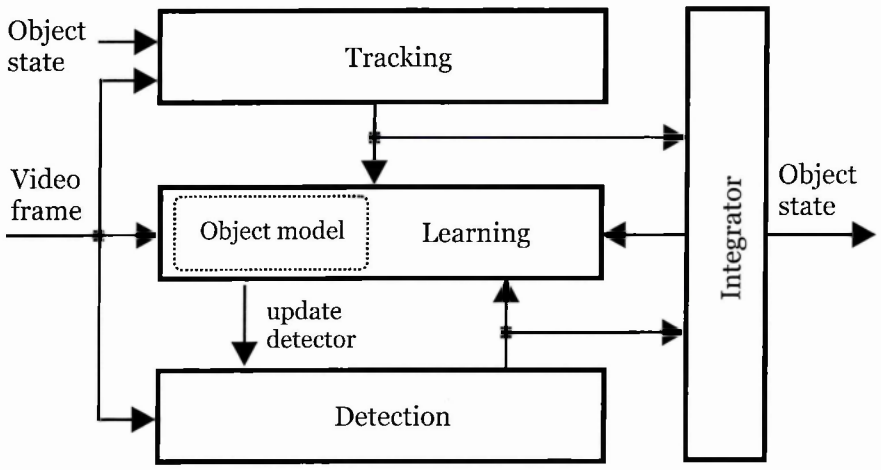

Figure 6.2: Detailed block diagram of the TLD framework.

6.2 Framework

TLD is designed for long-term tracking of unknown objects in unconstrained environments. In addition, TLD enables tracking of objects the class of which is known in advance. This section describes the TLD on the highest level. The block diagram is shown in figure 6.2.

6.2.1 Components

The framework consists of four components: tracker, learning, detector and integrator. These components have the following characteristics:

1. **Tracker** is an exploratory and error-prone component of TLD. The tracker estimates frame-to-frame object motion and is adaptive in order to handle appearance and illumination changes. It is not assumed that the tracker is correct all the time. Automatic detection of tracking failures is an important, but not required feature.

2. **Learning** is an analyzing component that maintains an *object model.* The object model. Learning constantly analyzes the output of the tracker and the detector, estimates errors performed by the detector and updates the object model to avoid these errors in the future.

3. **Detector** is a stabilizing component of the system that detect the appearances represented in the constantly updated object model. The detector is either build entirely online, or the online information is integrated with prior information about the object class. The detector must enable efficient incremental update.

4. **Integrator** is a component that merges the hypotheses from the detector and the tracker and outputs the *final hypothesis* about the object state.

TLD distinguishes two modes: (i) initialization, and (ii) run-time.

6.2.2 Initialization

The initialization requires the first frame and the corresponding object state indicated by a bounding box. In addition, the framework may accept images depicting the object from multiple views or background images where the object is not present. The following operations are then performed:

- *Initialization of the tracker:* involves setting the initial state (e.g. extraction of a template or training of a classifier).
- *Initialization of the object model:* involves inserting the given example(s) of the object and examples of the background into the object model.
- *Initialization of the detector:* involves training an object detector to detect the appearances represented in the object model. We shall refer to the resulting detector as the *Initial detector.*

After initialization, the TLD framework is prepared to process the video stream frame-by-frame.

6.2.3 Run-time

At each time instance, the framework accepts a video frame and passes it in parallel to the tracker, the detector and the learning component. The tracker estimates the object motion based on its previous state and outputs a single hypothesis. The detector returns a number of hypotheses about the location of the target object. The tracker's and detector's hypotheses are passed to the integrator, which merges them into the final state that is then output from the system. Outputs of the tracker, the detector and the integrator are analyzed by the learning block, which estimates errors and updates the detector to avoid these errors in the future.

6.3 Implementation

This section describes our implementation of the TLD framework, which we refer to as *TLD1.0*. We start by defining the object representation in section 6.3.1 and the object model in section 6.3.2. The following sections discuss the individual components. Section 6.3.3 introduces our detector, which is based on a cascaded classifier and enables integration of an offline learned detector developed in chapter 4. Section 6.3.4 mentions the adaptation of the Median-Flow tracker developed in chapter 3. Section 6.3.5 discusses the integration of the detector and the tracker. Finally, section 6.3.6 discusses the realization of the learning component that is based on the P-N learning developed in chapter 5.

6.3.1 Object representation

Object state. At any time instance, the object state is defined by a bounding box or indicates that the object is not visible. The bounding box has a fixed aspect ratio (given by the initial bounding box) and is parameterized by its location and scale. Other parameters such as in-plane rotation are not considered. Spatial similarity of two bounding boxes is measured using overlap, which is defined as a ratio between intersection and union of the two bounding boxes.

Object appearance. A single instance of the object's appearance is represented by an image patch P. The patch is sampled within the object bounding box and then is re-sampled to a normalized resolution (typically 15x15 pixels) regardless of the aspect ratio. The similarity between two patches $\mathrm{P_i}, \mathrm{P_j}$ is defined as

$$\mathrm{S(P_i, P_j)} = 0.5(\mathrm{NCC(P_i, P_j)} + 1), \tag{6.1}$$

where NCC is a Normalized Correlation Coefficient. The similarity ranges from 0 to 1.

Object trajectory. A sequence of object states defines a *trajectory* of an object in the video volume as well as the corresponding trajectory in the appearance space. Note that the trajectory is fragmented as the object may not be always visible. See figure 6.3 for illustration.

6.3.2 The object model

The object model M is a dynamic data structure that represents the object appearances and its surroundings observed so far. It is a collection of positive and negative patches, $M = \{\mathrm{P}_1^+, \mathrm{P}_2^+, \ldots, \mathrm{P}_\mathrm{m}^+, \mathrm{P}_1^-, \mathrm{P}_2^-, \ldots, \mathrm{P}_\mathrm{n}^-\}$, where P^+ and P^- represent the object and background patches, respectively. Positive patches are *ordered* according to the time when the patch was added to the collection. $\mathrm{P}_1^+$is the first positive patch added to the collection, P_m^+ is the last positive patch added to the collection.

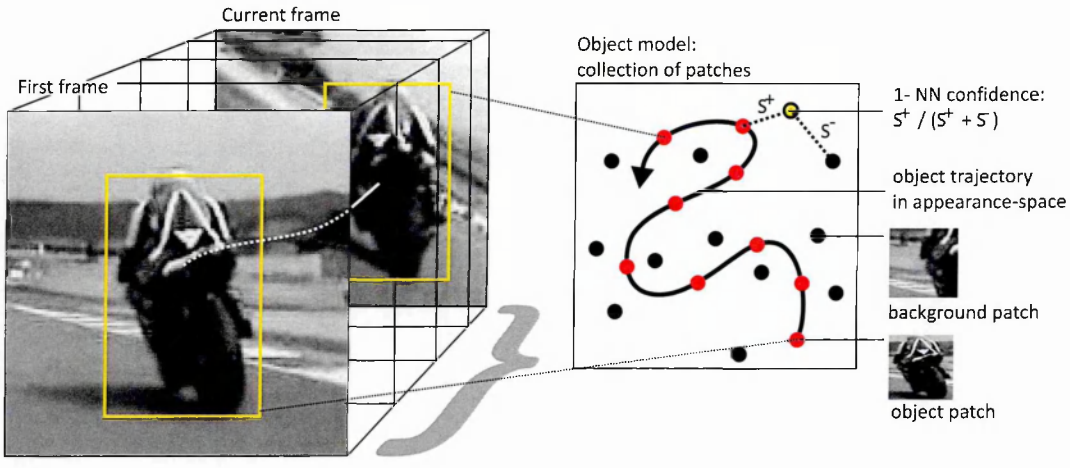

Figure 6.3: Illustration of a trajectory in video volume and corresponding trajectory in the appearance space.

We define several similarity measures which are used througout the system to indicate how much an arbitrary patch P resembles the object appearances represented in the model M:

1. Similarity with the positive nearest neighbor, $S^+(\mathrm{P}, M) = \max_{\mathrm{P}_i^+ \in M} S(\mathrm{P}, \mathrm{P}_i^+)$.
2. Similarity with the negative nearest neighbor, $S^-(\mathrm{P}, M) = \max_{\mathrm{P}_i^- \in M} S(\mathrm{P}, \mathrm{P}_i^-)$.
3. *Relative similarity*, $S^r = \frac{S^+}{S^+ + S^-}$. Relative similarity ranges from 0 to 1, higher values mean more confident that the patch depicts the object.
4. *Conservative similarity*, $S^c = \frac{S_\theta^+}{S_\theta^+ + S^-}$, similar to the relative similarity, however it considers only the first 50% of positive example in the object model. In order to realize the conservative similarity it is important to keep the positive patches ordered since then it is trivial to select the first half from them.

The Relative similarity is used to define the **Nearest Neighbor** (NN) classifier: a patch P is classified as positive if $S^r(\mathrm{P}, M) > \theta_{\mathrm{NN}}$. Parameter θ_{NN} enables tuning the nearest neighbor classifier either towards precision or recall. The classification margin is defined as $S^r(\mathrm{P}, M) - \theta_{\mathrm{NN}}$. The margin indicates the confidence of the classification.

Model update. To integrate a new labeled patch to the object model, the following strategy is used. The patch is first classified by the NN classifier and added to the collection only if the classification is incorrect. This strategy leads to a significant reduction of accepted patches [Aha 91] at the cost of coarser representation of the decision boundary. Therefore we alter this strategy by adding also patches where the classification margin is smaller than λ. With larger λ, the model accepts more patches which leads to better representation of the decision boundary. In our experiments, we use $\lambda = 0.1$ which compromises the accuracy of the representation and the speed by which is the collection grows. Exact setting of this parameter is not critical.

6.3.3 The object detector

The object detector is an algorithm that localizes the appearances represented in the object model. The detector scans the input image by a scanning-window and for each patch decides about presence or absence of the object.

Scanning-window grid. We generate all possible scales and shifts of an initial bounding box with the following parameters: scales step 1.2, horizontal step 10% of width, vertical step 10% of height, minimal bounding box size 20 pixels. This setting produces around 50 000 bounding boxes for a QVGA image (240x320), the exact number depends on the aspect ratio of the initial bounding box. In-plane rotations of the objects are not addressed explicitly.

Cascaded classifier. As the number of bounding boxes to be evaluated is large, the classification of individual patches has to be efficient. A straightforward approach of directly evaluating the NN classifier is problematic as it involves the search for two nearest neighbors (positive and negative) in a high dimensional feature space. To speed up the process, the classifier is structured into three stages: (i) patch variance, (ii) ensemble classifier, and (iii) nearest neighbor. Each stage either rejects the patch in question or passes it to the next stage. This cascaded architecture is common in

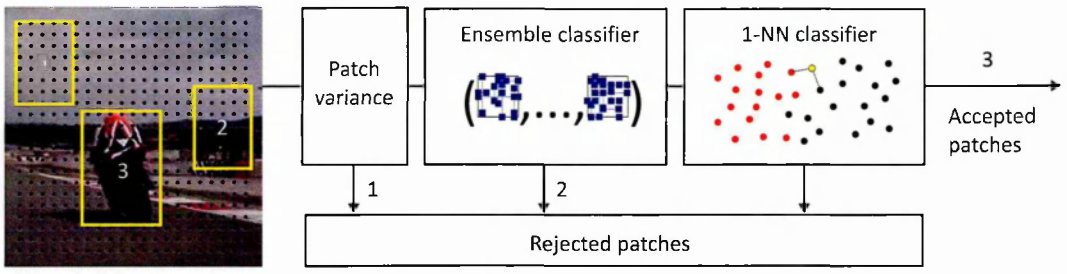

Figure 6.4: The block diagram of the object detector.

face detection [Viola 01] where it enabled real-time performance. Figure 6.4 shows the block diagram of our detector.

Patch variance. Patch variance is the first stage of our detector. This stage rejects all patches, for which the gray-value variance is smaller than a threshold. We set the threshold to 50% of the variance of the initial patch. Our implementation exploits the fact that variance of a patch p can be expressed as $\mathbb{E}(\mathrm{P}^2) - \mathbb{E}^2(\mathrm{P})$, and that the expected value $\mathbb{E}(\mathrm{P})$ can be measured in constant time using integral images [Viola 01]. This stage typically rejects more than 50% of non-object patches (sky, street, etc).

Ensemble classifier. The ensemble classifier is the second stage of our detector. The input to the ensemble is an image patch that was not rejected by the first stage. The ensemble consists of n *base classifiers*. Each base classifier i performs a number of *pixel comparisons* on the patch resulting in a binary code x, which indexes to an array of *posteriors* $\mathbf{P}_i(y|x)$, where $y \in \{-1, 1\}$. The posteriors of individual base classifiers are averaged. The patch is classified as positive if the average posterior is larger than 50%. Figure 6.5 shows the block diagram of the ensemble classifier.

Pixel comparisons. Every base classifier is based on a set of pixel comparisons. Similarly as in [Lepetit 06, Ozuysal 07, Calonder 10], the pixel comparisons are generated offline and stay fixed in run-time. The pixel comparisons are used to convert an image patch to a binary code. First, the image is convolved with a Gaussian kernel with standard deviation of 3 pixels to increase the robustness to shift and image noise. Next, the predefined set of pixel comparison is stretched to the patch. Each comparison re-

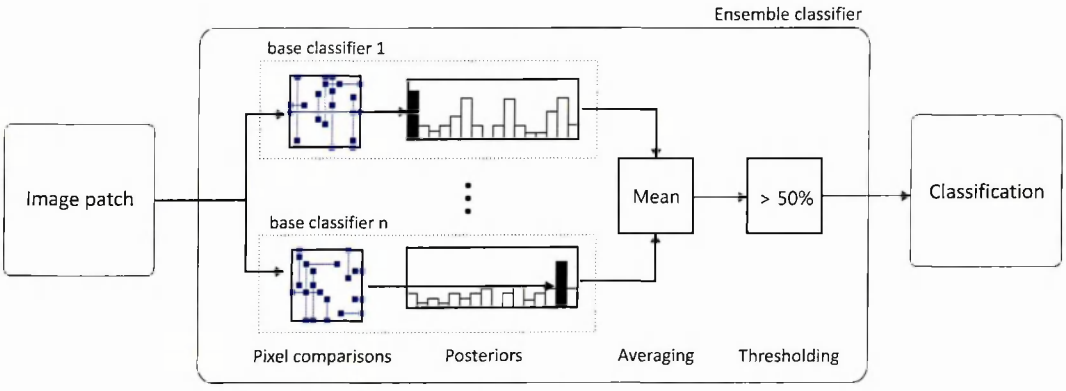

Figure 6.5: The block diagram of our ensemble classifier.

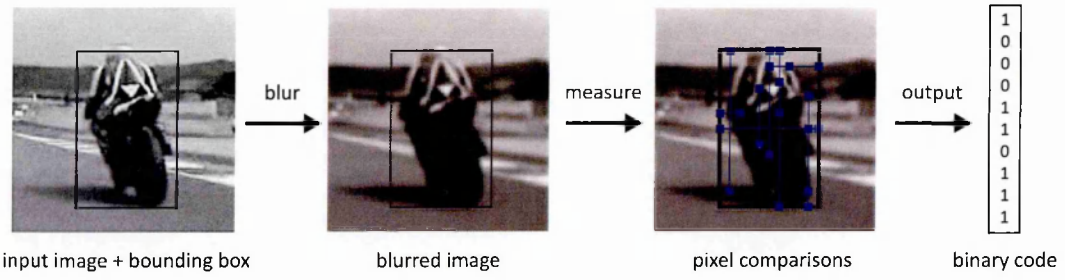

Figure 6.6: Conversion of a patch to a binary code using a set of pixel comparisons.

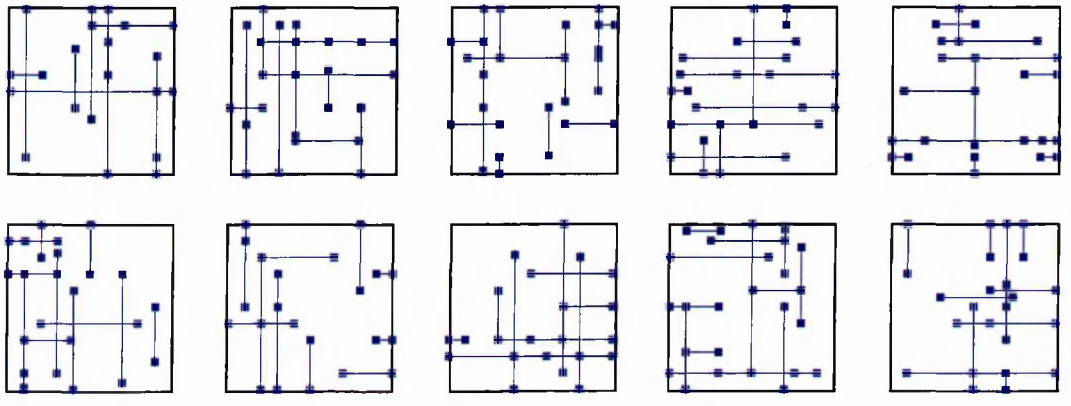

Figure 6.7: Pixel comparisons measured within individual base classifiers. The rectangles correspond to a normalized patch. Squares correspond to pixel locations, lines show which pixels are compared.

turns 0 or 1 and these measurements are concatenated into a binary code x. Figure 6.6 illustrates the process.

Generating pixel comparisons. The vital element of ensemble classifiers is the independence of the base classifiers [Breiman 01]. The independence of the classifiers is in our case enforced by measuring different pixel comparison by each base classifier. First, we discretize the space of pixel locations within a normalized patch and generate *all* possible horizontal and vertical pixel comparisons. Comparisons of zero length are not considered. Next, we permute the comparisons and split them into the base classifiers. As a result, every classifier is guaranteed to be based on a different set of features and all the features together uniformly cover the entire patch. This is in contrast to other approaches [Lepetit 06, Ozuysal 07, Calonder 10], where every pixel comparison is generated independently of other pixel comparisons. Figure 6.7 shows the pixel comparisons used in our implementation.

Posterior probabilities. Every base classifier i maintains a distribution of posterior probabilities $\mathbf{P}_i(y|x)$. The distribution has 2^d entries, where d is the number of pixel comparisons. We use 13 comparison, which gives 8192 possible codes that index to the posterior probability. The probability is estimated as $\mathbf{P}_i(y|x) = \frac{\#p}{\#p+\#n}$, where $\#p$ and $\#n$ correspond to number of positive and negative patches, respectively, that were assigned the same binary code. 10 base classifiers are used in our implementatin. This is mainly motivated by the requirement for real-time performance. If the speed is not an issue the number of base classifiers can be increased [Breiman 01] in order to increase the performance of the ensemble.

Initialization and update. In the initialization stage, all base posterior probabilities are set to zero, i.e. they vote for a negative class. During run-time, the ensemble classifier is updated as follows. The labeled example is classified by the ensemble and if the classification is incorrect, the corresponding $\#p$ and $\#n$ are updated which consequently updates $\mathbf{P}_i(y|x)$.

Nearest neighbor classifier. After filtering the patches by the first two stages, the last

stage is left with several bounding boxes that are not decided yet (≈ 50). The last stage employs the NN classifier based on the online model. A patch is classified as the object if $S^r > \theta_{\text{NN}}$. In our experiments we set $\theta_{\text{NN}} = 0.6$.

6.3.4 The object tracker

The tracking component of TLD1.0 is based on the Median-Flow tracker developed in chapter 3, which was augmented with failure detection. The Median-Flow tracker represents the object by a bounding box and estimates its motion between consecutive frames. Internally, the tracker estimates displacements of a number of points within the object's bounding box, estimates their reliability, and votes with 50% of the most reliable displacements for the motion of the bounding box using the median. A grid of 10×10 points is used. The motion of each individual point is estimated using the pyramidal implementation of Lucas-Kanade tracker [Bouguet 99]. The pyramidal Lucas-Kanade tracker uses 2 levels of the pyramid and represents the points by 11×11 patches.

Failure detection. Let δ_i denote the displacement of a single point of the Median-Flow tracker and δ_m be the median displacement of all points. A failure of the tracker is declared if Median Absolute Deviation (MAD) is larger than a threshold, $\text{median}(|\delta_i - \delta_m|) > 10$ pixels. This heuristic is able to reliably identify most failures caused by fast motion or fast occlusion of the object of interest. In that case, the individual displacement become scattered around the image and the MAD rapidly increases. If the failure is detected, the tracker does not return any bounding box.

6.3.5 The integrator

The integrator is a function that combines the responses of the tracker and the detector into a single response. If neither the tracker nor the detector output a bounding box,

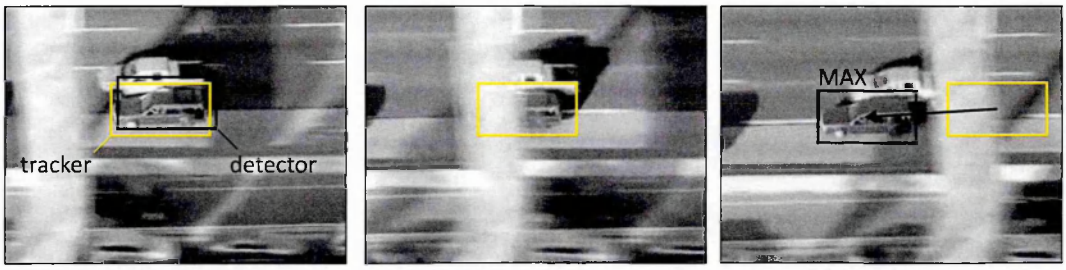

Figure 6.8: Illustration of integrator: (a) the object is tracked and detected, (b) the tracker is challenged by occlusion, detector has no response, (c) the tracker failed, the detector re-detects the object; these two patches are assigned conservative similarity S^c. Appearance that is in the online model earlier (car) receives higher score, new appearance (failed) receives lower score and the tracker is re-initialized (arrow).

the object is declared as not visible. Otherwise the integrator outputs the maximally confident bounding box, measured using the Conservative similarity S^c. The integrator is illustrated in figure 6.8.

Smoothing the trajectory. The object trajectory obtained by taking the maximally confident bounding box has one disadvantage: the trajectory tends to jitter. This is caused by the detector, which often has multiple responses close to the tracker, these might overrule the non-jittering tracker. Therefore, we further modified the integrator as follows. If the tracker's bounding box is defined and the maximally confident detection is in its vicinity (overlap > 0.8), the tracker bounding box is averaged with all detections that are in the tracker's vicinity. If the maximally confident detection is far from the tracker (overlap < 0.8), the tracker is re-initialized.

6.3.6 The learning component

The task of the learning component is to train the Initial detector in the first frame and bootstrap its performance at run-time using the P-expert and the N-expert.

Initialization

The Initial detector is trained using labeled examples that are generated as follows. The positive training examples are synthesized from the initial bounding box. First, we select 10 bounding boxes from the scanning grid that are closest to the initial patch. For each of the bounding boxes, 20 warped versions are generated. The parameters of the warping are drawn randomly from a uniform distribution of shift $\pm 1\%$, scale change $\pm 1\%$ and in-plane rotation $\pm 10°$. The warped patches are added with Gaussian noise ($\sigma = 5$). The result is 200 synthetic positive patches. Negative patches are collected from the surrounding of the initial patch, no synthetic negative examples are generated. If the application requires fast initialization, the training examples are sub-sampled. The labeled training patches are then update the object model as discussed in subsection 6.3.2 and the ensemble classifier as discussed in subsection 6.3.3. After the initialization, the Initial detector is ready for run-time.

The P-expert

The goal of the P-expert is to discover new appearances of the object and thus increase the generality the object detector. Section 5.3 suggested a P-expert that exploits the fact that the object moves on a trajectory. The object trajectory is generated by a combination of the tracker, the detector and the integrator. This combined process traces a discontinuous trajectory, which is by no means correct all the time as any of the components can fail. The challenge of the P-expert is to estimate *reliable* parts of the trajectory and use it to generate positive training examples.

Consider an object model represented as colored points in a feature space. Positive examples are represented by red dots connected by a directed curve suggesting their order, negative examples are black. Using the conservative similarity S^c, one can define a subspace in the feature space, where $S^c > \theta_L$. We refer to this subspace as the *core* of the object model.

The P-expert estimates the reliable parts of the trajectory as follows. The trajectory becomes reliable as soon as it enters the core and remains reliable until is re-initialized or the tracker declares its own failure. Any other trajectory is not considered by the P-expert. The reliable trajectory generates positive examples that are then added to the object model. See figure 6.9 for illustration.

Parameter θ_L defines the extend of the "core", influences the rate by which the trajectories are validated and hence the rate of learning. As we have seen in experiment 5.3.3, high values may result in situation when no learning takes place. On the other hand low value may lead to degradation of the classifier. The exact setting of the parameter is data dependent however it turned out that $\theta_L = 0.70$ works for majority of cases. This parameter is used in all of our experiments.

In every frame, the P-expert outputs a decision about the reliability of the current location output by the integrator. If the current location is reliable, the P-expert generates a set of positive examples that update the object model and the ensemble classifier. First, we select 10 bounding boxes from the scanning grid that are closest to the initial patch. For each of the bounding boxes, 10 warped versions are generated. The parameters of the warping are drawn randomly from a uniform distribution of shift $\pm 1\%$, scale change $\pm 1\%$ and in-plane rotation $\pm 5°$. The warped patches are added with Gaussian noise ($\sigma = 5$). This results in 100 synthetic positive examples for the ensemble classifier. For efficiency reasons, we consider only 10 patches for the update of the object model.

The N-expert

The N-expert generates negative training examples with the aim to discriminate the detector against background clutter. The key assumption of the N-expert is that the object can occupy at most one location in the image. The N-expert is applied at the same time as P-expert. In that case, patches that are far from current bounding box

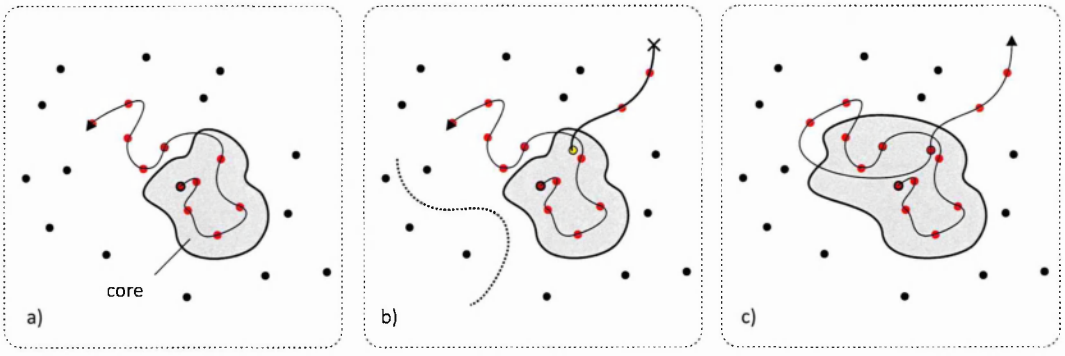

Figure 6.9: Illustration of the P-expert: (a) an object model in a feature space and the core (gray blob); (b) a non-reliable trajectory (dotted line) and a reliable trajectory (thick line); (c) the object model and the core after the update.

(overlap < 0.2) are all labeled as negative.

6.4 Quantitative evaluation

This section reports on a set of quantitative experiments comparing the TLD1.0 with relevant algorithms. The first two experiments evaluate the TLD1.0 on benchmark data sets that are commonly used in the literature. In particular, the experiment in section 6.4.1 extends the results reported in [Santner 10]. The experiment in section 6.4.2 extends the results from [Yu 08]. In both cases, a saturated performance is achieved. Section 6.4.3 therefore introduces a more challenging data set and performs further evaluation.

Every experiment in this section adopts the following evaluation protocol. A tracker is initialized in the first frame of a sequence and tracks the selected object up to the end of the sequence. The produced trajectory is then compared to ground truth. The particular evaluation measure is specified in every experiment. TLD1.0 has been compared with 11 comparable algorithms on 19 benchmark sequences. See Appendix A for more details about the algorithms and Appendix B for the sequences.

6.4.1 Comparison 1: CoGD

TLD1.0 was compared with results reported in [Yu 08], which reports on performance of 5 trackers: (i) Incremental Visual Tracking (IVT) [Ross 07], (ii) Online Discriminative Features (ODF) [Collins 05], (iii) Ensemble Tracking (ET) [Avidan 07], (iv) Multiple Instance Learning (MILTrack) [Babenko 09], and (v) Co-trained Generative and Discriminative tracker (CoGD) [Yu 08]). The evaluation was performed on 6 sequences that include full occlusions and disappearance of the object. CoGD [Yu 08] clearly dominated on these sequences as it is capable of re-detection of the object. The performance was assessed using the *Number of successfully tracked frames,* i.e. the number of frames where overlap with a ground truth bounding box is larger than 50%. Frames where the object were occluded were not counted. For instance, for a sequence of 100 frames where the object is occluded in 20 frames, the best possible score is 80 frames.

Table 6.1 shows the results. TLD1.0 achieved the maximal possible score in all sequences and matched the performance of CoGD [Yu 08]. It was reported in [Yu 08] that CoGD runs at 2 frames per second, and requires several frames (typically 6) for initialization. In contrast, TLD1.0 requires just a single frame and runs at 20 frames per second.

This experiment demonstrates that neither the generative trackers (IVT [Ross 07]), nor the discriminative trackers (ODF [Collins 05], ET [Avidan 07], MILTrack [Babenko 09]) are able to handle long-lasting full occlusions or disappearance of the object. CoGD is evaluated in detail on more challenging data in section 6.4.3.

6.4.2 Comparison 2: PROST

TLD1.0 was compared with the results reported in [Santner 10], which reports on performance of 5 algorithms: (i) Online Boosting (OB) [Grabner 06], (ii) Online Random

Sequence	Frames	Occlusion	IVT [Ross 07]	ODF [Collins 05]	ET [Avidan 07]	MILTrack [Babenko 09]	CoGD [Yu 08]	**TLD1.0**
David	761	0	17	-	94	135	759	**761**
Jumping	313	0	75	**313**	44	**313**	**313**	**313**
Pedestrian 1	140	0	11	6	22	101	**140**	**140**
Pedestrian 2	338	93	33	8	118	37	**240**	**240**
Pedestrian 3	184	30	50	5	53	49	**154**	**154**
Car	945	143	163	-	10	45	**802**	**802**

Table 6.1: The number of successfully tracked frames – TLD1.0 in comparison to results reported in [Yu 08]. Bold numbers indicate the best score; a dash indicates that the result was not reported. TLD1.0 achieved the best possible performance.

Forrest (ORF) [Saffari 09], (iii) Fragment-based Tracking (FT) [Adam 06], (iv) Multiple Instance Learning (MILTrack) [Babenko 09] and (v) PROST [Santner 10]). The evaluation was performed on 10 sequences, which includes partial occlusions and pose changes. The performance was reported using two measures: (i) *Recall* - number of true positives (50% overlap) divided by the sequence length, and (ii) *Localization error* - average distance between the predicted and the ground truth bounding box centers.

TLD1.0 estimates the scale of an object. However, the algorithms compared in this experiment perform tracking in single scale only. In order to make a fair comparison, the scale estimation was not used in this experiment.

Table 6.2 shows the performance measured by *Recall*. TLD1.0 scored best in 9/10 outperforming by more than 12% the second best. Table 6.3 shows the performance measured by *Localization error*. TLD1.0 scored best in 7/10 being 1.6 times more accurate than the second best.

6.4.3 Comparison 3: TLD data set

The previous experiments show that TLD1.0 performs well on benchmark sequences where the recall is in the range 90 - 100. We consider these sequences as saturated and

Sequence	Frames	OnlineBoost [Grabner 06]	OnlineRF [Saffari 09]	FragTrack [Adam 06]	MILTrack [Babenko 09]	Prost [Santner 10]	**TLD1.0**
Girl	452	24.0	-	70.0	70.0	89.0	**93.1**
David	502	23.0	-	47.0	70.0	80.0	**100.0**
Sylvester	1344	51.0	-	74.0	74.0	73.0	**97.4**
Face occlusion 1	858	35.0	-	**100.0**	93.0	**100.0**	98.9
Face occlusion 2	812	75.0	-	48.0	96.0	82.0	**96.9**
Tiger	354	38.0	-	20.0	77.0	79.0	**88.7**
Board	698	-	10.0	67.9	67.9	75.0	**87.1**
Box	1161	-	28.3	61.4	24.5	91.4	**91.8**
Lemming	1336	-	17.2	54.9	83.6	70.5	**85.8**
Liquor	1741	-	53.6	79.9	20.6	83.7	**91.7**
Mean	-	42.2	27.3	58.1	64.8	80.4	**92.5**

Table 6.2: Recall – TLD1.0 in comparison to results reported in [Santner 10]. Bold numbers indicate the best score; a dash indicates that the result was not reported. TLD1.0 scored best in 9/10 sequences.

Sequence	Frames	OnlineBoost [Grabner 06]	OnlineRF [Saffari 09]	FragTrack [Adam 06]	MILTrack [Babenko 09]	PROST [Santner 10]	**TLD1.0**
Girl	452	43.3	-	26.5	31.6	19.0	**18.1**
David	502	51.0	-	46.0	15.6	15.3	**4.0**
Sylvester	1344	32.9	-	11.2	9.4	10.6	**5.9**
Face occlusion 1	858	49.0	-	6.5	18.4	**7.0**	15.4
Face occlusion 2	812	19.6	-	45.1	14.3	17.2	**12.6**
Tiger	354	17.9	-	39.6	8.4	7.2	**6.4**
Board	698	-	154.5	154.5	51.2	37.0	**10.9**
Box	1161	-	145.4	145.4	104.5	**12.1**	17.4
Lemming	1336	-	166.3	166.3	**14.9**	25.4	16.4
Liquor	1741	-	67.3	67.3	165.1	21.6	**6.5**
Mean	-	32.9	133.4	78.0	46.1	18.4	**10.9**

Table 6.3: Localization error (pixels) – TLD1.0 in comparison to results reported in [Santner 10]. Bold numbers indicate the best score; a dash indicates that the result was not reported. TLD1.0 scored best in 7/10 sequences.

intorduce new, more challenging ones.

The **TLD data set** consists of 10 sequences. The sequences 1-6 have been used in experimentt 6.4.1 and include: David, Jumping, Pedestrian 1, Pedestrian 2, Pedestrian 3 and Car. The sequences 7-10 are new and include: Motorbike, Volkswagen, Car Chase and Panda. These sequences are long and contain all the challenges outlined in the chapter 1. All sequences were manually annotated with ground truth. In every frame, the object is defined by a bounding box or it is indicated that the object is not visible. More than 50% of occlusion or more than 90 degrees of out-of-plane rotation was annotated as "not visible". See Appendix B for more details. The TLD data set is available online at the website of the TLD project.[1]

Five tracking algorithms are compared on the TLD data set: (1) Online Boosting (OB) [Grabner 06], (2) Semi-Supervised Online Boosting (SOB) [Grabner 08], (3) Beyond Semi-Supervised Online Boosting (BSOB) [Stalder 09], (4) Multiple Instance Learning (MILTrack) [Babenko 09], and (5) Co-trained Generative and Discriminative tracker (CoGD) [Yu 08]. Binaries for trackers (1-3) are available in the Internet[2]. Tracker (4,5) were kindly evaluated directly by their authors.

The performance is evaluated using precision P, recall R and f-measure F. P is the number of true positives divided by number of all responses, R is the number true positivs divided by the number of object occurrences that should have been detected. F combines these two measures as $F = 2PR/(P+R)$. Since this experiment compares various trackers for which the default initialization (defined by the ground truth) might not be optimal, it was allowed to initialize the object arbitrarily. For instance, when tracking a motorbike racer, some algorithms might perform better when tracking only a part of the racer. Every trajectory was therefore normalized. A transformation that mapped the initializing bounding box to the ground truth bounding box was found (shift, aspect and scale) and this transformation was applied to every bounding box

[1] cmp.felk.cvut.cz/tld

[2] http://www.vision.ee.ethz.ch/boostingTrackers/

Sequence	Frames	OB [Grabner 06]	SOB [Grabner 08]	BSOB [Stalder 09]	MILTrack [Babenko 09]	CoGD [Yu 08]	**TLD1.0**
David	761	0.34	0.35	0.28	0.15	1.00	**1.00**
Jumping	313	0.09	0.17	0.15	1.00	1.00	**1.00**
Pedestrian 1	140	0.23	0.39	0.15	0.69	**1.00**	**1.00**
Pedestrian 2	338	0.21	0.77	0.04	0.11	0.81	**0.91**
Pedestrian 3	184	0.49	0.36	0.62	0.75	0.92	**0.99**
Car	945	0.73	0.80	0.72	0.24	**0.96**	0.94
Motocross	2665	0.01	0.05	0.00	0.03	0.45	**0.83**
Volkswagen	8576	0.04	0.04	0.01	0.07	0.11	**0.87**
Carchase	9928	0.06	0.09	0.19	0.07	0.08	**0.77**
Panda	3000	0.51	0.29	0.30	0.38	0.12	**0.60**
mean	26850	0.13	0.14	0.15	0.13	0.22	**0.81**

Table 6.4: F-measure – performance on the TLD data set. Bold numbers indicate the best score. TLD1.0 scored best in 9/10 sequences.

on the trajectory. The normalized trajectory was directly compared to ground truth using overlap and a true positive was considered if the overlap was larger than 25%. The earlier used threshold 50% was found to be too restrictive in this case. Sequences Motocross and Volkswagen were evaluated by the MILTrack [Babenko 09] only up to the frame 500 as the implementation required loading all images into memory in advance. Since the algorithm failed during this period the remaining frames were considered as failed.

Table 6.4 show the performance as measured by f-measure. The last row shows a weighted average performance (weighted by number of frames in the sequence). TLD1.0 achieved the best performance of 81% significantly outperforming the second best approach that achieved 22%, other approaches range between 13-15%. The performance is broken down to precision in table 6.5 and recall in table 6.6. This experiment demonstrates that TLD1.0 significantly outperforms state-of-the-art approaches on challenging data.

Sequence	Frames	OB [Grabner 06]	OSB [Grabner 08]	BOSB [Stalder 09]	MILTrack [Babenko 09]	CoGD [Yu 08]	**TLD1.0**
David	761	0.41	0.35	0.32	0.15	**1.00**	**1.00**
Jumping	313	0.47	0.25	0.17	1.00	1.00	**1.00**
Pedestrian 1	140	0.61	0.48	0.29	0.69	**1.00**	**1.00**
Pedestrian 2	338	0.77	0.85	**1.00**	0.10	0.72	0.89
Pedestrian 3	184	**1.00**	0.41	0.92	0.69	0.85	0.99
Car	945	0.94	**1.00**	0.99	0.23	0.95	0.92
Motocross	2665	0.33	0.13	0.14	0.05	**0.93**	0.89
Volkswagen	8576	0.39	0.04	0.02	0.42	0.79	**0.80**
Carchase	9928	0.79	0.80	0.52	0.62	**0.95**	0.86
Panda	3000	0.95	**1.00**	0.99	0.36	0.12	0.58
mean	26850	0.62	0.50	0.39	0.44	0.80	**0.82**

Table 6.5: Precision – performance on the TLD data set. Bold numbers indicate the best score. TLD1.0 achieved the precision of 82%, the second best achieved 80%.

6.5 Long-term tracking of faces

This section adopts the TLD1.0 system to tracking of human faces that we call the Face-TLD. We consider the same block structure of the system as outlined in figure 6.2 with the only modification in the object detector, where the ensemble classifier is replaced by a generic object detector developed in chapter 4. Our goal is to investigate whether the information about the object class helps in the long-term tracking or not.

6.5.1 Sitcom episode

This experiment compares the TLD1.0 with Face-TLD on a sitcom episode It Crowd (see appendix B). The episode is 22 minutes long (35471 frames) and contains a number of characters. For speed purposes the original frames were downsampled to resolution 320×176 pixels. Both systems were initialized on a face of one character (Roy) at his first appearance and automatically tracked the face up to the end of the sequence.

The TLD1.0 tracked correctly at the beginning of the episode, but failed to detect the

Sequence	Frames	OB [Grabner 06]	SOB [Grabner 08]	BSOB [Stalder 09]	MILTrack [Babenko 09]	CoGD [Yu 08]	TLD1.0
David	761	0.29	0.35	0.24	0.15	1.00	**1.00**
Jumping	313	0.05	0.13	0.14	1.00	0.99	**1.00**
Pedestrian 1	140	0.14	0.33	0.10	0.69	**1.00**	**1.00**
Pedestrian 2	338	0.12	0.71	0.02	0.12	**0.92**	**0.92**
Pedestrian 3	184	0.33	0.33	0.46	0.81	**1.00**	**1.00**
Car	945	0.59	0.67	0.56	0.25	0.96	**0.97**
Motocross	2665	0.00	0.03	0.00	0.02	0.30	**0.77**
Volkswagen	8576	0.02	0.04	0.01	0.04	0.06	**0.96**
Carchase	9928	0.03	0.04	0.12	0.04	0.04	**0.70**
Panda	3000	0.35	0.17	0.17	0.40	0.12	**0.63**
mean	26850	0.09	0.10	0.10	0.11	0.18	**0.81**

Table 6.6: Recall – performance on the TLD data set. Bold numbers indicate the best score. TLD1.0 achieved recall of 81%, the second best achieved 18%.

character in the second half. The overall recall was of 37% and precision of 70%. The Face-TLD was able to track the target throughout the entire episode leading to a recall of 54% and precision of 75%. The introduction of the face detector increased the recall by 17%. Both approaches processed the episode at 20 frames per second on laptop with Intel Core 2 Duo 2.4 GHz processor and 2GB RAM. Figure 6.10 shows several frames from the episode and the online model.

6.5.2 Surveillance footage

This section performs a quantitative comparison on sequence Surveillance (see appendix B). The sequence consists of 500 frames depicting interior of a shop with multiple people captured at 1 frame per second. The sequence cannot be tracked by pure face detector as there are multiple faces which occlude one another. Moreover, frame-to-frame tracking is difficult to apply because the frame-to-frame motion is large and the subjects move in and out of the camera view.

The TLD1.0 was again compared to Face-TLD. The TLD1.0 achieved a recall of 12%

Figure 6.10: Evaluation of Face-TLD on a sitcom episode "IT crowd". (TOP-LEFT) The initial frame. The entire sequence (22 minutes) was then processed automatically.

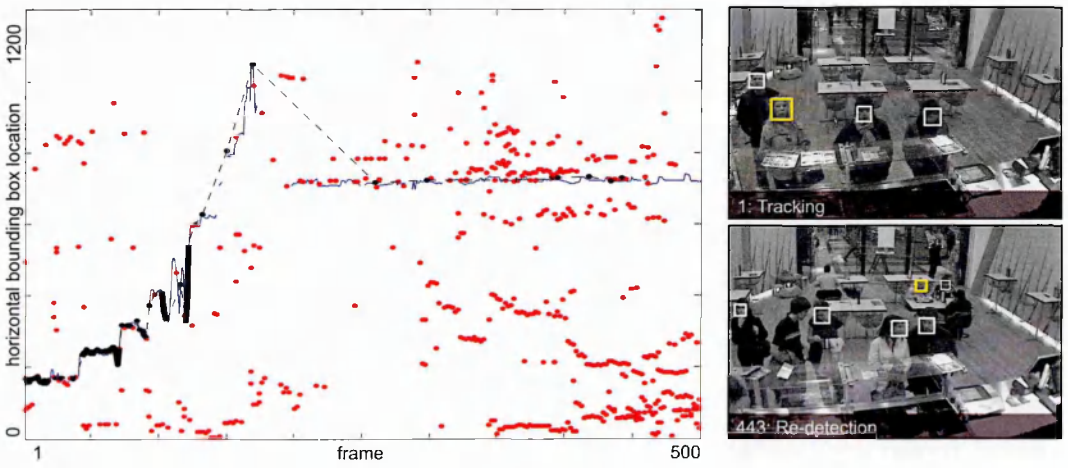

Figure 6.11: Evaluation of Face-TLD on sequence Surveillance. (LEFT) Responses of generic face detector (red), detections approved by online learned model (black), ground truth trajectory of the subject (blue). (RIGHT) The surveillance scenario.

and a precision of 57%, the Face-TLD achieved a recall of 35% and a precision of 79%. The introduction of face detector increased the recall by 23%. Figure 6.11 illustrates the scenario. This experiment demonstrates, that both TLD1.0 and Face-TLD are applicable to surveillance scenarios for tracking of faces. Furthermore, it shows that using a face detector increases the performance of the TLD system.

6.6 Qualitative analysis

This section discusses the strengths and weaknesses of TLD1.0 with respect to the challenges outlined in the chapter 1. The performance is illustrated on several snapshots from run-time of the system, where the following marking is used:

- *Yellow rectangle* - the bounding box output of the TLD1.0,
- *Gray dots* - detections output by the second stage of our detector,
- *Red dots* - detections output by the whole detector,
- *Blue dots* - the reliable points used by the Median-Flow tracker,
- *Patches to the left* - negative examples in the online model,
- *Patches to the right* - positive examples in the online model.
- Top left corner depict close-up of the object.

6.6.1 Strengths

Scale changes. TLD1.0 is robust to scale changes. Median-Flow estimates scale changes even when the target is partially out of the frame. Detector localizes the object in multiple scales. In sequence Volkswagen, the object of interest changes scale

Figure 6.12: TLD1.0 and scale changes.

Figure 6.13: TLD1.0 and illumination changes.

in the range from 20x20 to 100x100 pixels. The output of TLD1.0 is illustrated in figure 6.12.

Illumination changes. TLD1.0 is invariant to smooth changes in illumination. Median-Flow adapts the tracked templates and the detector is based on illumination invariant pixel comparisons and NCC. In sequence David, a face is tracked from a dark room to full illumination. Figure 6.13 shows the results.

Appearance changes. Median-Flow handles changes of appearance caused by pose change or articulations. The detector localizes all appearances observed in the past. In sequence Motocross, TLD1.0 learned all appearances of a motorbike from the rear view. However, it did not learn the side view. The detector was therefore not able to re-initialize a trajectory in that case. See figure 6.14 for illustration.

Figure 6.14: TLD1.0 and appearance changes.

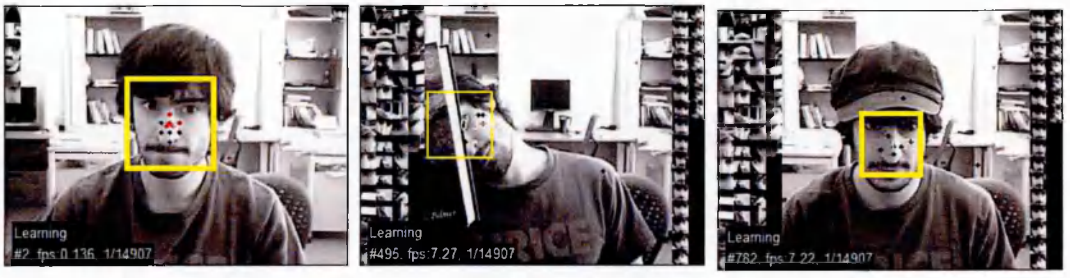

Figure 6.15: TLD1.0 and partial occlusions.

Partial occlusions. TLD1.0 deals with partial occlusions. Median-Flow tracker estimates reliable points within the bounding box and filters out parts of the object that are occluded. In sequence Face occlusion 2, the object of interest becomes partially occluded, but TLD1.0 is able to track these changes successfully as illustrated in figure 6.15.

Full occlusions and disappearances. The main power of TLD1.0 is the ability to re-detect the target after full occlusion or disappearance of the object from the scene. Figure 6.16 shows the re-detection in sequence Car. Note that the appearance of the car after occlusion is different from the initial appearance.

Similar targets. TLD1.0 is discriminative. If the object of interest is surrounded

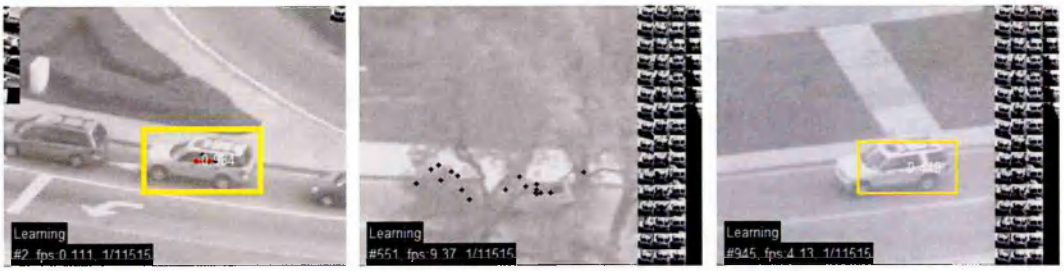

Figure 6.16: TLD1.0 and re-detection.

Figure 6.17: TLD1.0 and similar targets. The sequence appeared in [Kwon 10].

by objects of similar appearance or background clutter, the N-expert labels them as negative and inserts them to the online model. These negative examples then prevent the detector from confusing the object of interest with other objects. For instance in figure 6.17 the object of interest is a helmet of a football player. Notice that various appearances of the same helmet appear in positive examples, whereas different helmets occur in negative examples. This is best visible when zooming in on a display.

6.6.2 Weaknesses

Out-of-plane rotations. In case of out-of-plane rotation, Median-flow drifts away from the target. The tracker typically stays away until a detector re-initializes its position to previously seen appearance. For instance, figure 6.18 shows a sequence of an object performing out-of-plane rotation. From frame 1 to 168, the object performs out of plane rotation and the Median-Flow drifts. As the drift is slow, the failure of the tracker is not identified and the system is learning new incorrect appearances. In frame 176 the object re-appears in previously seen appearance and the trajectory is correctly

Figure 6.18: Out-of-plane rotations are challenging for TLD1.0. The sequence appeared in [Leichter 09].

Figure 6.19: TLD1.0 and sequences where the object never re-appear in a similar view. The sequence appeared in [Kwon 10].

re-initialized. Notice that the incorrect data produced by the drift did not prevent the tracker from correct re-initialization of the trajectory.

No previously seen appearances. Particularly challenging scenarios for TLD1.0 are scenes when the object never re-appears in previously observed appearance. For instance, figure 6.19 shows an example when tracking a face in a Soccer sequence from [Kwon 10]. The target object is tracked for a couple of frames but then fails due to occlusion combined with pose and expression changes. The target is never re-detected as the object never re-appears with previously observed appearance.

Chapter 7

Discussion

This chapter discusses the contributions of the thesis, reviews recent developments, and proposes possible avenues for future research.

7.1 Contributions

In this thesis, we have proposed a new paradigm for long-term tracking of unknown objects. Our approach was demonstrated on a number of challenging videos, and significantly outperformed state-of-the-art. The particular contributions are summarized below.

In chapter 3, we studied the long-term tracking problem from the perspective of frame-to-frame tracking. We accepted that frame-to-frame tracking is not a good model for this scenario as it leads to inevitable failures. Rather than trying to avoid these failures by directly designing a better frame-to-frame tracker, we proposed a novel measure that indicates the reliability of a tracker. The measure is based on the well known forward-backward consistency assumption. We demonstrated that the proposed measure provides complementary information to appearance-based NNC and SSD. Furthermore, we used the error measure to *improve* frame-to-frame tracking itself. We showed that

template tracking can be improved if the template is decomposed into independently tracked parts which are weighted based on their reliability and integrated using median estimator. The result is a novel template-based tracker (Median-Flow) which is robust to partial occlusions and appearance changes and outperforms comparable approaches.

In chapter 4, we studied the long-term tracking problem from the perspective of tracking-by-detection. We developed a novel learning method for supervised training of an object detector from a large data set. In particular, we focused on learning methods that combine bootstrapping and boosting. The theoretical contribution is the formalization of bootstrapping and boosting in a unified framework. Within this framework, we designed the optimal combination of the two approaches. The approach formulates bootstrapping as a weighted sampling where the weights are driven by boosting. The resulting combination demonstrated a significant improvement in terms of efficiency (both in training and testing) as well as the classifier accuracy in contrast to ad hoc combinations. The learning method has been applied to training face detectors (frontal and profile), which operate at video frame-rate on QVGA images. Such detectors are relevant to all long-term tracking scenarios, where the target object is a face. The learning method does not make any face-specific assumptions and can be applied to any other visual classes.

In chapter 5, we investigated the task of learning during long-term tracking. We have demonstrated that an accurate object detector can be trained from a single example and an unlabeled video stream using the following strategy: (i) evaluate the detector, (ii) estimate its errors, and (iii) update the detector. The main novelty of the method is the estimation of the detector errors, which is guided by two rules, which we call the *P-expert* and *N-expert*, respectively. P-expert estimates only false negatives and improves the detector generality. N-expert estimates only false positives and increases the detector discriminability. Estimation of the detector's errors independently based on their type enabled not only simpler design of the experts, but also mutual compensation of their errors. The theoretical contribution is the formalization of this learning

process as a discrete dynamical system, which allowed us to specify conditions, under which the learning guarantees improvement of the detector. We demonstrated, that the experts can be designed when considering spatio-temporal relationships in the video.

In chapter 6, we proposed a novel tracking framework (TLD) that decomposes the long-term tracking task into three sub-tasks: tracking, learning and detection. Building on the components developed in chapters 3, 4 and 5, we showed how to implement the TLD framework and how to achieve real-time performance. An extensive quantitative evaluation on benchmark sequences demonstrated saturated performance. Therefore, we introduced a new data set, ground truth and evaluation protocol and showed a significant improvement over state-of-the-art approaches. Finally, we applied TLD to the tracking of human faces and demonstrated how to incorporate an offline trained detector to further improve long-term tracking.

7.2 Recent development

The source code of TLD1.0 has been released under GPL v3.0 license and is available online [1]. A corresponding discussion group has currently over 1000 registered users. A presentation video[2] that explains TLD crossed 0.5 million hits within one month on YouTube. Moreover the author has been invited to give a Google Tech Talk [3].

The implementation of TLD has been demonstrated at Computer Vision and Pattern Recognition, 2010. The system has been running for more than 8 hours, tracking various objects in real-time. Figure 7.1 shows the setup of the demo and several snapshots taken automatically from the demo camera.

[1] https://github.com/zk00006/OpenTLD
[2] http://youtu.be/1GhNXHCQGsM
[3] http://youtu.be/lmG_FjG4Dy8

Figure 7.1: TLD demo at Computer Vision and Pattern Recognition conference, 2010.

7.3 Future work

Feedback. This thesis has shown that by introducing the P-N experts, one can improve an offline trained detector. In broader context, we have used feedback that is commonly used in control engineering or in artificial intelligence. On the other hand, in computer vision, is feedback not common. Traditionally, vision is more considered as a "sensor" that provides measurements. Majority of current approaches follow this philosophy and design systems that stay fixed in run-time and have constant performance characteristics. This approach leads to increasingly complex systems that essentially attempt to "avoid" errors in runtime. By introducing feedback to vision, one can reconsider the error as the opportunity to learn. A long term goal would be therefore to investigate computer vision systems, that extensively rely on feedback in run-time and therefore have the ability to improve them self.

Tracking multiple objects. A particularly promising direction is to adapt the TLD for tracking of a large number of small patches. One could imagine a scenario when hun-

dreds of points are tracked simultaneously, each of which has the property to learn its appearance on the fly, detect its disappearance and re-initialize its own trajectory when it becomes visible. Such an approach would be applicable in a number of applications. Extension of the ideas of TLD to optical flow is also an very promising direction that is becoming realistic with the increasing speed of processors and availability of GPU.

Tracking. In chapter 7, we have demonstrated that a relatively simple tracker coupled with a learning method and detector, significantly outperforms competing approaches. On the other hand, we observed that if the tracker fails too quickly (e.g. due to out-of-plain rotation), the detector is not able to re-initialize the tracker. Therefore one promising way to proceed is to strengthen the tracking itself, e.g. by running multiple trackers in parallel [Kwon 10] each of which would be based on different features and motion models. Such an approach would lead to a set of P-experts that would train the detector more quickly.

Detection. The detector used in our system is based on a scanning window and global representation of the object and as such is prone to occlusions. However, as we have reviewed in chapter 2, a number of detectors are based on local representations [Lowe 04] where partial occlusions are not an issue.

Learning. In chapter 5, we proposed a learning method (P-N Learning) which processes a video stream in one pass, considering only one frame at a time. Frames observed in the past were not used. While our motivation was mainly speed, this is no longer an issue for a multi-threaded architecture. One can imagine a second thread analysing the already processed frames, thus providing more training data for the detector. In an ideal case, the detector should reflect all the information received up to current time.

Faster implementation. While the current implementation of TLD1.0 is running in real-time on QVGA images, for larger images the frame-rate drops since the detector has to evaluate a larger number of windows. A GPU implementation is a potential way

to increase the speed as the scanning window approach can be parallelized. Implementation of pieces of code using SSE instruction set is also a promising direction.

Apply P-N Learning to other problems. In chapter 5, P-N Learning was applied to data from a video stream with a specific spatio-temporal structure. The structure is, however, present in many other problems as well. One possible way is to exploit search engines such as Google Image Search. Search for a particular object (e.g. a dog) returns a set of images where the object is likely to appear (P-expert). A search for other object categories returns a set of images where the object is typically not present (N-expert).

Sophisticated experts. The P-N experts used in this thesis are relatively simple, as they were describing motion of a single object in a video stream. Apart from the assumption that the object is unique in the image and the object moves on a trajectory, the experts did not take any other assumption. In more complex scenarios, e.g. when tracking multiple object in parallel, one can formalise more complex rules to describe the problem.

Appendix A

Compared algorithms

1. **FT:** Fragment-based Tracker [Adam 06], a static template tracker which represents the object by a set of parts. In presence of partial occlusions, the method have demonstrated better performance than Mean-Shift [Comaniciu 03].

2. **IVT:** Incremental Visual Tracking [Ross 07], a particle filter that incrementally builds a PCA-based model of the object.

3. **ET:** Ensemble Tracking [Avidan 07], a mean shift-based tracker that adapts an discriminative model classifying pixels.

4. **ODF:** Online Discriminative Features [Collins 03], a mean shift-based tracker that adapts color projections to separate the object from background.

5. **OB:** Online Boosting Tracker [Grabner 06], an approach similar to ODF, but the classification is performed on bounding box level.

6. **ORF:** Online Random Forests [Saffari 09], an approach similar to OB but more robust with respect to noise.

7. **SOB:** Semi-supervised Online Boosting [Grabner 08], an extension of OB that internally trains 2 classifiers.

8. **BSOB:** Beyond Semi-supervised Online Boosting [Stalder 09], an extension of SOB that trains 3 classifiers to simultaneously increase adaptability and stability.

9. **MILTrack:** Multiple Instance Learning tracker [Babenko 09], an approach similar to OB but with a modified, drift-resistant updating strategy.

10. **CoGD:** Co-trained Generative and Discriminative [Yu 08], a particle filter that co-trains a pair of classifiers.

11. **PROST:** Parallel Robust Online Simple Tracking [Santner 10], a method based on three complementary trackers: template, optical flow and random forest.

Appendix B

Sequences used for evaluation

The TLD1.0 system has been quantitatively evaluated on 21 sequences specified in table B.1 and shown in figure B.1.

Id	Sequence name	Frames	First appeared in	Moving camera	Partial occlusion	Full occlusions	Out-of-plane rotation	Illumination change	Scale change	Similar objects
1	David	761	D. Ross et al., IJCV'08	yes	yes	no	yes	yes	yes	no
2	Jumping	313	Q. Yu, ECCV'08	yes	no	no	no	no	no	no
3	Pedestrian 1	140	S. Avidan, PAMI'07	yes	no	no	no	no	no	no
4	Pedestrian 2	338	Q. Yu et al., ECCV'08	yes	yes	yes	no	no	no	yes
5	Pedestrina 3	184	Q. Yu et al., ECCV'08	yes	yes	yes	no	no	no	yes
6	Car	945	Q. Yu et al., ECCV'08	yes	yes	yes	no	no	no	yes
7	Girl	502	S. Birchfield, CVPR'89	yes	yes	no	yes	no	yes	yes
8	Silvester	1,344	D. Ross et al., IJCV'08	no	no	no	yes	yes	no	no
9	Face occlusion 1	885	A. Adam et al., CVPR'06	no	yes	no	no	no	no	no
10	Face occlusion 2	812	B. Babenko et al., CVPR'09	no	yes	no	no	no	no	no
11	Tiger	354	B. Babenko et al., CVPR'09	no	yes	no	yes	yes	no	no
12	Board	698	J. Santner et al., CVPR'10	no	no	no	yes	no	no	no
13	Box	1,161	J. Santner et al., CVPR'10	no	yes	no	yes	no	no	no
14	Lemming	1,336	J. Santner et al., CVPR'10	no	yes	no	yes	no	no	no
15	Liquor	1,741	J. Santner et al., CVPR'10	no	yes	no	yes	no	no	yes
16	Motocross	2,665	Z. Kala et al.l, CVPR'10	yes	yes	yes	yes	yes	yes	yes
17	Volkswagen	8,576	Z. Kalal et al., CVPR'10	yes	yes	yes	yes	yes	yes	yes
18	Car Chase	9928,	Z. Kalal et al., CVPR'10	yes	yes	yes	yes	yes	yes	yes
19	Panda	3,000	Z. Kalal et al., CVPR'10	yes	yes	yes	yes	yes	yes	no
20	IT Crowd	35,471	Z. Kalal et al., CVPR'10	yes	yes	yes	yes	yes	yes	yes
21	Surveillance	500	Z. Kalal et al., CVPR'10	no	yes	yes	yes	no	yes	yes

Table B.1: Description of sequences used for evaluation. A horizontal line separates the standard and the introduced sequences. The red color indicates the TLD data set.

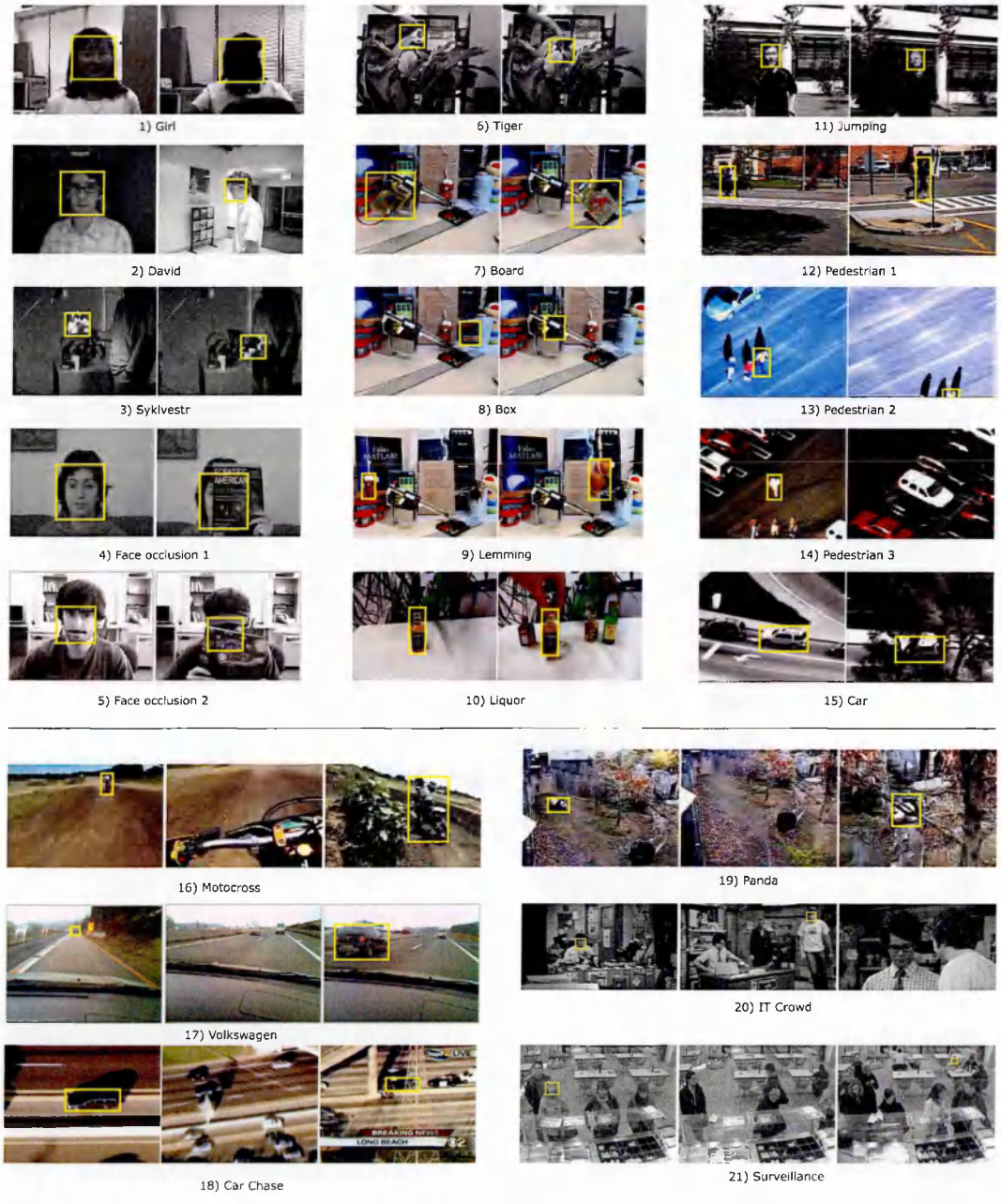

Figure B.1: Snapshots from the sequences used for evaluation. A horizontal line separates the standard and the introduced sequences.

Bibliography

[Adam 06] A. Adam, E. Rivlin & I. Shimshoni. *Robust Fragments-based Tracking using the Integral Histogram.* Conference on Computer Vision and Pattern Recognition, pages 798–805, 2006.

[Aha 91] D W Aha, D Kibler & M K Albert. *Instance-based learning algorithms.* Machine Learning, vol. 6, no. 1, pages 37–66, 1991.

[Alvarez 07] L Alvarez, R Deriche, T Papadopoulo & J Sanchez. *Symmetrical dense optical flow estimation with occlusions detection.* International Journal of Computer Vision, vol. 75, no. 3, pages 371–385, 2007.

[Amit 97] Y Amit & D Geman. *Shape quantization and recognition with randomized trees.* Neural computation, vol. 9, no. 7, pages 1545–1588, 1997.

[Avidan 04] S Avidan. *Support Vector Tracking.* IEEE Transactions on Pattern Analysis and Machine Intelligence, pages 1064–1072, 2004.

[Avidan 07] S Avidan. *Ensemble Tracking.* IEEE Transactions on Pattern Analysis and Machine Intelligence, vol. 29, no. 2, pages 261–271, 2007.

[Babenko 09] B Babenko, Ming-Hsuan Yang & S Belongie. *Visual Tracking*

with Online Multiple Instance Learning. Conference on Computer Vision and Pattern Recognition, 2009.

[Baker 04] S Baker & I Matthews. *Lucas-Kanade 20 Years On: A Unifying Framework.* International Journal of Computer Vision, vol. 56, no. 3, pages 221–255, February 2004.

[Barron 94] J L Barron, D J Fleet & S S Beauchemin. *Performance of Optical Flow Techniques.* International Journal of Computer Vision, vol. 12, no. 1, pages 43–77, 1994.

[Belhumeur 97] P Belhumeur, J Hespanha & D Kriegman. *Eigenfaces vs. Fisherfaces: recognition using class specific linearprojection.* IEEE Transactions on Pattern Analysis and Machine Intelligence, 1997.

[Bibby 08] C Bibby & I Reid. *Robust real-time visual tracking using pixel-wise posteriors.* European Conference on Computer Vision, 2008.

[Bibby 10] C Bibby & I Reid. *Real-time Tracking of Multiple Occluding Objects using Level Sets.* Computer Vision and Pattern Recognition, 2010.

[Birchfield 98] S Birchfield. *Elliptical head tracking using intensity gradients and color histograms.* Conference on Computer Vision and Pattern Recognition, 1998.

[Black 98] M J Black & A D Jepson. *Eigentracking: Robust matching and tracking of articulated objects using a view-based representation.* International Journal of Computer Vision, vol. 26, no. 1, pages 63–84, 1998.

[Blum 98] A Blum & T Mitchell. *Combining labeled and unlabeled data with co-training.* Conference on Computational Learning Theory, page 100, 1998.

[Bouguet 99] J Y Bouguet. *Pyramidal Implementation of the Lucas Kanade Feature Tracker Description of the algorithm.* Technical Report, Intel Microprocessor Research Labs, 1999.

[Bradski 98] G R Bradski. *Computer vision face tracking for use in a perceptual user interface.* Intel Technology Journal, vol. 2, no. 2, pages 12–21, 1998.

[Breiman 96] L Breiman. *Bagging predictors.* Machine Learning, vol. 24, no. 2, pages 123–140, 1996.

[Breiman 01] L Breiman. *Random forests.* Machine Learning, vol. 45, no. 1, pages 5–32, 2001.

[Brox 04] T Brox, A Bruhn, N Papenberg & J Weickert. *High accuracy optical flow estimation based on a theory for warping.* European Conference on Computer Vision, pages 25–36, 2004.

[Buchanan 06] A. M. Buchanan & A. W. Fitzgibbon. *Interactive Feature Tracking using K-D Trees and Dynamic Programming.* In IEEE Conference on Computer Vision and Pattern Recognition, volume 1, pages 626–633, 2006.

[Buehler 08] P Buehler, M Everingham, D P Huttenlocher & A Zisserman. *Long term arm and hand tracking for continuous sign language TV broadcasts.* British Machine Vision Conference, 2008.

[Calonder 08] M Calonder, V Lepetit & P Fua. *Keypoint signatures for fast learning and recognition.* European Conference on Computer Vision, pages 58–71, 2008.

[Calonder 10] M Calonder, V Lepetit & P Fua. *BRIEF : Binary Robust Independent Elementary Features.* European Conference on Computer Vision, 2010.

[Cauwenberghs 01] G Cauwenberghs & T Poggio. *Incremental and decremental support vector machine learning.* Advances in neural information processing systems, page 409, 2001.

[Chapelle 06] O Chapelle, B Schölkopf & A Zien. Semi-Supervised Learning. MIT Press, Cambridge, MA, 2006.

[Collins 03] R Collins & Y Liu. *On-line selection of discriminative tracking features.* Proceedings Ninth IEEE International Conference on Computer Vision, pages 346–352 vol.1, 2003.

[Collins 05] R Collins, Y Liu & M Leordeanu. *Online Selection of Discriminative Tracking Features.* IEEE Transactions on Pattern Analysis and Machine Intelligence, vol. 27, no. 10, pages 1631–1643, 2005.

[Comaniciu 03] D Comaniciu, V Ramesh & P Meer. *Kernel-Based Object Tracking.* IEEE Transactions on Pattern Analysis and Machine Intelligence, vol. 25, no. 5, pages 564–577, 2003.

[Dalal 05] N Dalal & B Triggs. *Histograms of oriented gradients for human detection.* Conference on Computer Vision and Pattern Recognition, 2005.

[Davison 03] A J Davison. *Real-time simultaneous localisation and mapping with a single camera.* International Conference on Computer Vision, 2003.

[Dietterich 97] T G Dietterich, R H Lathrop & T Lozano-Perez. *Solving the multiple instance problem with axis-parallel rectangles.* Artificial Intelligence, vol. 89, no. 1-2, pages 31–71, 1997.

[Dowson 05] N Dowson & R Bowden. *Simultaneous Modeling and Tracking (SMAT) of Feature Sets.* Conference on Computer Vision and Pattern Recognition, 2005.

[Dowson 06] N Dowson & R. Bowden. *N-tier simultaneous modelling and tracking for arbitrary warps.* In British Machine Vision Conference., 2006.

[Dowson 08] N Dowson & R Bowden. *Mutual information for Lucas-Kanade Tracking (MILK): an inverse compositional formulation.* IEEE transactions on pattern analysis and machine intelligence, vol. 30, no. 1, pages 180–5, January 2008.

[Efron 93] B Efron & R Tibshirani. An Introduction to the Bootstrap. Chapman & Hall/CRC, 1993.

[Fergus 03] R Fergus, P Perona & A Zisserman. *Object class recognition by unsupervised scale-invariant learning.* Conference on Computer Vision and Pattern Recognition, vol. 2, 2003.

[Fischler 73] M A Fischler & R A Elschlager. *The representation and matching of pictorial structures.* IEEE Transactions on Computers, vol. 100, no. 22, pages 67–92, 1973.

[Fleuret 01] F Fleuret & D Geman. *Coarse-to-Fine Face Detection.* International Journal of Computer Vision, 2001.

[Fleuret 08] F Fleuret & D Geman. *Stationary features and cat detection.* Journal of Machine Learning Research, vol. 9, pages 2549–2578, 2008.

[Freund 95] Y Freund. *Boosting a weak learning algorithm by majority.* Information and Computation, 1995.

[Freund 97] Y Freund & R E Schapire. *A Decision-Theoretic Generalization of On-Line Learning and an Application to Boosting,*. Journal of Computer and System Sciences, vol. 55, no. 1, pages 119–139, August 1997.

[Freund 01] Y Freund. *An Adaptive Version of the Boost by Majority Algorithm.* Machine Learning, 2001.

[Friedman 00] J Friedman, T Hastie & R Tibshirani. *Additive logistic regression: a statistical view of boosting (With discussion and a rejoinder by the authors).* The Annals of Statistics, vol. 28, no. 2, pages 337–407, 2000.

[Goldman 07] D B Goldman, B Curless, D Salesin & S M Seitz. *Interactive Video Object Annotation.* ACM Computing Surveys, pages 1–7, 2007.

[Grabner 06] H Grabner & H Bischof. *On-line boosting and vision.* Conference on Computer Vision and Pattern Recognition, 2006.

[Grabner 08] H Grabner, C Leistner & H Bischof. *Semi-Supervised On-line Boosting for Robust Tracking.* European Conference on Computer Vision, 2008.

[Hadid 04] A Hadid, M Pietikainen & T Ahonen. *A Discriminative Feature Space for Detecting and Recognizing Faces.* IEEE Computer Society, no. ii, 2004.

[Harris 88] Ch Harris & M Stephens. *A Combined Corner and Edge Detector.* Alvey vision conference, vol. 15, page 50, 1988.

[Hinterstoisser 09] S Hinterstoisser, O Kutter, N Navab, P Fua & V Lepetit. *Real-time learning of accurate patch rectification.* Conference on Computer Vision and Pattern Recognition, 2009.

[Hinterstoisser 10] S Hinterstoisser, V Lepetit, S Ilic, P Fua & N Navab. *Dominant Orientation Templates for Real-Time Detection of Texture-Less Objects*. Conference on Computer Vision and Pattern Recognition, 2010.

[Horn 81] B K P Horn & B G Schunck. *Determining optical flow*. Artificial intelligence, vol. 17, no. 1-3, pages 185–203, 1981.

[Huang 07] C Huang, H Ai, Y Li & S Lao. *High-Performance Rotation Invariant Multiview Face Detection*. IEEE Transactions on Pattern Analysis and Machine Intelligence, 2007.

[Isard 98] M Isard & A Blake. *CONDENSATION - Conditional Density Propagation for Visual Tracking*. International Journal of Computer Vision, vol. 29, no. 1, pages 5–28, 1998.

[Javed 05] O Javed, S Ali & M Shah. *Online detection and classification of moving objects using progressively improving detectors*. Conference on Computer Vision and Pattern Recognition, 2005.

[Jepson 03] A D Jepson, D J Fleet & T F El-Maraghi. *Robust Online Appearance Models for Visual Tracking*. IEEE Transactions on Pattern Analysis and Machine Intelligence, pages 1296–1311, 2003.

[Jones 03] M Jones & P Viola. *Fast multi-view face detection*. Conference on Computer Vision and Pattern Recognition, 2003.

[Klein 07] G Klein & D Murray. *Parallel Tracking and Mapping for Small AR Workspaces*. International Symposium on Mixed and Augmented Reality, November 2007.

[Kolsch 04] M. Kolsch & M. Turk. *Fast 2D Hand Tracking with Flocks of Features and Multi-Cue Integration*. Conference on Computer Vision and Pattern Recognition Workshop, 2004.

[Kwon 10] J Kwon & K M Lee. *Visual Tracking Decomposition.* Conference on Computer Vision and Pattern Recognition, 2010.

[Laptev 06] I Laptev. *Improvements of object detection using boosted histograms.* British Machine Vision Conference, 2006.

[Leibe 07] B Leibe, K Schindler & L Van Gool. *Coupled Detection and Trajectory Estimation for Multi-Object Tracking.* 2007 IEEE 11th International Conference on Computer Vision, pages 1–8, October 2007.

[Leichter 09] I Leichter, M Lindenbaum & E Rivlin. *Tracking by affine kernel transformations using color and boundary cues.* IEEE transactions on pattern analysis and machine intelligence, vol. 31, no. 1, pages 164–71, January 2009.

[Lepetit 05] V Lepetit, P Lagger & P Fua. *Randomized trees for real-time keypoint recognition.* Conference on Computer Vision and Pattern Recognition, 2005.

[Lepetit 06] V Lepetit & P Fua. *Keypoint recognition using randomized trees.* IEEE transactions on pattern analysis and machine intelligence, vol. 28, no. 9, pages 1465–79, September 2006.

[Levi 04] K Levi & Y Weiss. *Learning object detection from a small number of examples: the importance of good features.* Conference on Computer Vision and Pattern Recognition, 2004.

[Levin 03] A Levin, P Viola & Y Freund. *Unsupervised improvement of visual detectors using co-training.* International Conference on Computer Vision, 2003.

[Lewis 94] D Lewis & W Gale. *Training text classifiers by uncertainty sampling*. International Conference on Research and Development in Iformation Retrieval, 1994.

[Li 04] S Z Li & Z Q Zhang. *FloatBoost Learning and Statistical Face Detection*. IEEE Transactions on Pattern Analysis and Machine Intelligence, 2004.

[Li 07] Y Li, H Ai, T Yamashita, S Lao & M Kawade. *Tracking in Low Frame Rate Video: A Cascade Particle Filter with Discriminative Observers of Different Lifespans*. Conference on Computer Vision and Pattern Recognition, 2007.

[Lienhart 02] R Lienhart & J Maydt. *An extended set of Haar-like features for rapid object detection*. International Conference on Image Processing, 2002.

[Lowe 04] D G Lowe. *Distinctive image features from scale-invariant keypoints*. International Journal of Computer Vision, vol. 60, no. 2, pages 91–110, 2004.

[Lucas 81] B D Lucas & T Kanade. *An iterative image registration technique with an application to stereo vision*. International Joint Conference on Artificial Intelligence, vol. 81, pages 674–679, 1981.

[Maggio 07] E Maggio, E Piccardo, C Regazzoni & A Cavallaro. *Particle {PHD} filtering for multi-target visual tracking*. IEEE International Conference on Acoustics, Speech and Signal Processing, vol. 1, 2007.

[Matas 04] J Matas, O Chum, M Urban & T Pajdla. *Robust wide-baseline stereo from maximally stable extremal regions*. Image and Vision Computing, vol. 22, no. 10, pages 761–767, 2004.

[Matthews 04] I Matthews, T Ishikawa & S Baker. *The Template Update Problem.* IEEE Transactions on Pattern Analysis and Machine Intelligence, vol. 26, no. 6, pages 810–815, 2004.

[Mikolajczyk 04] K Mikolajczyk, C Schmid & A Zisserman. *Human detection based on a probabilistic assembly of robust part detectors.* European Conference on Computer Vision, 2004.

[Mikolajczyk 05] K Mikolajczyk, T Tuytelaars, C Schmid, A Zisserman, J Matas, F Schaffalitzky, T Kadir & L V Gool. *A comparison of affine region detectors.* International journal of computer vision, vol. 65, no. 1, pages 43–72, 2005.

[Murase 95] H Murase & S K Nayar. *Visual learning and recognition of 3-D objects from appearance.* International Journal of Computer Vision, vol. 14, no. 1, pages 5–24, 1995.

[Newman 06] P Newman. *SLAM-Loop Closing with Visually Salient Features.* International Conference on Robotics and Automation, 2006.

[Nickels 02] K Nickels & S Hutchinson. *Estimating uncertainty in SSD-based feature tracking.* Image and vision computing, vol. 20, no. 1, pages 47–58, 2002.

[Nigam 00] K Nigam, A K McCallum, S Thrun & T Mitchell. *Text classification from labeled and unlabeled documents using EM.* Machine Learning, vol. 39, no. 2, pages 103–134, 2000.

[Obdrzalek 05] S Obdrzalek & J Matas. *Sub-linear indexing for large scale object recognition.* British Machine Vision Conference, vol. 1, pages 1–10, 2005.

[Ogata 09] K Ogata. Modern control engineering. Prentice Hall, 2009.

[Ojala 02] T Ojala, M Pietikainen & T Maenpaa. *Multiresolution Gray-Scale and Rotation Invariant Texture Classification with Local Binary Patterns.* IEEE Transactions on Pattern Analysis and Machine Intelligence, vol. 24, no. 7, pages 971–987, 2002.

[Okuma 04] K Okuma, A Taleghani, N de Freitas, J J Little & D G Lowe. *A boosted particle filter: Multitarget detection and tracking.* European Conference on Computer Vision, 2004.

[Osuna 97] E Osuna, R Freund & F Girosi. *Training support vector machines: an application to face detection.* Conference on Computer Vision and Pattern Recognition, 1997.

[Oza 05] N C Oza. *Online bagging and boosting.* International Conference on Systems, Man and Cybernetics, 2005.

[Ozuysal 06] M Ozuysal, V Lepetit, F Fleuret & P Fua. *Feature Harvesting for Tracking-by-Detection.* European Conference on Computer Vision, 2006.

[Ozuysal 07] M Ozuysal, P Fua & V Lepetit. *Fast Keypoint Recognition in Ten Lines of Code.* Conference on Computer Vision and Pattern Recognition, 2007.

[Papageorgiou 98] C P Papageorgiou, M Oren & T Poggio. *A general framework for object detection.* International Conference on Computer Vision, 1998.

[Pilet 10] J Pilet & H Saito. *Virtually augmenting hundreds of real pictures: An approach based on learning, retrieval, and tracking.* 2010 IEEE Virtual Reality Conference (VR), pages 71–78, March 2010.

[Poh 09] N Poh, R Wong, J Kittler & F Roli. *Challenges and Research Directions for Adaptive Biometric Recognition Systems.* Advances in Biometrics, 2009.

[Polikar 06] R Polikar. *Ensemble based systems in decision making.* IEEE Circuits and Systems Magazine, vol. 6, no. 3, pages 21–45, 2006.

[Press 92] W Press, S Teukolsky, W Vetterling & B Flannery. Numerical Recipes in C. Cambridge University Press, 1992.

[Quinlan 96] J R Quinlan. *Bagging, boosting, and C4. 5.* National Conference on Artificial Intelligence, 1996.

[Rahimi 08] A Rahimi, L P Morency & T Darrell. *Reducing drift in differential tracking.* Computer Vision and Image Understanding, vol. 109, no. 2, pages 97–111, 2008.

[Ramanan 05] D Ramanan, D A Forsyth & A Zisserman. *Strike a pose: Tracking people by finding stylized poses.* Conference on Computer Vision and Pattern Recognition, 2005.

[Ramanan 07] D Ramanan, D A Forsyth & A Zisserman. *Tracking people by learning their appearance.* IEEE Transactions on Pattern Analysis and Machine Intelligence, pages 65–81, 2007.

[Reddy 02] B S Reddy & B N Chatterji. *An FFT-based technique for translation, rotation, and scale-invariant image registration.* Image Processing, IEEE Transactions on, vol. 5, no. 8, pages 1266–1271, 2002.

[Rosenberg 05] C Rosenberg, M Hebert & H Schneiderman. *Semi-supervised self-training of object detection models.* Workshop on Application of Computer Vision, 2005.

[Ross 07] D Ross, J Lim, R Lin & M Yang. *Incremental Learning for Robust Visual Tracking*. International Journal of Computer Vision, vol. 77, no. 1-3, pages 125–141, August 2007.

[Rosten 06] E Rosten & T Drummond. *Machine learning for high-speed corner detection*. European Conference on Computer Vision, May 2006.

[Rowley 98] H A Rowley, S Baluja & T Kanade. *Neural network-based face detection*. IEEE Transactions on Pattern Analysis and Machine Intelligence, vol. 20, no. 1, pages 23–38, 1998.

[Saffari 09] A Saffari, Ch Leistner, J Santner, M Godec & H Bischof. *On-line Random Forests*. Online Learning for Computer Vision Workshop, 2009.

[Sand 08] P Sand & S Teller. *Particle video: Long-range motion estimation using point trajectories*. International Journal of Computer Vision, vol. 80, no. 1, pages 72–91, 2008.

[Santner 10] J Santner, C Leistner, A Saffari, T Pock & H Bischof. *PROST: Parallel Robust Online Simple Tracking*. Conference on Computer Vision and Pattern Recognition, 2010.

[Schapire 90] R E Schapire. *The strength of weak learnability*. Machine Learning, 1990.

[Schapire 98a] R E Schapire, Y Freund, P Bartlett & W S Lee. *Boosting the margin: A new explanation for the effectiveness of voting methods*. The Annals of Statistics, 1998.

[Schapire 98b] R E Schapire & Y Singer. *Improved boosting algorithms using confidence-rated predictions*. Proceedings of the eleventh an-

nual conference on Computational learning theory - COLT' 98, vol. 37, no. 3, pages 80–91, 1998.

[Schapire 99] R Schapire & Y Singer. *Improved Boosting Using Confidence-rated Predictions.* Machine Learning, 1999.

[Schapire 02] R E Schapire. *The boosting approach to machine learning: An overview.* Lecture Notes in Statistics, 2002.

[Schneiderman 04] H Schneiderman & T Kanade. *Object Detection Using the Statistics of Parts.* International Journal of Computer Vision, 2004.

[Schweitzer 02] H Schweitzer, J Bell & F Wu. *Very fast template matching.* European Conference on Computer Vision, pages 145–148, 2002.

[Shi 94] J Shi & C Tomasi. *Good features to track.* Conference on Computer Vision and Pattern Recognition, 1994.

[Shotton 08] J Shotton, M Johnson & R Cipolla. *Semantic texton forests for image categorization and segmentation.* In Computer Vision and Pattern Recognition,. IEEE, June 2008.

[Sinha 94] P Sinha. *Object Recognition via Image Invariants: A Case Study.* Investigative Ophthalmology and Visual Science, 1994.

[Sochman 05] J Sochman & J Matas. *WaldBoost: learning for Time Constrained Sequential Detection.* Conference on Computer Vision and Pattern Recognition, 2005.

[Sochman 09] J Sochman & J Matas. *Learning Fast Emulators of Binary Decision Processes.* International Journal of Computer Vision, vol. 83, no. 2, pages 149–163, March 2009.

[Stalder 09] S Stalder, H Grabner & L V Gool. *Beyond semi-supervised tracking: Tracking should be as simple as detection, but not simpler than recognition.* 2009 IEEE 12th International Conference on Computer Vision Workshops, ICCV Workshops, pages 1409–1416, September 2009.

[Strecha 03] C Strecha, T Tuytelaars & L Van Gool. *Dense matching of multiple wide-baseline views.* International Conference on Computer Vision, 2003.

[Sung 98] K K Sung & T Poggio. *Example-based learning for view-based human face detection.* IEEE Transactions on Pattern Analysis and Machine Intelligence, vol. 20, no. 1, pages 39–51, 1998.

[Takacs 10] G Takacs, V Chandrasekhar, D Chen, S Tsai, R Grzeszczuk & B Girod. *Unified Real-Time Tracking and Recognition with Rotation-Invariant Fast Features.* Conference on Computer Vision and Pattern Recognition, 2010.

[Tang 07] F Tang, S Brennan, Q Zhao, H Tao & U C Santa Cruz. *Co-tracking using semi-supervised support vector machines.* International Conference on Computer Vision, pages 1–8, 2007.

[Taylor 09] S Taylor & T Drummond. *Multiple target localisation at over 100 fps.* British Machine Vision Conference, 2009.

[Turk 91] M Turk & A Pentland. *Eigenfaces for recognition.* Journal of cognitive neuroscience, vol. 3, no. 1, pages 71–86, 1991.

[Tuytelaars 07] T Tuytelaars & K Mikolajczyk. *Local Invariant Feature Detectors: A Survey.* Foundations and Trends in Computer Graphics and Vision, vol. 3, no. 3, pages 177–280, 2007.

[Vacchetti 04] L Vacchetti, V Lepetit & P Fua. *Stable real-time 3d tracking using online and offline information.* IEEE Transactions on Pattern Analysis and Machine Intelligence, vol. 26, no. 10, page 1385, 2004.

[Vapnik 98] V N Vapnik. Statistical learning theory. Wiley New York, 1998.

[Veenman 01] C J Veenman, M J T Reinders & E Backer. *Resolving motion correspondence for densely moving points.* IEEE Transactions on Pattern Analysis and Machine Intelligence, vol. 23, no. 1, pages 54–72, 2001.

[Viola 01] P Viola & M Jones. *Rapid object detection using a boosted cascade of simple features.* Conference on Computer Vision and Pattern Recognition, 2001.

[Wang 03] L Wang, W Hu & T Tan. *Recent developments in human motion analysis.* Pattern Recognition, vol. 36, no. 3, pages 585–601, 2003.

[Wu 04] B Wu, H Ai, C Huang & S Lao. *Fast rotation invariant multi-view face detection based on real Adaboost.* International Conference on Automatic Face and Gesture Recognition, 2004.

[Wu 07] H Wu, A C Sankaranarayanan & R Chellappa. *In Situ Evaluation of Tracking Algorithms Using Time Reversed Chains.* Conference on Computer Vision and Pattern Recognition, 2007.

[Xiao 03] R Xiao, L Zhu & H J Zhang. *Boosting chain learning for object detection.* International Conference on Computer Vision, 2003.

[Yang 94] G Yang & T S Huang. *Human face detection in a complex background.* Pattern Recognition, 1994.

[Yilmaz 04] A Yilmaz, X Li & M Shah. *Contour-based object tracking with occlusion handling in video acquired using mobile cameras.* IEEE Transactions on Pattern Analysis and Machine Intelligence, pages 1531–1536, 2004.

[Yilmaz 06] A Yilmaz, O Javed & M Shah. *Object tracking: A survey.* ACM Computing Surveys, vol. 38, no. 4, page 13, 2006.

[Yu 08] Q Yu, T B Dinh & G Medioni. *Online tracking and reacquisition using co-trained generative and discriminative trackers.* European Conference on Computer Vision, 2008.

[Zeisl 10] B Zeisl, C Leistner, A Saffari & H Bischof. *On-line Semi-supervised Multiple-Instance Boosting.* Conference on Computer Vision and Pattern Recognition, 2010.

[Zhou 96] K Zhou, J C Doyle & K Glover. Robust and optimal control. Prentice Hall Englewood Cliffs, NJ, 1996.

[Zhu 09] X Zhu & A B Goldberg. Introduction to semi-supervised learning. Morgan & Claypool Publishers, 2009.

[Zimmermann 09] K Zimmermann, J Matas & T Svoboda. *Tracking by an optimal sequence of linear predictors.* IEEE transactions on pattern analysis and machine intelligence, vol. 31, no. 4, pages 677–92, April 2009.